INORGANIC CHEMISTRY FRONTIERS

REVIEW

View Article Online
View Journal | View Issue

Check for updates

Cite this: *Inorg. Chem. Front.*, 2025, **12**, 6398

The inorganic chemist's guide to actinide radiation chemistry: a review†

Samantha J. Kruse, *[a,b] Sarah K. Scherrer, [a] Gregory P. Horne, [c] Jay A. LaVerne [b,d] and Tori Z. Forbes *[a]

Received 17th April 2025,
Accepted 8th July 2025

DOI: 10.1039/d5qi00975h

rsc.li/frontiers-inorganic

This review aims to provide an overview of the current state of radiation chemistry with respect to the actinide elements, thorium through californium. Despite the inherent radioactivity of the actinides, only a few studies explore the effects of ionizing radiation on their redox chemistry and surrounding environment. This fundamental knowledge gap, coupled with the current renaissance in actinide-based technologies such as nuclear power, space exploration, and medicine, underscores the importance of research in this interdisciplinary area. This review will focus on the interactions between reactive species formed by radiolysis with actinides and their complexes, offering an inorganic chemist's perspective on research in radiation chemistry. In addition, a thorough discussion of our current understanding of radiation-induced changes in actinide speciation in both aqueous solution and the solid-state will be provided, focusing on changes in oxidation state distribution, complexation, and secondary coordination effects within inorganic materials. Finally, this review will discuss challenges and opportunities for inorganic chemists to explore this unique intersection of fields.

Open Access Article. Published on 10 juli 2025. Downloaded on 20-05-2026 01:21:34.
This article is licensed under a Creative Commons Attribution 3.0 Unported Licence.

1. Introduction

The actinides are a series of complex elements that continue to challenge and fascinate the inorganic chemistry community.[1] Positioned at the bottom of the periodic table, these elements exhibit chemical behavior significantly influenced by relativistic effects, such as expansion of the 5f-orbitals and extensive spin–orbit coupling. These physical attributes strongly influence their electronic structure, resulting in complex spectroscopic signatures, magnetic properties, and redox behavior. Unlike their 4f congeners, the lanthanides, actinides display increased involvement of their 5f-orbitals in chemical bonding, leading to enhanced covalency.[2] The intricacies of actinide electronic structures and the resulting variability in their chemical interactions have led many inorganic chemists to delve deeper into the fundamental behavior of these elements.

A frequently overlooked aspect of actinide chemistry is the impact of their inherent radioactivity or the ionizing radiation fields in which they are associated. All actinides possess isotopes that are susceptible to radioactive decay, resulting in the emission of ionizing radiation in the form of energetic particles (alpha particles [α], beta particles [β], neutrons [n], fission fragments, and recoiling daughter nuclei) and photons (gamma rays [γ] and X-rays). Harnessing this energy is essential for energy production by nuclear power reactors[3,4] and radioisotope thermoelectric generators for space exploration.[5,6] Conversely, managing the impacts of ionizing radiation fields is a significant challenge for used nuclear fuel (UNF) reprocessing,[7–9] nuclear waste storage,[10–13] environmental remediation,[14,15] and nuclear medicine[16] because the energy deposited by ionizing radiation generates reactive radicals, ions, and molecular species. These radiolysis products can initiate redox chemistry, degrade molecules, create defects in solid-state materials, and alter the physical and chemical properties of matter.[17] Each of these radiation-induced modifications can influence the chemical behavior, speciation, and transport of actinides, which is further complicated by actinide elements often being intermixed with other radionuclides in real-world scenarios.[18,19] Consequently, understanding actinide radiation chemistry is one of the basic research needs in nuclear science.

There is an existing understanding of the effects of ionizing radiation on actinide chemistry thanks to the foundational work of radiation chemists and physicists, but the primary focus has been on resolving long-standing challenges in the reprocessing of UNF.[20–23] However, there remains a gap

[a]Department of Chemistry, University of Iowa, Iowa City, IA, 52240, USA. E-mail: tori-forbes@uiowa.edu, Samantha.Kruse@inl.gov
[b]Radiation Laboratory, University of Notre Dame, Notre Dame, IN, 46556, USA
[c]Center for Radiation Chemistry Research, Idaho National Laboratory, Idaho Falls, ID, 83415, USA
[d]Department of Physics and Astronomy, University of Notre Dame, Notre Dame, IN, 46556, USA

† Electronic supplementary information (ESI) available. See DOI: https://doi.org/10.1039/d5qi00975h

This journal is © the Partner Organisations 2025

Open Access Article. Published on 10 juli 2025. Downloaded on 20-05-2026 01:21:34.
This article is licensed under a Creative Commons Attribution 3.0 Unported Licence.

between the insights of radiation chemists and the tools and techniques utilized by inorganic chemists to explore fundamental actinide science. Bridging this gap could yield valuable insights and new discoveries in the field. Thus, this review aims to summarize the current state of ionizing radiation research on actinides in both aqueous solutions and the solid-state, focusing on the interactions between radiolysis products and actinide ions, their complexes, and the surrounding chemical environment. Additionally, this review will highlight gaps in the literature, key tools for the characterization of actinides, and potential future research directions.

In this review, we focus on inorganic actinide species in aqueous solutions and solid-state materials. For solid-state materials, we cover inorganic crystalline solids that demonstrate significant changes in actinide speciation upon irradiation. Given the importance to the field, we also include discussion on organic ligands coordinated to actinide ions in the solid-state and briefly highlight emerging metal–organic frameworks (MOFs). This review is also limited to radiation-induced processes involving α-particles and γ-rays, as these radiation types are predominant in the radioactive decay of actinide isotopes and have been extensively studied in the literature. Furthermore, it is important to note that discussions of γ-rays also apply to β-particle effects due to their equivalent mechanisms of radiation energy deposition.[24]

2. Ionizing radiation basics

The absorption of ionizing radiation by matter primarily causes the ejection of electrons from atoms, ions, and molecules to create "holes" (the site vacated by the electron) and a free electron.[25] In this context, α-particles, β-particles, γ-rays, X-rays, fast electrons (e^-), fission fragments, recoiling daughter nuclides, accelerated protons (p^+), and heavy ions are all forms of ionizing radiation that can induce physical and chemical changes in matter. Note that β-particles are electrons/negatrons (β^-) or positrons (β^+) emitted by the decay of a nucleus, while fast electrons are artificially produced. The terms are often interchanged, especially as the chemistry induced by these species is equivalent. Note that a low energy β-particle will not induce the same radiation chemistry as a fast electron due to differences in the track structure. Neutrons have been omitted from the above list as they do not directly ionize matter; instead, they activate nuclei through neutron capture processes, generating unstable isotopes that subsequently undergo radioactive decay, or generate recoil ions that then ionize the surrounding medium.

Not all energy transfer events result in ionization; those below the energetic threshold promote an electron to a higher energy orbital, forming an excited state.[26] Excited states can also form by charge recombination reactions between electrons and holes. These initial radiolytic species—the free electron, the corresponding hole, and excited states—subsequently relax by solvation, fragmentation, chemical reaction, or charge recombination to ultimately generate thermal energy. The latter of which is the predominant process in the absence of solutes and reactive surfaces. In more complex systems, the branching of these relaxation pathways determines the extent to which radiolysis impacts the physical and chemical properties of an irradiated system. Each species formed by radiolysis, initial and subsequent, has an associated yield per unit of energy absorbed, a *G*-value (mol J^{-1} or species per 100 eV energy absorbed), representing the efficiency of radiation-induced chemical change.

Initial energy loss by charged particles is through Coulombic interactions with the electrons of the medium. In a mixed medium, the energy deposition to each component is proportional to the electron density of each component, which to a first approximation is equal to their relative masses. The passage of ionizing radiation through matter creates a path of energy transfer events known as a radiation track—a non-homogenous distribution of radiolytic species that evolves in time and space due to a competition between diffusion and chemical reaction. The structure of a radiation track is determined by the type of incident radiation and the composition of the absorbing medium. The number and separation of energy transfer events is directly related to the linear energy transfer (LET) of a charged particle; defined as the average amount of energy deposited by ionizing radiation per unit path length of the medium it travels through ($-\frac{dE}{dx}$).[25,27] LET increases as a particle's velocity decreases, goes through a maximum (the Bragg peak), and ultimately reaches zero when the particle thermalizes with the surrounding medium. At a given velocity, heavier particles have a higher LET than light particles and travel shorter distances.

Track structure is important for the subsequent chemistry that occurs with constituents of the irradiated system. For instance, high-LET leads to energy loss events sufficiently close in space that they can overlap, creating a columnar structure that promotes second-order radical combination reactions, affording relatively lower *G*(radicals) and higher *G*(ions/molecules) values. Conversely, low-LET results in energy loss events that are well separated in space, with each event evolving independently, affording relatively higher *G*(radicals) and lower *G*(ions/molecules) values.

Photon radiation interacts with matter *via* (1) the photoelectric effect, where the incident photon is absorbed to create a hole and a free electron; (2) Compton scattering, where the photon scatters like a particle to produce a free electron and corresponding hole; or (3) pair production, where an electron and positron are produced.[28] In water, the photoelectric effect is dominant below approximately 30 keV, then Compton scattering up to about 25 MeV, and pair production beyond that energy range. Given these modes of interaction, photon radiation tracks are comprised of few, well-separated energy transfer events, and thus, classified as low-LET radiation. γ-Rays are generally in the MeV energy range, so they produce high energy electrons through the Compton effect and the radiation chemistry they induce is the same as an incident fast electron. Electrons ejected by X-rays will induce radiation chemistry con-

Open Access Article. Published on 10 juli 2025. Downloaded on 20-05-2026 01:21:34.
This article is licensed under a Creative Commons Attribution 3.0 Unported Licence.

sistent with low energy β-particles or fast electrons depending on their initial energy.

It is important to note that if electrons are ejected with sufficient kinetic energy (approximately >5 keV), they propagate their own radiation tracks. However, in most cases, these "secondary" electrons do not travel far from the initial ionization event and ultimately produce a cluster of ionizations and excitations, known as a spur. As alluded to above, the lifetime of a radiation track is finite, on the order of microseconds in aqueous solution. The surviving species become homogenously distributed in bulk solution and available for further reaction.

3. Radiation sources

Ionizing radiation sources can be external, where a radioactive material or accelerator is used to supply the radiation, or internal where a radioisotope is deposited or dissolved in the medium. Experimental radiation chemistry studies typically utilize external sources of γ-radiation due to the limited penetration depth of external α-sources and the challenges of working with radioisotopes for internal source irradiations. External radiation sources provide more accurate dosimetry and are useful for simulating the long-term effects of radiation in an experimentally feasible time. External γ-radiation sources often utilize ^{60}Co ($\tau_{1/2}$ = 5.27 years) or ^{137}Cs ($\tau_{1/2}$ = 30.71 years), which require a significant amount of expertise and safety and security procedures to use. Accelerators are common sources for charged particles or X-rays and can be run in a continuous mode for high dose rate studies or in a pulsed mode for time resolved studies. Accelerators can provide advanced capabilities, including electron pulse radiolysis experiments that utilize short bursts of high energy electrons to examine radical reactions and other chemical changes as a function of time and absorbed dose. Fewer studies focus on α-radiation, with external sources utilizing particle accelerators to generate He^{2+} ion beams (α-particle surrogates), and internal sources incorporating a radioactive α-emitter, such as ^{241}Am ($\tau_{1/2}$ = 432.2 years), for so-called self-radiolysis experiments.[29] The incorporation of an internal α-emitter provides a more uniform dose as a He-ion beam can only penetrate a short distance into a medium given its high LET.[30] Therefore, the use of both external and internal radiation sources are essential in experimental studies.

4. Radiation chemistry in aqueous solutions

4.1. Water radiolysis and its chemistry

Water, as the universal solvent, is important in numerous processes; thus, the interaction of ionizing radiation with water is a key factor in understanding fundamental mechanisms occurring in ionizing radiation environments. As depicted in Fig. 1, water radiolysis can be described in three main stages. The initial timepoint is the physical stage, where the absorption of radiation causes either excitation (H_2O^*) or ionization ($H_2O^{\bullet+}$ + e^-) of a water molecule. During the subsequent physicochemical stage, these initial water radiolysis species undergo a variety of reactions to create a range of primary radiolysis products. From the excited state, dissociative relaxation can occur to either form a $^\bullet$OH + H$^\bullet$ pair or create H_2 and an O(^{1}D,^{3}P) atom. The O(^{3}P) atom can interact with neighboring water molecules to create two more $^\bullet$OH radicals. From the ionization branch, $H_2O^{\bullet+}$ can either transfer a proton to a nearby water molecule to form H_3O^+ + $^\bullet$OH, or undergo recombination with an electron to give H_2O^*. Any e^- that escape recombination becomes solvated by the surrounding water molecules to yield the hydrated electron (e_{aq}^-). Finally, each of the species produced from the excitation and ionization processes can interact with other constituents in the system during the

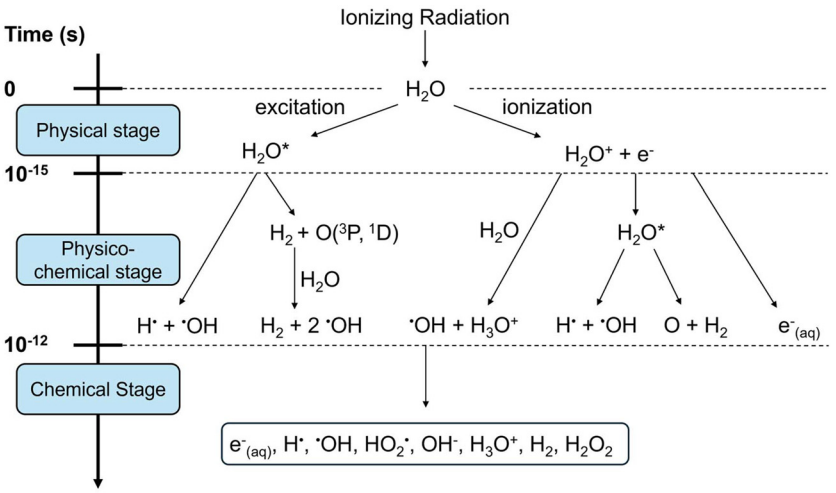

Fig. 1 Reaction scheme for the radiolysis of neat water.[31]

 This journal is © the Partner Organisations 2025

Open Access Article. Published on 10 juli 2025. Downloaded on 20-05-2026 01:21:34.
This article is licensed under a Creative Commons Attribution 3.0 Unported Licence.

chemical stage. The chemical stage also includes the formation of additional reactive oxygen species, such as H_2O_2, $HO_2^{\bullet}$, and $O_2^{\bullet-}$, through interactions between free radicals ($^{\bullet}OH + {}^{\bullet}OH \rightarrow H_2O_2$; $H_2O_2 + {}^{\bullet}OH \rightarrow HO_2^{\bullet} + H_2O$) or molecular oxygen ($O_2 + e^- \rightarrow O_2^{\bullet-}$). These reactions occur over the range of nanoseconds to microseconds depending on the type and energy of the incident radiation.

Although each of these radiation-induced species has a *G*-value in neat water, these yields are highly sensitive to the presence of solutes and radiation quality (type and energy). For example, at about a microsecond the e_{aq}^- has a *G*-value of 2.8–2.9 ions per 100 eV from the γ-radiation of neat water.[32] This yield decreases to 2.47 ions per 100 eV for 5 MeV accelerated He^{2+} ions,[33] and zero in the presence of 1 mM $NaNO_3$.[34] Therefore, one must consider all components of an irradiated system when comparing and invoking *G*-values in the study of actinide-containing solutions.

Fig. 2 provides a timeline correlating the various time regimes in water radiolysis and the appropriate experimental techniques currently used by radiation chemists and inorganic chemists alike. We have expanded the chemical stage from Fig. 1 into two categories—the non-homogeneous radiation track stage and the homogeneous bulk solution stage. The typical initiation of the non-homogeneous stage begins at picosecond timescales, where spur geometry drives competition between the chemical reaction of radiolysis products and their diffusion into homogenous bulk solution. The timeframe of the non-homogeneous stage extends to microseconds for low-LET radiation but cannot be generalized due to differences in track structure for different radiation qualities and dependence on the medium. Upon complete spatial relaxation of the radiation track the concentrations of water radiolysis products can be considered to be homogeneous.

The rate of reaction between a water radiolysis product (P) and a solute (S) is given by the following equation:

$$\frac{d[P]}{dt} = -k_s[P][S]. \quad (1)$$

Generally, [S] does not change much over the course of the reaction so it can be considered constant giving a pseudo first-order reaction rate, and the value of $k_s[S]$ is referred to as the "scavenging capacity" of this reaction. The inverse of the scavenging capacity provides the time regime of the scavenging reaction. For example, scavenging of the e_{aq}^- by NO_3^- occurs at 9×10^9 M^{-1} s^{-1}.[35] Therefore, in an aqueous 1 mM $NaNO_3$ solution, the scavenging capacity is 9×10^6 s^{-1} occurring within the sub-microsecond time regime (1.11×10^{-7} s), *i.e.*, the non-homogenous chemical stage.[36] Care must be taken with interpreting the chemistry of efficient radical scavenging solutes because at high solute concentrations they can scavenge the precursors of certain radiolysis products. For instance, at concentrations >1 M, NO_3^- can scavenge the precursor to the e_{aq}^- and $H_2O^{\star}$.[37] Note, unless there are additional driving forces, such as Coulombic attraction between charged species or extended ion networks, rate coefficients cannot be faster than the diffusion limit of a reactive species in a specific solution. Rate coefficients can, however, be much slower than the diffusion-controlled limit due to a variety of factors, including steric hindrance and high activation energies.

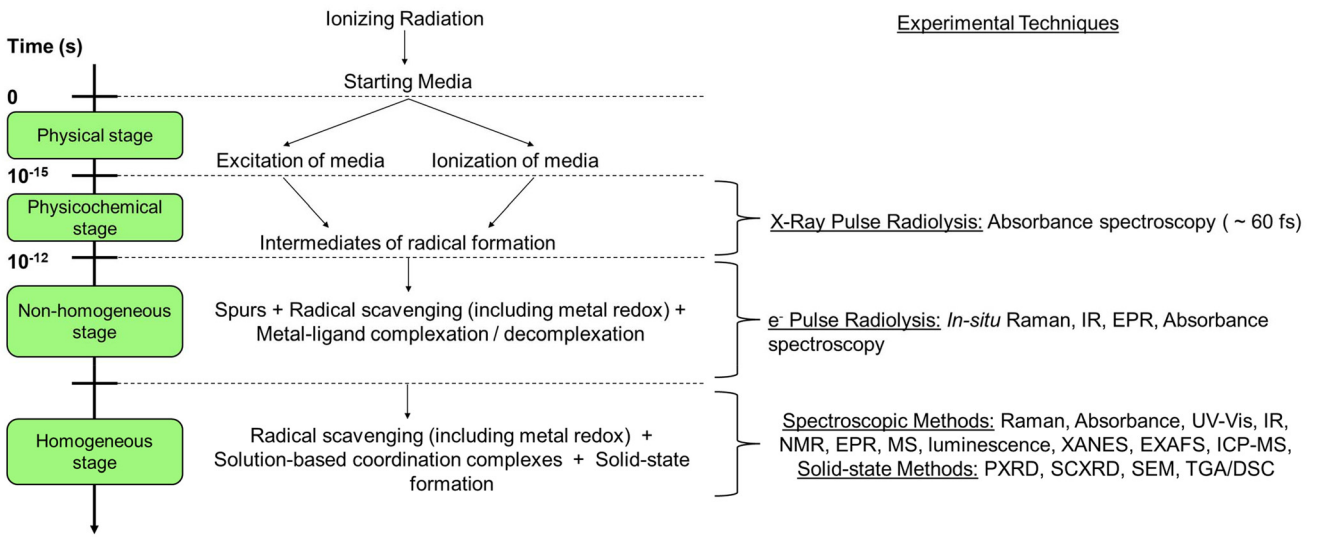

Fig. 2 Left – Timeline of radiation chemistry with the incorporation of metals for solution and solid-state media. Right – Experimental techniques that can be used for different irradiation analyses and associated timescales including spectroscopic techniques such as absorbance, *in situ* Raman spectroscopy, Raman spectroscopy, absorbance spectroscopy, ultraviolet-visible (UV-vis) spectroscopy, infrared spectroscopy (IR), nuclear magnetic resonance spectroscopy (NMR), electron paramagnetic resonance spectroscopy (EPR), mass spectroscopy (MS), luminescence, X-ray absorption near-edge spectroscopy (XANES), extended X-ray absorption fine structure spectroscopy (EXAFS), and inductively coupled plasma mass spectrometry (ICP-MS). Solid-state characterization techniques also include powder X-ray diffraction (PXRD), single crystal X-ray diffraction (SCXRD), scanning electron microscopy (SEM), and thermogravimetric analyses (TGA)/differential scanning calorimetry (DSC).

Open Access Article. Published on 10 juli 2025. Downloaded on 20-05-2026 01:21:34.
This article is licensed under a Creative Commons Attribution 3.0 Unported Licence.

The presence of multiple solutes can lead to competition for water radiolysis products, the partitioning of which is based on simple competition kinetics. Consider the scavenging of the e_{aq}^- by NO_3^- with a rate coefficient of k_a in competition with the reduction of U(VI) by the e_{aq}^- with a rate coefficient of k_b. The fraction of e_{aq}^- that reduces U(VI) is given by:

$$k_b[U(VI)]/(k_b[U(VI)] + k_a[NO_3^-]) \quad (2)$$

The scavenging capacity of each competing species is independent of the concentration of the e_{aq}^- and applies to both the non-homogeneous and homogeneous bulk regimes. Important limitations to consider when selecting a radical scavenging solute include its solubility, its reactivity towards a species of interest, and potential issues from radiolysis of the solute and solvent at high concentration.[38]

Finally, water radiolysis leads to the formation of strong reductants (e_{aq}^-) and oxidants ($^\bullet$OH) in about equal yields,[39,40] and thus, both oxidation and reduction can occur simultaneously in irradiated aqueous solutions. This competition can lead to difficulties in determining which species is responsible for the observed chemistry. Consequently, radiation chemists commonly resort to saturating aqueous solutions with nitrous oxide (N_2O), which converts the reducing products of water radiolysis into additional $^\bullet$OH radicals:[40]

$$e_{aq}^-/H^\bullet + N_2O \rightarrow O^{\bullet -}/OH + N_2, \quad (1)$$

$$O^{\bullet -} + H_2O \rightarrow {}^\bullet OH + OH^-. \quad (2)$$

This conversion is nearly stoichiometric, leading to a doubling of $G(^\bullet OH)$ and the associated yields of oxidizing reactions. In contrast, the yields of reducing reactions will decrease to zero in N_2O saturated solutions. Note, not all systems are completely oxidizing or reducing, so some variation of these results can be expected.

The discussed reaction kinetics are a result of indirect radiation effects. Direct radiation effects refer to chemical change arising from the direct absorption of radiation energy by a species, typically the solvent, whereas indirect effects arise from the interaction of radiolysis products with solutes. That said, under high solute concentration conditions (approximately >1 M in aqueous solution), a solute will receive a fraction of the radiation energy absorbed by the medium, leading to the direct radiolysis of the solute. These direct radiation effects may decompose the solute in a completely different manner from the oxidation/reduction processes occurring by indirect processes. For instance, the direct radiolysis of NO_3^- leads to:[41]

$$NO_3^- \rightsquigarrow e_{aq}^-, NO_3^\bullet, NO_2^-, O. \quad (3)$$

4.2. A short overview on actinide elements

The actinides consist of elements 89–103 on the periodic table and the complexity of their aqueous chemistry is driven by their electron configuration. Valence electrons associated with the actinide elements are located within the 7s, 6d, and 5f-orbitals and the close proximity of the orbital energy levels leads to multiple oxidation states for a majority of the actinide cations. Table 1 summarizes information on the known oxidation states of the actinides from Chapter 15 of the Actinide and Transactinide Elements book,[42] which provides an excellent detailed overview of the chemistry in this series. The authors also note that the most unstable oxidation states have been observed in solid state compounds or, more relevant for this audience, produced as transient species in solution by pulse radiolysis. Fig. 3 provides a standard redox potential scale for the actinide elements and common radicals produced from aqueous solutions (with common co-solutes) to further highlight how radicals produced during pulse radiolysis could influence the redox behavior of the metal cation. We note that the standard reduction potentials provided in Fig. 3 are taken from equilibrium conditions in 1 M HCl or $HClO_4$, but that non-equilibrium conditions can exist during radiolysis processes and are influenced by pH. For readers interested in additional information on the impact of pH on actinide redox behavior, we refer them to the "Atlas of Eh-pH Diagrams" published by the Geological Survey of Japan.[43]

Across the actinide series, cations of the same charge tend to have similarities in coordination environments and some chemical properties. Both trivalent, An(III), and tetravalent, An(IV) cations have coordination numbers that vary between 8–10 and show a strong tendency to solvate, hydrolyze, and oligomerize in aqueous solutions. Both pentavalent, An(V), and hexavalent, An(VI), actinides form strong covalent bonds to oxygen atoms to create actinyl ions (AnO_2^{n+}, where n = 1 or 2) whereas heptavalent, An(VII), actinides form the tetraoxo species (AnO_4^-). These high valent moieties can further coor-

Table 1 Possible oxidation states for the actinide elements.[42,44,45] The most stable oxidation states are shown in bold and unsubstantiated are indicated with question marks

Ac	Th	Pa	U	Np	Pu	Am	Cm	Bk	Cf	Es	Fm	Md	No	Lr
			1										**1(?)**	
	2		**2**	**2**	**2**	**2**	**2**	**2**	**2**	**2**	**2**	**2**	**2**	
3	**3**	**3**	**3**	**3**	**3**	**3**	**3**	**3**	**3**	**3**	**3**	**3**	**3**	**3**
	4	**4**	**4**	**4**	**4**	4	**4**	**4**	**4**	**4(?)**				
		5	**5**	**5**	**5**	**5**	**5(?)**		**5(?)**					
			6	**6**	**6**	**6**	**6(?)**							
				7	**7**	**7(?)**								
					8(?)									

This journal is © the Partner Organisations 2025

Open Access Article. Published on 10 juli 2025. Downloaded on 20-05-2026 01:21:34.
This article is licensed under a Creative Commons Attribution 3.0 Unported Licence.

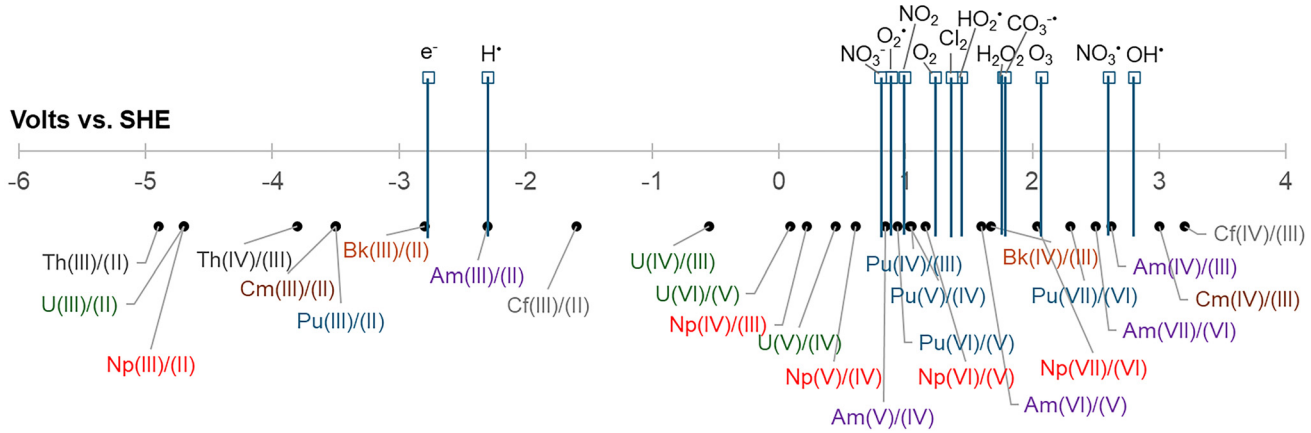

Fig. 3 Standard reduction potentials *versus* the Standard Hydrogen Electrode (SHE) for free radicals produced during the radiolysis of water and aqueous solutions of common solutes compared to the common oxidation states for the actinide elements under acidic conditions.[42]

dinate to additional ligands in solution to create an overall coordination number between 6–8. Given the limited evidence of the divalent and octavalent states, the coordination environments of these species are unknown. The An(IV)/An(III) and An(V)O_2^+/An(VI)O_2^{2+} redox couples are reversible, but the others are not, likely due to the barrier caused by the breakage/formation of the covalent actinyl bonds. Changes in standard redox couples and the overall chemical behavior of the actinides are observed in the presence of co-solutes and are also relevant to consider when evaluating how these cations will interact with free radicals produced during water radiolysis.

4.3. Actinide interactions with aqueous radiolysis products and common solutes

Adding actinide cations to aqueous solutions adds additional complexity to the cascade of radiation-induced processes discussed thus far, resulting in deviations in the expected chemical behavior. In the current section, we summarize the existing state of knowledge regarding the irradiation of actinide-containing aqueous solutions and highlight key inorganic chemistry drivers that may be important to consider in these systems. To support these efforts, we have also created a series of tables (ESI, Tables S1–S22†) that summarizes the previously reported radiation results for actinide elements Th–Cf in aqueous solutions. These tables consolidate information regarding experimental conditions (*i.e.*, solutes, actinide concentration, and pH) and oxidation state changes of the actinide cations before and after irradiation to provide a clearer picture of the experimental conditions that have previously been reported in the literature. This review does not include discussions of Ac, Pa, or Es through Lr due to the limited information on the inorganic chemistry and irradiation of these species—opportunities for future study!

4.3.1. Hydrated electron (e_{aq}^-). The e_{aq}^- is a powerful reducing agent (E° = −2.77 V) capable of participating in single-electron reduction reactions with actinide ions in aqueous media.[46] Reduction by the e_{aq}^- is considered an elementary process, meaning that an intermediate actinide species does not form prior to the reduction process. An important consideration for inorganic actinide chemists is that the e_{aq}^- can reduce actinide ions traditionally considered stable in aqueous media, such as Th(IV) and Cm(III). Th(IV) has a calculated E°_{red} ranging from −2.09 to −2.36 V for its hydrated monomeric form, which means that the e_{aq}^- is capable of reducing Th(IV) to Th(III).[47,48] Electron pulse radiolysis of Cm(III), a species which is predominantly present as a trivalent ion in aqueous solution, has resulted in its transient reduction to Cm(II).[49] Although this species re-oxidized within approximately 20 μs, one could envisage that under constant irradiation in a system that favored the formation of the e_{aq}^-, a small steady-state concentration of Cm(II) could be established. Morss reported an E°_{red} of −3.7 V for the Cm(III)/Cm(II) couple in 1994,[50] which is significantly larger than the reducing potential of the e_{aq}^- at −2.77 V. However, Mikheev *et al.* reported a Cm(III)/Cm(II) E°_{red} of −2.78 V,[51] indicating that reduction is thermodynamically feasible, but the resulting Cm(II) would be ultimately unstable under these conditions, aligning with the findings from pulse radiolysis.[49] The curium study highlighted that validation of standard reduction potentials under a range of chemical conditions, particularly for the transuranic elements, is needed to provide better predictive capabilities for redox properties of the actinides elements subjected to ionizing radiation.

When considering the impact of the e_{aq}^-, pH and coordination environment of the actinide ion must be considered because redox properties are predicted to vary with metal hydrolysis and speciation. As mentioned above, Th(IV) has a calculated standard reduction potential ranging from −2.09 to −2.36 V for its hydrated monomeric form.[47,48] When factoring in hydrolysis, the standard reduction potential for the hydrolyzed forms of Th(IV)—

Open Access Article. Published on 10 juli 2025. Downloaded on 20-05-2026 01:21:34.
This article is licensed under a Creative Commons Attribution 3.0 Unported Licence.

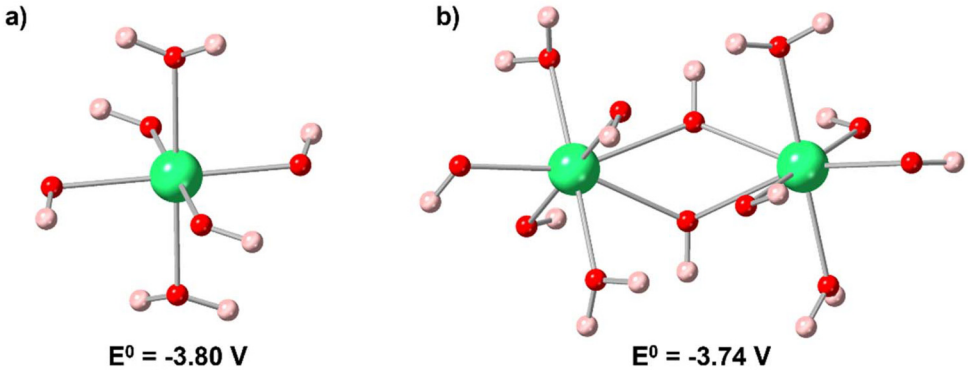

Fig. 4 Ball and stick models of (a) $Th(OH)_4(H_2O)_2$ and (b) $Th_2(OH)_8(H_2O)_4$ molecular hydrolysis products with their calculated reduction potentials. H, O, and Th atoms are colored pink, red, and green spheres, respectively.[48]

such as $Th(OH)_4(H_2O)_2$ and $Th_2(OH)_8(H_2O)_4$—shifts to −3.80 and −3.74 V, respectively[52] (Fig. 4), where the former is a monomer and the latter is a dimeric species. This shift suggests that actinide hydrolysis products may be less reactive towards the e_{aq}^-, although this is yet to be explored experimentally. Similar considerations need to be made beyond Th(IV), as other tetravalent actinides readily undergo hydrolysis. For example, Np(V) is reduced to Np(IV) by the e_{aq}^-, and further reduction to Np(III) can occur under acidic condition.[53] However, in neutral or basic conditions, the formation of a trivalent species may be limited because the resulting hydrolysis product, $Np(OH)_4$, may be less prone to subsequent reduction.[54]

While interactions between actinide ions and the e_{aq}^- clearly demonstrate that reduction will take place, the lifetime of the reduced species is variable and strongly dependent on the chemical environment. Nenoff *et al.*[55] reported that the γ-irradiation of U(VI) in acidic media results in the formation of U(IV) as UO_2 nanoparticles. In this case, the one-electron reduction of U(VI) by the e_{aq}^- forms U(V), which is unstable in aqueous solution. The resulting U(V) rapidly disproportionates into U(IV) and U(VI), cascading the reduction process. This chemistry demonstrates the dynamic nature of these irradiated redox active systems and how subtle differences in chemical environment can influence the long-term behavior actinides.

4.3.2. Hydrogen radical ($H^\bullet$). The $H^\bullet$ is another strongly reducing ($E^\circ = -2.3$ V) water radiolysis product generated by a combination of excited state water (H_2O^*) fragmentation (reaction (4)) and protonation of the e_{aq}^- (reaction (5)):[56]

$$H_2O* \rightarrow H^\bullet + {}^\bullet OH, \quad (4)$$

$$e_{aq}^- + H_{aq}^+ \rightarrow H^\bullet \; pK_a = 9.6. \quad (5)$$

Consequently, the yield and availability of the $H^\bullet$ for reaction with actinide ions is tied directly to the acidity of the solution (number of free protons). Therefore, $H^\bullet$-mediated reduction reactions are less likely in basic pH media. Under acidic conditions, the $H^\bullet$ has been shown to reduce several actinide ions and oxidation states[46] at rates typically one-to-two orders of magnitude slower than by the e_{aq}^-, which is consistent with their fundamental differences in chemical reactivity and respective redox potentials. Reduction of an actinide ion by the $H^\bullet$ has been postulated to occur *via* an inner-sphere mechanism in which the $H^\bullet$ adds to a coordinated water molecule, forming the hydronium radical ($H_3O^\bullet$). This species then undergoes an electron transfer with the metal ion center to generate the hydronium ion (H_3O^+), as shown in Scheme 1.[57]

Similar to the e_{aq}^--mediated reduction, the long-term stability of $H^\bullet$ reduced actinide species is dependent on the overall chemical environment. For example, the reduction of Cf(III) to Cf(II) by the $H^\bullet$ radical[45] resulted in the reoxidation back to Cf (III) within the μs timeframe.[45] Metal ion reduction can induce disproportionation reactions as Saini *et al.*[58] observed for the γ-radiation of U(IV). The initially formed U(V) further transforms into a mixture of U(IV) and U(VI). Similarly, interactions with the $H^\bullet$ reduces Am(V) to Am(IV)[59] but can also cause disproportionation to Am(IV) and Am(VI).[44] It is worth noting that all of the examples described above include the presence of $HClO_4$ as a co-solute, providing excess H_{aq}^+ to increase $G(H^\bullet)$ from water radiolysis. Yet, the presence of co-solutes (described in more detail in section 4.3.6) further complicates the underlying chemistry (*e.g.*, generation of $ClO_4^\bullet$ and $ClO_3^\bullet$ radicals, section 4.3.6), which must also be considered beyond

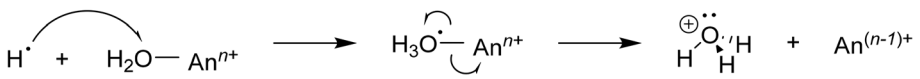

Scheme 1 Proposed mechanism describing the redox process for $H^\bullet$-mediated actinide ion (An^{n+}) reduction.[57]

This journal is © the Partner Organisations 2025

Open Access Article. Published on 10 juli 2025. Downloaded on 20-05-2026 01:21:34.
This article is licensed under a Creative Commons Attribution 3.0 Unported Licence.

the primary products of water radiolysis. Therefore, the discussed studies may not solely reflect H$^{\bullet}$ chemistry, but other radical-driven processes as well.

Interestingly, unlike the e_{aq}^{-}, the H$^{\bullet}$ has been shown to oxidize the trivalent oxidation states of Np and Pu.[60,61] This unusual behavior is likely driven by the more negative standard reduction potentials of Np(III) and Pu(III), −2.83 and −2.79 V, respectively.[52] This observation adds an additional layer of redox complexity to multivalent irradiated actinide systems that needs further study.

4.3.3. Hydroxyl ($^{\bullet}$OH) and oxide anion ($O^{\bullet-}$) radicals. The $^{\bullet}$OH is the most important oxidizing radical ($E°$ = 2.8 V) produced by water radiolysis due to its persistence beyond the lifetime of the radiation track and has been shown to interact with a wide variety of chemicals.[62] This radical primarily exists in acidic to weakly basic media, whereas its deprotonated form ($O^{\bullet-}$, pK_a = 11.9) predominates under alkaline conditions.[57,62] In acidic environments, the $^{\bullet}$OH undergoes one-electron oxidation processes with the majority of the actinide elements and their oxidation states, even with those whose redox potentials would suggest otherwise (*e.g.*, Am(III), Cm(III), and Cf(III)).[63]

Two mechanisms for the $^{\bullet}$OH-mediated oxidation of trivalent actinides have been proposed and explored using experimental and computational techniques. The first mechanism, proposed by Berdnikov *et al.*,[64] occurs through a H-atom abstraction/electron transfer from a $^{\bullet}$OH in the second coordination sphere (Fig. 5a). Codorniu-Hernández and Kusalik[65] investigated this pathway in bulk solution using density functional theory (DFT)-based *ab initio* molecular dynamics methods, predicting a rapid three-step process: (1) preorganization of the [H_2O–OH]$^{\bullet}$ transition state with weakening of the O–H bonds in the ligated water; (2) formation of an $H_3O_2^{\bullet}$ molecule and subsequent electron transfer from the coordinated An^{3+} ion to the bonded radical species; and (3) electron transfer/H-atom abstraction resulting in the formation of free H_2O and coordinated OH^-. The second proposed mechanism is an inner-sphere process proposed by Golub *et al.*[66] In this mechanism, the $^{\bullet}$OH directly complexes to the actinide ion, leading to the rearrangement of the first coordination sphere (Fig. 5b). This rearrangement is followed by electron transfer from the metal center to $^{\bullet}$OH, elimination of OH^-, and a return to the original coordination environment. This proposed mechanism is supported in part by Lierse *et al.*,[67] who measured rate coefficients using transient conductivity pulse radiolysis experiments for Np(III), Cm(III), Bk(III), and Cf(III). The kinetic values were in good agreement with those predicted (~5×10^8 M^{-1} s^{-1}),[67] however, the Lierse *et al.* study is limited to nanosecond time resolution, which may not be fast enough to provide definitive evidence for distinguishing between the two mechanisms.

Oxidation of the early actinides (*i.e.*, U, Np, Pu, and Am) from their lower valence states to higher valence actinyl states (AnO_2^{n+}, n = 1 or 2) involves more than just a simple electron transfer. It requires the additional formation of two axial oxygen bonds, leading to reaction rates that are significantly slower—by orders of magnitude—compared to the oxidation of An(III) to An(IV).[66]

The penta- and hexavalent oxidation states form the actinyl moiety that can accommodate coordinating ligands in the

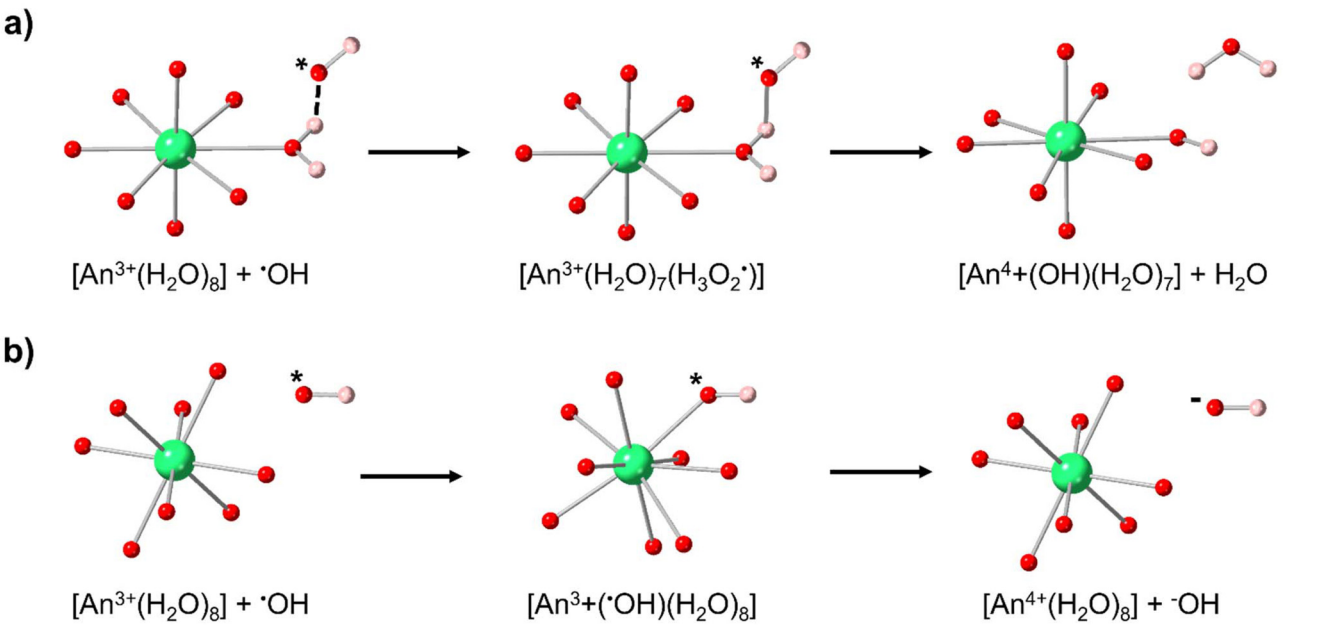

Fig. 5 Proposed $^{\bullet}$OH-mediated oxidation schemes for H-abstraction by $^{\bullet}$OH of the inner hydration shell of the actinides (a, outer sphere) and rearrangement of the inner hydration shell followed by a OH^- elimination (b, inner sphere). The * indicates a radical species and – indicates an anion. Actinides (An), O, and H are represented as green, red, and pink, respectively. Hydrogen atoms were omitted from the aqua ligands for clarity unless deprotonation is described. Adapted from Lierse *et al.*[68]

Open Access Article. Published on 10 juli 2025. Downloaded on 20-05-2026 01:21:34.
This article is licensed under a Creative Commons Attribution 3.0 Unported Licence.

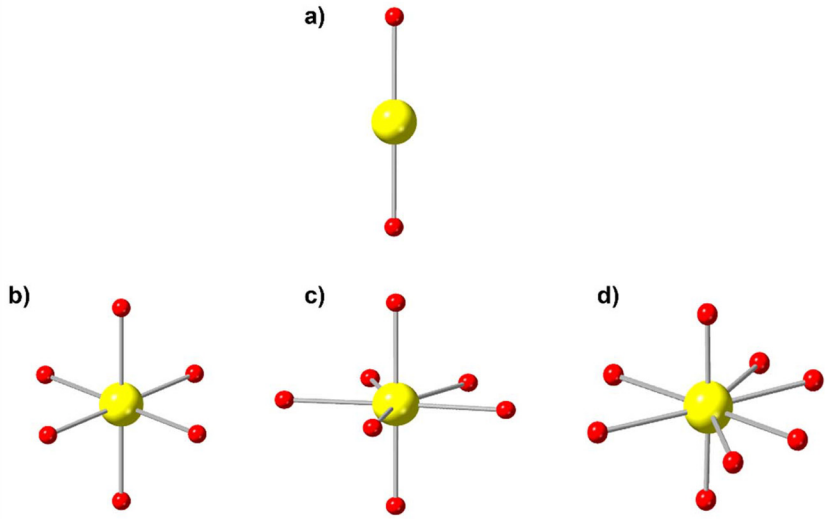

Fig. 6 Ball-and-stick models of the hexavalent and pentavalent (a) uranyl cation (UO_2^{2+}/UO_2^{+}) and potential geometries—(b) tetragonal, (c) pentagonal, and (d) hexagonal bipyramids—that are found in solution and solid-state materials. Adapted from Plášil.[70]

equatorial plane, adopting square, pentagonal, or hexagonal bipyramidal geometries, as illustrated in Fig. 6.[69] It is theoretically possible for the $^{\bullet}OH$ to coordinate through the equatorial plane as hydrolysis species are known in a wide range of compounds (Fig. 5).[71] U(VI) is known for binding strongly to OH^- and there is some evidence that $^{\bullet}OH$ can be complexed by U(VI) within peroxide clusters as reported by Lottes *et al.*[72] Formation of $^{\bullet}OH$ in this case is likely due to the breakdown of peroxide and may be enhanced by the formation of the molecular cluster. However, it is unclear if the $^{\bullet}OH$ or $O^{\bullet-}$ radicals can be captured within monomeric U(VI) species, $[UO_2(OH)_4]^{2-}$ (Fig. 7a). Further, it is unclear if stabilization can occur through bridging OH^- groups (Fig. 7b and c) or if weak interactions can induce the stabilization of these reactive species in solution.

As the available oxidation state increases to heptavalent for Np and Pu, there are additional considerations regarding interactions with $^{\bullet}OH$ or $O^{\bullet-}$ beyond metal redox processes. Gamma radiation can induce the formation of Np(VII), as evidenced when Pikaev *et al.*[73] irradiated alkaline solutions saturated with N_2O, and it can be chemically induced under basic conditions using ozone as the oxidant. Plutonium in alkaline conditions can also form the heptavalent state in the presence of oxidizing species, such as $O^{\bullet-}$.[57] While ozonolysis can create a variety of reactive oxygen species within the solution, a recent study by Kravchuk *et al.*[74] utilized DFT calculations to determine that $^{\bullet}OH$ is the most favorable oxidant under these conditions. Oxidation from Np(VI) to Np(VII) again requires a change in the coordination geometry from the initial $[Np(VI)O_2(OH)_4]^{2-}$ species found in basic conditions to the $[Np(VII)O_4(OH)_2]^{3-}$ species observed for the heptavalent state (Fig. 8). As described earlier, the reaction of $^{\bullet}OH$ with an actinide ion involves both H-abstraction and electron transfer. Kravchuk *et al.*[74] evaluated the energetics of the individual steps of this reaction. The $[Np(VI)O_2(OH)_4]^{2-}$ is more stable than the related $[Np(VI)O_2(O)(OH)_3]^{3-}$ suggesting that deprotonation may not be

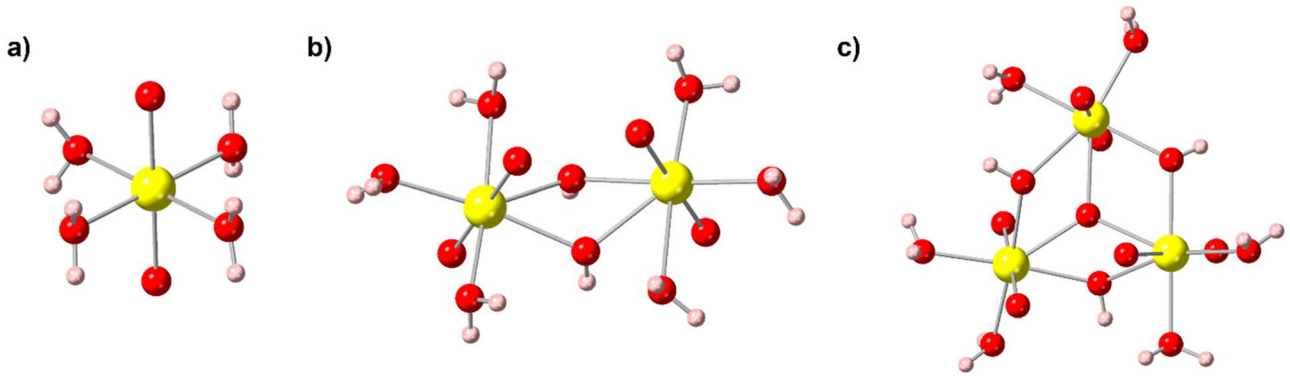

Fig. 7 Uranyl (UO_2^{2+}) complexes that can exist in aqueous solutions with hydroxide anions. (a) $[UO_2(H_2O)_4]^{2+}$, (b) $[UO_2(OH)_2(H_2O)_4]^{2+}$, and (c) $[UO_2(O)(OH)_3(H_2O)_4]^{+}$. U, O, and H are depicted as yellow, red, and pink spheres, respectively. Adapted from Quilès *et al.*[71]

 This journal is © the Partner Organisations 2025

Open Access Article. Published on 10 juli 2025. Downloaded on 20-05-2026 01:21:34.
This article is licensed under a Creative Commons Attribution 3.0 Unported Licence.

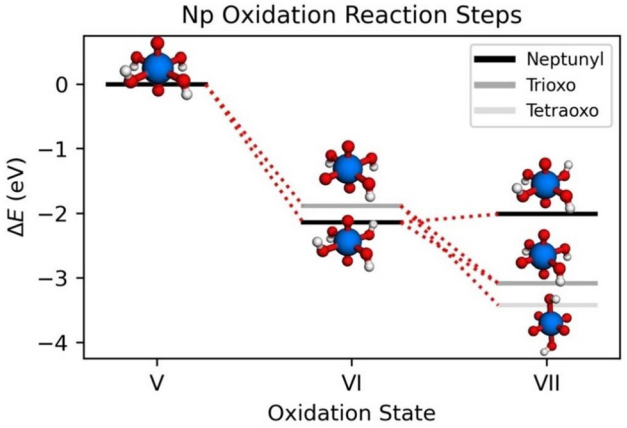

Fig. 8 Diagram describing the formation of a stable Np(VII) species from Np(V) oxidation under basic conditions that was originally proposed by Kravchuk *et al.*[74] The ˙OH was determined to be the most likely oxidant and two metastable Np(VI) complexes were identified before oxidation to the Np(VII) occurs. Np, O, and H are depicted as blue, red, and white spheres, respectively.

the first step in the reaction. Both Np(VII) forms ($[Np(VII)O_4(OH)_2]^{3-}$ and $[Np(VII)O_3(OH)_3]^{2-}$) are predicted to be more stable than the Np(VI) forms, indicating that the electron transfer and protonation steps may occur simultaneously as the initial step in the process. This process is then followed by a second deprotonation step to form the final $[Np(VII)O_4(OH)_2]^{3-}$ species. The caveat to this study is that it does not contain additional hydrogen bonding interactions as did the work performed by Codorniu-Hernández and Kusalik;[75] thus, additional theoretical studies could yield new insights into the electron and hydrogen transfer steps in these reactions.[65]

4.3.4. Oxygen radicals ($HO_2^{\bullet}$, $O_2^{\bullet-}$, and $O_3^{\bullet-}$). Formation of $HO_2^{\bullet}$ (E° = 1.44 V), $O_2^{\bullet-}$ (E° = 0.89 V), and $O_3^{\bullet-}$ (E° = 1.60 V) radicals occur upon the irradiation of oxygenated aqueous solutions, where the concentration of these species is dependent on the incident radiation and the media. In aerated solutions, the e_{aq}^- and H˙ react with dissolved O_2 to form $O_2^{\bullet-}$ and $HO_2^{\bullet}$, respectively.[57] The yields of $HO_2^{\bullet}$ and $O_2^{\bullet-}$ from heavy ion radiolysis are greatly increased due to intratrack reactions.[76] The $O_2^{\bullet-}$ reacts with H_2O (1.0×10^5 M^{-1} s^{-1}) to form O_2, HO_2^-, and OH^-.[77] In the presence of proton sources (*i.e.*, in acidic media), $O_2^{\bullet-}$ will disproportionate to form either H_2O and O_2 or protonate to $HO_2^{\bullet}$, but the lifetime of $O_2^{\bullet-}$ is prolonged with OH^- concentrations >1 M. The $O_3^{\bullet-}$ is said to form solely in basic media where $O^{\bullet-}$ reacts with O_2 but decays to form $O_2^{\bullet-}$ with a rate coefficient of 6.0×10^8 M^{-1} s^{-1}.

Due to the reactive nature of these radicals in aqueous solution, most radiation studies mention $HO_2^{\bullet}$, $O_2^{\bullet-}$, and $O_3^{\bullet-}$ in the context of intermediates for the formation of peroxides. The work by Gogolev *et al.*[78] evaluated the reactions of $O_2^{\bullet-}$ with Np(VI) and Np(VII) using pulse radiolysis, where they found no significant impacts to the oxidation state of either actinide ion. Both Np(VI) and Np(VII) were more susceptible to reduction by the e_{aq}^- rather than $O_2^{\bullet-}$. Similarly, ozonolysis is widely used by the actinide chemistry community to oxidize metal ions to higher valent states, but it is often other radical species such as ˙OH that are engaging in the oxidation process in radiolysis.

While there is limited information in the radiation chemistry literature on these species, there are a handful of studies from inorganic and physical chemists that evaluate interactions of $O_2^{\bullet-}$ and $HO_2^{\bullet}$ with actinide cations. Very little is known about their interactions with the tetravalent state, however, Meisel *et al.*[79] reported that a Th(IV)–$HO_2^{\bullet}$ exists in solution through use of EPR spectroscopy. Gibson *et al.* have explored gas phase Pu(V) chemistry, noting the formation of a [Pu(V)O_2(O_2)] complex through the decomposition of the oxalate starting material, which spontaneously oxidizes to [Pu(VII)O_4]$^-$.[80] During this process, $O_2^{\bullet-}$ reduces into two O^{2-} ions to create the tetroxide Pu(VI) species. This suggests that in the absence of ˙OH, $O_2^{\bullet-}$ can also engage in metal redox processes. More recently, there is evidence that $O_2^{\bullet-}$ can be stabilized both in solution and the solid-state when coordinated to U(VI). Scherrer *et al.*[81] recently demonstrated oxidation of O_2^{2-} to $O_2^{\bullet-}$ within U(VI) triperoxide solids. They observed $O_2^{\bullet-}$ EPR spectral feature two days after dissolution of potassium uranyl triperoxide. These findings were the first known report using EPR detection of $O_2^{\bullet-}$ stabilized in water at room temperature without the addition of a spin trapping agent. This suggests that the U(VI) cation can stabilize $O_2^{\bullet-}$, which may influence the ability of $O_2^{\bullet-}$ to engage in subsequent chemical reactivity. Recent work has probed such reactivity within the solid-state,[81] but additional studies are necessary to fully understand the bonding and reactivity of actinide superoxide complexes in ionizing radiation fields.

4.2.5. Hydrogen peroxide (H_2O_2, HO_2^-). Hydrogen peroxide (H_2O_2; E° = 0.88 V, pH 14) and its deprotonated form (HO_2^-, pK_a = 11.65)[82] are considered the more chemically stable species produced by the radiolysis of aqueous solutions.[83] Molecular radical species typically occur in higher yields with increasing LET, but H_2O_2 is produced by both γ- and α-irradiation of aqueous solution.[83] A majority of the H_2O_2 is produced within 1 μs following irradiation and its final steady-state concentrations is governed by e_{aq}^- and H˙ chemistry in the homogeneous phase of radiolysis.[84] Studies with γ-radiation have found negligible changes in H_2O_2 concentrations over a pH range of 5–9, while lower pH affords higher H_2O_2 yields due to the protonation of e_{aq}^- in H.[84] With high LET systems (>100 eV nm^{-1}), there was little-to-no change in the yield of H_2O_2 across the pH range of 3–10.[83–85]

Interactions between H_2O_2 and actinide ions can either result in oxidation or reduction of the metal center, depending on the conditions present and a given actinide oxidation state's redox potential (Fig. 3). While Th(IV) is unreactive towards H_2O_2, uranium(III,IV,V) readily undergoes one-electron oxidation reactions with H_2O_2.[66,86] These oxidations will result in the formation of $O_2^{\bullet-}$; thus, the chemistry of the latter must also be considered when exploring H_2O_2 chemistry. Shilov *et al.*[87] also explored the radiolysis of Np(V) in pure water and determined that the formation of H_2O_2 did not change its oxi-

Open Access Article. Published on 10 juli 2025. Downloaded on 20-05-2026 01:21:34.
This article is licensed under a Creative Commons Attribution 3.0 Unported Licence.

dation state under these conditions, but instead formed a neptunyl peroxo-complex.

Given the stability of H_2O_2 and HO_2^-, much of our knowledge on actinide redox behavior with peroxide comes from the direct addition of H_2O_2 to solution. Th(IV) remains stable in the presence of H_2O_2, but U(IV) and U(V) will oxidize to U(VI) species. Neptunium is more complex due to its variable redox behavior, with the resulting redox reactions being pH dependent. When Np(III) or Np(IV) are dissolved in acid and exposed to radiolysis products such as H_2O_2, the metal center oxidizes through a one-step oxidation process. However, Tananaev *et al.*[88] reported that Np(V) reduced to Np(IV) in 4.5 M HNO_3, but oxidized to Np(VI) when the concentration increased to 7.5 M. With Np(VI) and Np(VII), the presence of H_2O_2 formed from solvent radiolysis results in reduction to lower valent states under basic conditions in lithium hydroxide.[89] Similar complexities exist for plutonium, where Pu(III) in the presence of H_2O_2 will oxidize to Pu(IV) in strong acidic conditions, but Pu(IV) will reduce to Pu(III) under weakly acidic conditions.[90] Pu(VI) will form either Pu(V) or a mixed Pu(V)/Pu(VI) solution.[90,91] Interactions of HO_2^- with Am(IV) result in either the oxidation to Am(V) in HNO_3,[44] or Am(V) and Am(IV) peroxo-complexes in weakly acidic aqueous solutions.[92,93]

Peroxides tend to form complexes with actinide cations, but there is a limited understanding of these species for lower valent oxidation states. Trivalent actinides do not typically form peroxide complexes, likely due to redox instability, but Th(IV) and Pu(IV) peroxide complexes have previously been reported.[94–96] Only one Th(IV) peroxide coordination complex has been reported by Galley *et al.* that contains three Th(IV) cations linked through μ_2-peroxide bridges and capped by 2,2′,6′,2″-terpyridine and nitrate anions.[94] This sole complex could only be formed through the use of 40-year-old, unpurified ^{232}Th, which contained three orders of magnitude more disintegrations per second than fresh materials, resulting in radiolysis of the solution. Pu(IV) peroxo-complexes are postulated to form, including dimers ($[Pu_2(O_2)(OH)]^{5+}$ and $[Pu_2(O_2)_2]^{4+}$) (Fig. 9a and b), but the two structurally characterized Pu(IV) peroxo-dimers were formed in a carbonate solution ($K_8[Pu_2(\mu\text{-}\eta_2\text{-}\eta_2\text{-}O_2)_2(CO_3)_6]\cdot 12H_2O$)[95] and $Na_8[Pu_2(\mu\text{-}\eta_2\text{-}\eta_2\text{-}O_2)_2(CO_3)_6]\cdot 12H_2O$ (Fig. 9c).[97] These complexes contain two Pu(IV) cations bridged through μ_2:η^2-O_2 ligands and further bonded to six bidentate carbonate ligands.[95] A tetrameric $[Pu_4(O_2)_6(O)(H_2O)_{12}]_n^{2+}$ species (Fig. 9d) has also been suggested based upon spectroscopic evidence, but has yet to be structurally characterized using X-ray diffraction techniques.[96] Pu(IV) peroxide complexes have previously been noted to form within irradiation experiments and are important within the nuclear fuel cycle, so additional efforts are needed to understand these phases.

U(VI) peroxide chemistry is the most well-studied of the actinides outside of the radiation chemistry field and there are a range of complexes that can be formed depending on the pH. We refer the reader to review articles on U(VI) peroxides for a complete understanding of these complexes,[98,99] but highlight several important species herein. Upon α-radiolysis of water, the formation of uranyl peroxide complexes readily occur[100] and eventually lead to the precipitation of $[(UO_2)(O_2)(H_2O)_2]\cdot 2H_2O$ (studtite) under acidic conditions.[101] Using the direct addition of 30% H_2O_2 has led to a large range of struc-

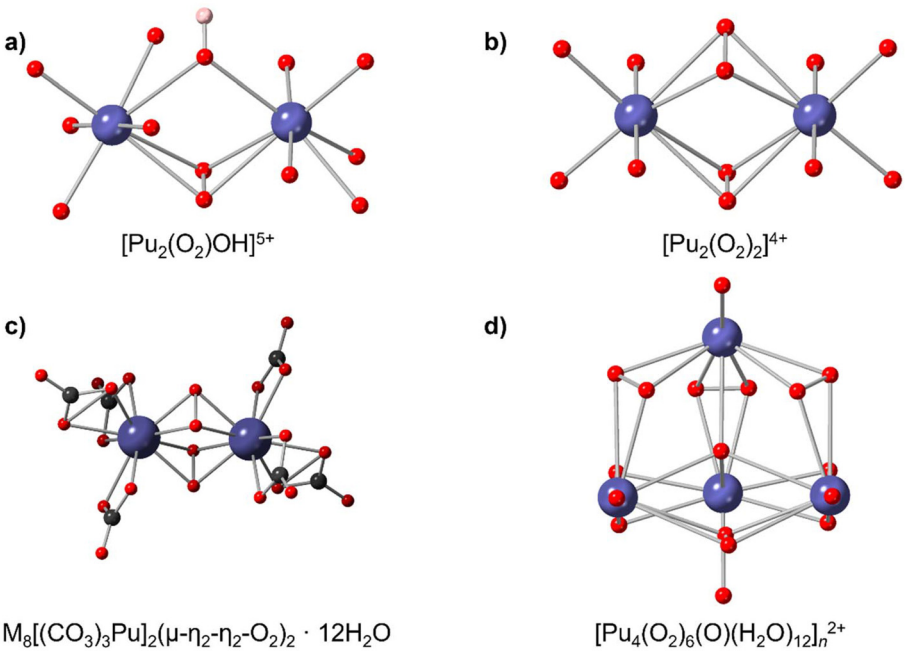

Fig. 9 Pu(IV) peroxo-complexes such as (a) $[Pu_2(O_2)(OH)]^{5+}$, (b) $[Pu_2(O_2)_2]^{4+}$, (c) $M_8[(CO_3)_3Pu]_2(\mu\text{-}\eta_2\text{-}\eta_2\text{-}O_2)_2\cdot 12H_2O$ (where M = K or Na), and (d) $[Pu_4(O_2)_6(O)(H_2O)_{12}]_n^{2+}$. Pu, O, C, and H are represented as purple, red, grey, and pink spheres, respectively. Hydrogens on aqua ligands, outer sphere waters molecules, and counter cations were omitted for clarity.[95–97]

 This journal is © the Partner Organisations 2025

Open Access Article. Published on 10 juli 2025. Downloaded on 20-05-2026 01:21:34.
This article is licensed under a Creative Commons Attribution 3.0 Unported Licence.

tural topologies, including the formation of uranyl peroxide coordination complexes,[102–104] sheets,[105] crowns,[106] bowls,[106] and spherical clusters.[98,107,108] Transformation from the monomeric coordination complexes $[(UO_2)(O_2)_3]^{4-}$ to the larger spherical clusters containing twenty-four U(VI) cations in $[((UO_2)(O_2)(OH))_{24}]^{24-}$ can occur through both the use of a transition metal catalyst (*e.g.*, Cu(II)) or with exposure to γ-radiation.[109] This alteration suggests that the mechanism is the degradation of bound peroxide into OH^- but warrants additional investigation.

Neptunyl peroxide complexes are also expected to occur for the pentavalent and hexavalent states, but their exact speciation is complicated because H_2O_2 can oxidize or reduce Np depending on the chemical conditions.[110–112] In both oxidation states, Np has been reported to form complexes with the peroxide ligand. For Np(V), there is some controversy over where stable peroxo-complexes form as it was originally postulated that the peroxo phase forms as a yellow-brown solution at high γ doses, but the exact oxidation state has not been definitively proven using spectroscopic techniques. Under acidic conditions, a fine precipitate forms but this has also not been conclusively linked to Np(V).[32] A mixed phase Np(V)/Np(VI) peroxide cluster has been reported, with the Np (V) potentially inhabiting the central position inside the spherical molecular cluster, but that again has not been supported spectroscopically.[113] A $[Np(VI)O_2(O_2)_3]^{4-}$ species has been crystallized in the presence of Ca(II) anions under highly basic conditions.[110] This species is isostructural to the U(VI) triperoxide phases, suggesting that the broad structural topology observed for U(VI) may also be observed for Np(VI) peroxide phases.

Higher valent plutonyl peroxides may also have importance although there is limited information about these species in solution. Reduction of Pu(VI) to Pu(IV) occurs quite readily under acidic conditions, but the reaction is influenced by acidity and temperature.[114,115] In this case, H_2O_2 causes the reduction of Pu(VI) to Pu(V) and the acidity determines the rate of disproportionation to form the Pu(IV) species. There is no evidence of a Pu(V) peroxide phase, but this may be due to instability of the complex in acidic media and needs further study. Nash *et al.*[116] noted the formation of a transient reddish-brown color when they added H_2O_2 to a 0.6 mM Pu(VI) stock under basic conditions, which they assumed to be a transient Pu(VI) peroxide phase based upon an absorption at 480 nm observed in the UV-Vis spectrum. They noted that the species undergoes reduction to Pu(V) over longer periods of time and that mixed valent Pu(V)/Pu(VI) peroxo-complexes may form upon aging.[117]

4.3.6 Impacts of co-solutes on the radiolysis of actinide cations. Aqueous solutions of actinides are often accompanied by co-solutes that can influence the range of radiolysis products available for reaction. These additional solutes or their radiation products can play a significant role in the overall chemistry of an irradiated actinide solution. The extent of co-solutes affecting the chemistry is dependent on competition kinetics; that is, the relative reactivity of the actinide or the co-solute with water radiolysis products. We will focus on co-solutes commonly used in the manipulation of actinide cations in solution, specifically NO_3^-, nitrite (NO_2^-), carbonate (CO_3^{2-}), sulfate (SO_4^{2-}), and halogen (X^-) anions.

4.3.6.1. Nitrate and nitrite. Actinide nitrates are widely used as precursors in basic science research and are ubiquitous in the reprocessing of UNF and the management of legacy waste.[118] The direct radiolysis of NO_3^-/HNO_3 solutions (reaction (6)) leads to formation of additional NO_2^-/HNO_2 and $NO_3^{\bullet}$.[119] The nitrate anion (NO_3^-) is an effective scavenger of the e_{aq}^- (reaction (7)), as well as the $H^{\bullet}$ atom to a lesser extent:[120]

$$HNO_3^- \rightsquigarrow e_{aq}^-, NO_3, HNO_2^{\bullet -}, \quad (6)$$

$$NO_3^- + e_{pre}^-/e_{aq}^- \rightarrow NO_3^{\bullet 2-}. \quad (7)$$

As a result, in the presence of NO_3^-, the reducing species from water radiolysis are transformed through a series of reactions (reactions (8)–(14)) into nitrogen dioxide ($NO_2^{\bullet}$), nitrite (NO_2^-), and nitrous acid (HNO_2):[36,121,122]

$$NO_3^- + H \rightarrow HNO_3^{\bullet -}. \quad (8)$$

$$NO_3^{\bullet 2-} + H_2O \rightarrow NO_2^{\bullet} + 2OH^-, \quad (9)$$

$$NO_3^{\bullet 2-} + H^+ \rightarrow HNO_3^-, \quad (10)$$

$$HNO_3^{\bullet -} \rightarrow NO_2^{\bullet} + OH^-, \quad (11)$$

$$NO_3^{\bullet 2-} + H_2O \rightarrow NO_2^{\bullet} + 2OH^-, \quad (12)$$

$$2NO_2^{\bullet} \rightleftharpoons N_2O_4, \quad (13)$$

$$N_2O_4 + H_2O \rightarrow HNO_3 + HNO_2. \quad (14)$$

Although less reducing than their precursors, these indirect NO_3^- radiolysis products participate in redox reactions with most actinide oxidation states.[123–125] For instance, HNO_2 has been shown to play a critical role in the radiation-induced redox chemistry of Np(VI), Pu(VI), and Am (VI) in concentrated HNO_3 solutions.[124–126] In concentrated HNO_3 solutions, there is a non-negligible amount of undissociated HNO_3 that can react with $^{\bullet}OH$ to produce the similarly oxidizing nitrate radical ($NO_3^{\bullet}$, E° = 2.30–2.60 V)[127] (reaction (15)):[128]

$$HNO_3 + {}^{\bullet}OH \rightarrow NO_3^{\bullet} + H_2O. \quad (15)$$

The $NO_3^{\bullet}$ radical has been demonstrated to be an integral part of the radiation-induced redox cycling of actinide oxidation states.

Though regarded as an oxidizer, neither Th(IV) nor U(VI) are reactive with $NO_3^{\bullet}$, but there is a model study that suggests U(IV) can be oxidized to U(V) in the presence of this species.[129] Although not directly impacting the actinide itself, a study by Boyle *et al.*[130] aimed to explore the role of the e_{aq}^- reducing an actinide cation but quickly discovered that the presence of minimal amounts of HNO_3 in solution in addition to that coordinated to the Th(IV) center impacted this chemistry. The

Open Access Article. Published on 10 juli 2025. Downloaded on 20-05-2026 01:21:34.
This article is licensed under a Creative Commons Attribution 3.0 Unported Licence.

radiolysis of Th(IV) nitrate solutions produced O_2, H_2, N_2, N_2O, and NO_2/N_2O_4.[130] However, no changes in the oxidation state distribution of thorium were reported, so the stability of the Th(IV) cation under these conditions remains unclear in terms of the e_{aq}^-. If the Th(IV) cation is stable in this scenario, it may be due to the presence of NO_3^-, which can more readily capture the e_{aq}^- to form $NO_3^{\bullet 2-}$, which decomposes into NO_2^-, creating oxidizing conditions. Previous work by Cook *et al.*[35] indicates that the strongly reducing $NO_3^{\bullet 2-}$ (E° = −1.1 V) persists in solution for no more than ~20 μs before converting into the oxidizing $NO_2^\bullet$. Therefore, the NO_3^- ligands coordinated to Th(IV) and in the solvation sphere may provide a shielding effect for the Th(IV) cation, but further research is needed to confirm this hypothesis. Therefore, coordination complexes used to enhance actinide solubility create a more complex environment where not only must one consider the effects of water radiolysis on the actinide, but also the additional formation of reactive species from the coordinated ligands, which can behave as a co-solute.

Though the early actinides have yet to be shown to be directly impacted by $NO_3^\bullet$, transuranic species have been experimentally reported to react with $NO_3^\bullet$. For a mixed Np(V)/Np(VI) system, Mincher *et al.*[41] and Shilov *et al.*[131] indicated that the oxidation of Np(V) to Np(VI) is due to $NO_3^\bullet$. In media containing HNO_3 or NO_3^-, Pu(III) was reported to oxidize to Pu(IV) regardless of aeration, doping with various gases, or left under ambient conditions.[132–134] HNO_3 solutions of Am(III) have been reported to oxidize to a mixture of Am(IV) and Am(V).[135,136] Asprey *et al.*[137,138] reported the oxidation of Am(III) to Am(VI). This oxidation likely occurs due to the interaction of $NO_3^\bullet$ with Am cations. In the case of Cm(III), a one-electron oxidation occurred in the presence of $NO_3^\bullet$,[49] which was also observed for Cf(III) in 6.0 M HNO_3.[45]

One of the challenges in understanding the redox behavior of these systems is the ingrowth of NO_2^- and how that may impact the resulting actinide redox behavior. This complexity is exemplified in the mixed Np(V)/Np(VI) system explored by Mincher *et al.*,[41] where after the initial oxidation to Np(VI), there was subsequent reduction to Np(V) at higher radiation doses. This reduction was linked to the formation of HNO_2 that influenced the overall redox distribution of the metal. This effect may also explain the behavior observed by Frolova *et al.*[139] where α-irradiation of Np(IV) at HNO_3 concentrations <1 M formed Np(V), while concentrations >1 M resulted in a mixture of oxidation states including (IV), (V), and (VI). Garaix *et al.*,[140] noted that the yields of HNO_2 increase with NO_3^- concentration until it reaches a plateau at HNO_3 concentration >2 M. Reduction has also been observed for Pu(VI)[141] and depends on the exact chemical conditions.[44,142] Interestingly, when the reactive species was $NO_2^\bullet$, the resulting optical spectra observed the formation of a mixture of both Pu(III) and Pu(V),[143] likely from the disproportionation of intermediate oxidation states.

Both NO_3^- and NO_2^- ligands can coordinate to actinide cations in solution, which has implications on interactions with the corresponding radical species. There is some evidence that a weak inner-sphere $Th(NO_3)^{3+}$ complex exists in 1 M NO_3^- solutions,[144] but for others it requires concentrations of 6 M NO_3^- or higher.[145] There are no experimental studies reporting Th(IV)–NO_2^- molecular species,[146] but there are suggestions that the NO_2^- complexes should be stronger than the corresponding NO_3^- species given that NO_2^- is a stronger base. A $Np(V)O_2NO_{2(aq)}$ species may exist, but the results were challenging as the $\log_{10}\beta$ was determined to be −0.05 ± 0.05.[145] Similarly, plutonium species are assumed to be negligible. This speciation data suggests that direct inner sphere interactions between actinide cations and $NO_3^\bullet$ or $NO_2^\bullet$ will be relatively insignificant, except when the actinide cations are in high acid concentrations. Thus, additional work in this area is needed to fully understand these interactions.

Vladimirova *et al.*[147,148] reported that the irradiation of Pu(VI) can form the intermediate excited-state Pu(VI)* species, which dimerizes with ground-state Pu(VI). These Pu(VI)*/Pu(VI) dimers are then reduced to Pu(V) in concentrated (>8 M) HNO_3. Plutonyl–NO_3^- complexes are understudied as there are only a handful of reports containing structural or spectroscopic characterization, but no dimeric species have been identified. Reilly *et al.*[149] isolated a hydrolyzed Pu(VI) dimer under basic conditions (Fig. 10) suggesting the potential speciation present in nitrate systems. In this case, the two Pu(VI) O_2^{2+} cations are connected through μ_2-OH bridges and surrounded by additional aqua ligands in the equatorial plane and may be similar to the species that could exist in the nitrate system. Maurice *et al.*[150] utilized DFT calculations to explore the nature of Pu(V/VI)–NO_3^- complexes created from electrospray ionization and noted that $[Pu(V)O_2(NO_3)_2]^-$ and $[Pu(VI)O_2(NO_3)_3]^-$ can be formed under these conditions. They also noted the formation of a $[Pu(VI)O_2(NO_3)_2(O)]^-$ can be created from the release of $NO_2^\bullet$ and is more favored than oxidation to a Pu(VII) phase.

Alpha particle irradiation of plutonium in HNO_3 has also been explored under a range of concentrations. Pu(III) can be stabilized in a solution that contains mixtures of $HNO_3/HNO_2/NO_2$, oxidized to Pu(IV) in 1 M HNO_3 or HNO_2, and form Pu(IV) peroxo-complexes or Pu(VI) in dilute (0.12 M) HNO_3 (Scheme 2). Andreichuk *et al.*[151,152] observed stabilization of Pu(IV) if the α-particle flux was kept below 0.3 Gy s^{-1} for several years; however, exceeding this dose rate resulted in a mixture of Pu(IV) and Pu(VI). They indicated that this oxidation at higher doses was due to the formation of $^\bullet OH$ and $NO_2^\bullet$ species, and that the

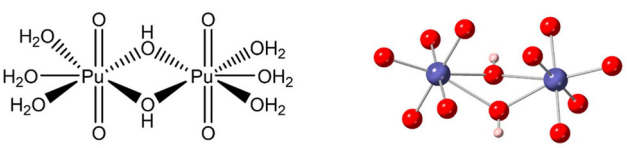

Fig. 10 Pu(VI) dimer $[Pu_2O_2(OH)_2(H_2O)_6]^{2+}$ observed experimentally in solution under basic conditions by Reilly *et al.*,[149] displayed as line (left) and ball and stick models (right). Hydrogens on aqua ligands were removed for clarity. H, O, and Pu atoms are depicted as pink, red, and purple spheres, respectively.

This journal is © the Partner Organisations 2025

Open Access Article. Published on 10 juli 2025. Downloaded on 20-05-2026 01:21:34.
This article is licensed under a Creative Commons Attribution 3.0 Unported Licence.

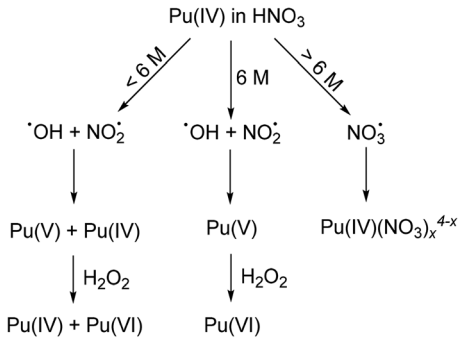

Scheme 2 Concentration dependence of α-particle irradiated HNO_3 solutions leads to the formation of Pu(IV), Pu(V), and/or Pu(VI).[151,152]

presence of H_2O_2 would reduce any higher-valent species in the system, resulting in mixed valence states.[151,152] If the dose rate remained below 4.6 Gy s^{-1} in 6 M HNO_3, the only product was Pu(VI), but once this concentration was exceeded Pu(IV)–NO_3^- complexes were observed in the solution.

An additional study by Vladimirova *et al.*[147,153] explored γ-irradiation of a mixed Pu(VI) and Np(VI) stock in HNO_3. Under all irradiation scenarios, Np(VI) was reduced to Np(V), but a dose >320 Gy was necessary for Pu(VI) to reduce to Pu(V). Vladimirova *et al.*[154] suggested the easier reduction of neptunium was due to Np(VI) having higher reduction rate coefficients with radiolysis products, allowing for the reduction of Np(VI) to Np(V) prior to the reduction of the Pu(VI) species. Initial stages were confirmed *via* kinetic modeling to support the reduction of Np(VI), but the model could not account for the reduction rates of Pu(VI), other than that the dependence of Pu(VI) retention relies on the concentration of Np(VI) and Pu(VI).

4.3.6.2. Carbonate. The carbonate radical ($CO_3^{\bullet-}$, E° = 1.78 V) is formed upon radiolysis of solutions containing carbonate (CO_3^{2-}) or hydrogen carbonate (HCO_3^-). Direct ionization of CO_3^{2-} and interactions with $^\bullet OH$ are described in reactions (16)–(18):[155,156]

$$CO_3^{2-} \rightsquigarrow CO_3^{\bullet-} + e_{aq}^-, \quad (16)$$

$$CO_3^{2-} + {}^\bullet OH \rightarrow CO_3^{\bullet-} + OH^-, \quad (17)$$

$$HCO_3^- + {}^\bullet OH \rightarrow CO_3^{\bullet-} + H_2O. \quad (18)$$

The formation of $CO_3^{\bullet-}$ through interactions with $O^{\bullet-}$ has been postulated, yet there is lack of experimental evidence that provides characteristic spectroscopic signatures associated with this species; therefore, a reaction scheme has yet to be reported involving $O^{\bullet-}$. Oxidation of actinide cations is predicted to occur upon interacting with $CO_3^{\bullet-}$ as it is known for being a strong one-electron oxidant, but the formation of e_{aq}^- may cause additional complexities in the redox behavior of the system.

The challenges with understanding the redox behavior of actinides in the presence of irradiated carbonate solutions is highlighted by studies with the neptunyl cation. Pikaev *et al.*[157] specifically noted oxidation of Np(V) to Np(VI) in $NaHCO_3$ after irradiation, but Np(V) in a Na_2CO_3 solution does not change valence states. In the case of Np(VI), reduction to Np(V) occurs in Na_2CO_3 but it remains stable in $NaHCO_3$. It has been suggested that the redox stability is related to the metal center being protected by the ligated carbonate anions in the molecular complex. Carbonate forms strong complexes with Np(V) and Np(VI), where $[Np(V/VI)O_2(CO_3)]^{-/0}$, $[Np(V/VI)O_2(CO_3)_2]^{3-/2-}$, and $[Np(VI)O_2(CO_3)_3]^{4-}$ are all possible, depending on pH and carbonate concentration.[158–166] However, the exact carbonate speciation has yet to be determined in these systems.

Similar redox behavior has been observed for the interactions between $CO_3^{\bullet-}$ and plutonium. Gogolev *et al.*[167,168] reported both the reduction and oxidation of a Pu(IV)–CO_3^{2-} complex to Pu(III) and Pu(V), but did not comment on the outcome. For low-valent species like Pu(III) and Pu(IV), the metal cations undergo a one-electron oxidation when exposed to $CO_3^{\bullet-}$.[53,169] Pu(IV) is predicted to form $[Pu(CO_3)]^{2+}$,[170] but Pu(IV) carbonatohydroxo complexes (reactions (19) and (20)) can also form because OH^- is a competitive ligand in these systems:

$$[PuO_2(H_2O)_x] + 2HCO_3^- \rightarrow [Pu(OH)_2(CO_3)_2]^{2-} + xH_2O, \quad (19)$$

$$[PuO_2(H_2O)_x] + 2CO_3^- \rightarrow [Pu(OH)_4(CO_3)_2]^{2-} + (x-2)H_2O, \quad (20)$$

$$2[PuO_2(CO_3)_3]^{5-} + 2CO_2 \rightleftharpoons [PuO_2(CO_3)_3]^{4-} + [Pu(CO_3)_5]^{6-}. \quad (21)$$

Pu(V) was noted to be stable within irradiated carbonate solution.[171] The stability of the Pu(V) state is interesting because $[Pu(V)(CO_3)_3]^{5-}$ generally occurs in equilibrium with its disproportionation species (reaction (21)).[172] This result suggests that potentially another Pu(V) carbonate species is responsible for the redox stability under these conditions.

4.3.6.3. Sulfate. Sulfate radical ions ($SO_4^{\bullet-}$, E° = 2.43 V)[173] are formed through the direct ionization of sulfate (SO_4^{2-}) (reaction (22)) or indirect interactions between SO_4^{2-} or hydrogen sulfate (HSO_4^-) with $^\bullet OH$, $^\bullet H$, and $HO_2^\bullet$ (reactions (23)–(26)).[174] In acidic media, the predominant species is HSO_4^-, yet in weakly acidic (pK_a = 1.9) or neutral conditions, the primary form present is SO_4^{2-}. There is, therefore, a concentration dependence for the formation of $SO_4^{\bullet-}$, where the starting reactant will lead to varying secondary radical species.[175]

$$SO_4^{2-} \rightsquigarrow SO_4^{\bullet-} + e_{aq}^-, \quad (22)$$

$$HSO_4^- \rightsquigarrow HSO_4^\bullet + e_{aq}^-, \quad (23)$$

$$H_2SO_4 \rightsquigarrow H_2SO_4^{\bullet+} + e_{aq}^-, \quad (24)$$

$$SO_4^{\bullet-} + H^+ \rightarrow SO_4^- + H^\bullet, \quad (25)$$

$$SO_4^{\bullet-} + H^\bullet \rightarrow HSO_4^-. \quad (26)$$

The presence of $SO_4^{\bullet-}$ in most systems will lead to oxidation of the actinide cation. For example, $SO_4^{\bullet-}$ reacts with U(IV)[176] and U(V)[177] to induce a one-step oxidation. Similarly, Np(III), Np(IV), and Np(V) are all readily oxidized by $SO_4^{\bullet-}$.[157,169,178–181] In H_2SO_4, the generated $SO_4^{\bullet-}$ has been shown to oxidize both Pu(III) and Pu(IV) to Pu(IV) and Pu(V), respectively.[132,169]

Open Access Article. Published on 10 juli 2025. Downloaded on 20-05-2026 01:21:34.
This article is licensed under a Creative Commons Attribution 3.0 Unported Licence.

Similarly, Am(III) and Cf(III) react with $SO_4^{\bullet-}$, to form their respective tetravalent species.[57] These experimental results were collected by pulse radiolysis studies and the steady-state species were not reported. It is important to evaluate the longer timescales consequences of $SO_4^{\bullet-}$ chemistry (*i.e.*, steady-state conditions) to provide additional information regarding the persistence of non-equilibrium actinide species and complexes in radiation environments, such as monomeric cations, hydrolyzed species, or sulfate complexes.

Sulfate radicals may play a secondary role in the redox behavior of the actinides when other radicals are present in the system. While α-particle irradiation of U(IV) in neat H_2SO_4 results in a one-electron oxidation, U(IV) is stabilized in a mixed $H_2SO_4/HClO_4$ solution.[32,58] The importance of $HClO_4$ in the mixture was not discussed, but reactive species formed from $HClO_4$ may interact with water radiolysis products or $SO_4^{\bullet-}$, preventing further oxidation from taking place. In addition, the presence of O_2 in the solution may also drive the redox chemistry in irradiated sulfate solutions. Boyle *et al.*,[182] determined that in O_2 saturated systems, U(IV) is oxidized but subsequently undergoes a one-electron reduction step. The valence state remained unchanged in deaerated systems, suggesting the oxidation of U(IV) to U(VI) may be driven by $^{\bullet}OH$ and $HO_2^{\bullet}$, and at a later stage U(VI) is reduced back to U(IV) by the e_{aq}^-. More systematic studies are necessary to elucidate the mechanisms that prohibit or enhance radical formation and what controls the metal redox behavior in SO_4^{2-} containing actinide solutions.

With more redox active actinide cations, like plutonium, irradiation of SO_4^{2-} containing solutions leads to complex behavior. When a mixture of Pu(V) and Pu(VI) or pure Pu(VI) was irradiated in H_2SO_4, it resulted in the reduction of both species to Pu(IV).[141] Molecular complexes have been identified by Wilson *et al.* including $[Pu(SO_4H)]^{3+}$, $[Pu(SO_4)]^{2+}$, and $[Pu(SO_4)_2]$,[183] and it was determined that bidentate coordination of the sulfate to Pu(IV) is more thermodynamically favorable than the monodentate form.[183]

4.3.6.4. Halogens. Dihalogen radical anions ($X_2^{\bullet-}$) are well-known oxidants that can be formed by irradiating halide-containing solutions, although they are typically less oxidizing than $SO_4^{\bullet-}$. Monoatomic halide radicals ($X^{\bullet}$) are also formed upon radiolysis of halogen-containing solutions,[184] but nothing has been reported on their interaction with actinide cations. When $HClO_4$ is present in solution, both $ClO_4^{\bullet}$ and $ClO_3^{\bullet}$ radicals can be formed (reaction (27)):[185]

$$ClO_4^- \rightsquigarrow e_{aq}^-, ClO_4^{\bullet}, ClO_3^-, ClO_3^{\bullet}, O^{\bullet-}, O(^3P), \quad (27)$$

in addition to other reactive species such as e_{aq}^-, $O^{\bullet-}$, and $O^{\bullet}$.[180]

The interactions between $X_2^{\bullet-}$—specifically $Cl_2^{\bullet-}$, $Br_2^{\bullet-}$, and $I_2^{\bullet-}$—and actinide cations have been investigated in acidic media using pulse radiolysis. In $HClO_4$, $X_2^{\bullet-}$ species oxidized U(III) to U(IV), while $Cl_2^{\bullet-}$ generated from irradiated NaCl and HCl led to the one-electron oxidation of U(V) to U(VI).[138,181] U(III) and U(IV) irradiated in both aerated and deaerated HCl resulted in the oxidation of each species,[32] likely due to the formation of $Cl_2^{\bullet-}$ from the media. One-electron $X_2^{\bullet-}$ mediated oxidations have also been reported for Np(III), Np(V), Pu(III), Am(III), and Cf(III).[32,128,181,186]

Both reduction and oxidation of the actinide cations can be observed in $HClO_4$ solutions depending on experimental conditions. In dilute $HClO_4$ (<1 M), Np(IV) oxidizes to Np(V)[187] with α-particles and at higher concentrations (>1 M), Np(IV) can be converted to Np(VI). In solutions containing both Pu(III) and Pu(IV) in $HClO_4$, the product contained only Pu(III);[141] thus, the Pu(IV) was reduced under these conditions. In samples containing Pu(IV) in concentrated $HClO_4$, both Pu(III) and Pu(VI) was observed and the formation of Pu(VI) peroxo-complexes were suggested to form in solution.[141] When Pu(V) in $LiClO_4$ was irradiated with α-particles, Pu(V) disproportionated into Pu(IV) and Pu(VI) and led to the formation of insoluble Pu(IV) colloids formed from Pu(IV) hydrolysis.[188] Frolov *et al.*[189] observed similar behavior when Am(III) and Cm(III) were placed in a saturated solution of $NaClO_4$ where Am(V), Am(III) hydroxides, and Cm(III) hydroxides formed upon α-particle radiolysis. The only clean reduction reaction reported in halogen systems is that by Zielen *et al.*,[190] where α-particle radiolysis of Np(VI) in $HClO_4$ of varying concentrations reduced to Np(V).

In general, halogens form weak interactions with the actinide elements, with the F^- anion being the exception.[188,191] Actinide speciation in $HClO_4$ media is dominated by aqua complexes because of weak interactions with the ClO_4^- anion, meaning that the previously reported studies are representative of those complexes.[189] This result is likely why the Pu(V) reduction to Pu(IV) in $LiClO_4$ [141] and studies on Am(III) and Cm(III) in $NaClO_4$ [189] enabled hydrolysis and formation of colloidal particles.[188] Similarly, in HCl, HBr, and HI, the X^- concentrations reach several molar before the halogen anions can complex with the actinide cation.[192] Fluoride is the only halogen that binds strongly to the actinide and forms stable complexes under dilute solutions; however, there are no studies exploring the irradiation of these solutions in the current literature.[193]

5. Solid-state chemistry

Irradiation of compounds in the solid-state provides atomistic-level perspectives on defects and changes in materials when exposed to radiation. Diffusion is hindered in the solid state, so irradiation of these materials gives an understanding of their initial decomposition due to direct radiation effects. Moreover, a thorough understanding the behavior of actinides in ionizing radiation fields relevant to nuclear fuel is a high priority for their safe and effective storage. Solid nuclear fuel materials are subjected to extreme conditions[3] such as high radiation, high temperatures and aggressive media like strong acids that promote corrosion processes. Corrosion of UNF presents significant long-term risks for their storage and sequestration from the environment.[194,195] While the development of radiation-resistant solid materials remains of interest for the

 This journal is © the Partner Organisations 2025

Open Access Article. Published on 10 juli 2025. Downloaded on 20-05-2026 01:21:34.
This article is licensed under a Creative Commons Attribution 3.0 Unported Licence.

disposal of UNF, it is crucial to determine what risks may be present following irradiation of the actinides to mitigate the release of potentially harmful radioactive materials in the environment.[196] Therefore, understanding the behavior of solid-state actinides, specifically in terms of the metal center and complexes formed, following exposure to ionizing radiation is crucial in determining what risks may arise after a breach of UNF containment vessels.

Herein, we highlight the current state of radiation research on solid-state materials and discuss the impact of radiation fields on redox behavior, metal complexation, and changes to the crystalline lattice. The solid-state chemistry covered in this review will be limited to inorganic crystalline materials and MOFs, which have previously reported structural characterization or detailed atomistic-level understanding. Glasses and ceramics will only be briefly summarized, as there are several high-quality reviews dedicated to these materials in the literature.[10,11,197–199] Again, we provide a summary of the studies that explored the irradiation of actinide-bearing solid materials in the ESI section, Tables S23–S26.†

5.1. Brief summary of glasses and ceramics

Glasses remain a high priority for the long-term disposal of actinide-bearing nuclear materials where the elements of concern have half-lives in the thousands to millions of years.[11] Transforming liquid waste into a glass product is termed *vitrification* and this process has the potential to immobilize problematic radionuclides, while minimizing the space required for storage relative to liquid waste forms. However, studies have unveiled that both intense short-term and prolonged radiation exposure lead to decomposition of the glass and induce bubble formations from ionization-driven radiolytic processes.[10] Additionally, microfracturing can take place (viewable by optical microscopy) after prolonged radiation exposure and decay events within glasses,[10] which is problematic because it increases the surface area within the material and results in leaching of the radionuclide from the wasteform.[200] For a more in-depth assessment of glasses, we refer readers to Gin *et al.*,[198] who has provided an extensive review discussing factors that can be considered to rationally design durable materials for long-term nuclear waste storage.

Ceramics have been investigated as host materials to immobilize actinides in high-level nuclear waste due to their ability to withstand significant radiation damage, but there are notable defects that occur within this group of solids. In ceramics (*e.g.*, apatite, perovskite, pyrochlore/fluorite, zircon, and zirconolite structure types),[201] the most typical defects resulting from irradiation of solid-state materials is an anion vacancy or F-center (also called a color center), which is caused by a free electron inhabiting a void space in the lattice (Fig. 11).[202] Formation of F-centers result in a color change due to band gap filling; thus, optical spectroscopy is an excellent tool for this subset of materials.[203] Within metal–oxide crystals it is typical to observe F_s-centers (F-centers isolated on the surface), which have smaller transition energies than a traditional F-center and usually form on the surface of the material.[204] These defects can quickly deteriorate under ambient conditions *via* the adsorption of oxygen or by thermal induced escape of the electron from the trapped site. The other class of defects that are common among radiation studies are Frenkel defects, where the smaller ion, typically the cation, leaves its position in the crystalline lattice, thus creating a vacancy, then relocates in a nearby site becoming an interstitial cation. The formation of both the vacancy and interstitial cation is often denoted as a Frenkel pair.[205] Some defects produced from ionizing radiation exposure can be annealed, ultimately reversing the observed radical formation and damage. One study by Griffiths *et al.*[206] reported that additional impurities imbedded within the material can lead to a variety of defects and those impurities (*i.e.*, Pb), observed oxidation state changes that further perturb the equilibrium in the lattice.

While ceramics, like many insulators, are considered relatively impervious to radiation damage, the crystalline materials eventually become amorphous upon radiation exposure (whether externally or internally generated). Amorphization is typically accompanied by swelling (increased material volume), increase in tensile strength, and higher levels of leachability for the actinide immobilized within the ceramic (rates on

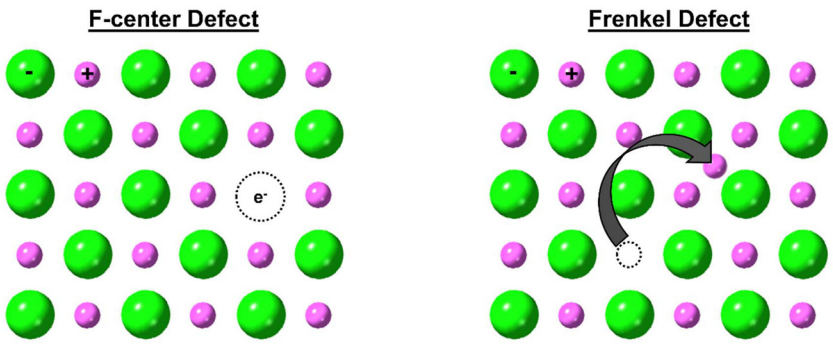

Fig. 11 Model of F-center defects (left) and Frenkel defects (right) in the solid-state. Cation and anions are represented by pink and green spheres, respectively, whereas the dashed circle represents a vacancy site. Adapted from Leitner *et al.*[202]

Open Access Article. Published on 10 juli 2025. Downloaded on 20-05-2026 01:21:34.
This article is licensed under a Creative Commons Attribution 3.0 Unported Licence.

average increase by factors of 10–100).[207] For a more detailed review regarding physical changes in ceramics upon irradiation, comprehensive reviews have been provided by Weber *et al.*,[208] Thomé *et al.*,[199] and Tracy *et al.*[209]

Though previous literature provides insightful findings regarding macroscopic effects and lattice expansion, few studies report atomistic-level details such as vibrational mode changes or radical formation from experimental spectra. Thus, the next sections focus on atomistic-level details—those beyond physical changes discussed *vide supra*—to understand the chemistry associated with changes upon irradiation.

5.2. Metallic and intermetallic materials

Metals exhibit varying degrees of radiation resistance, influenced by their atomic structure, alloy composition, and microstructural characteristics. In general exposure to ionizing radiation can harden a metal as atoms are moved from their original site within the crystallographic lattice, forming defects and dislocations. This hardening process strengthens the material at the same time it embrittles it, resulting in a loss of ductility. Within intermetallic or alloys, exposure to radiation can lead to atom diffusion and segregation, creating phase separations and voids. The formation of defects and voids can also impact the behavior of electrons and phonons in the system, increasing electrical resistivity and thermal conductivity. Similarly, semiconducting materials can display both transient and permanent changes upon exposure to ionizing radiation due to the formation of charge carriers.[210] These charge carriers can temporarily increase the conductivity but will lead to permanent failure of the semiconducting material when they are accumulated or trapped within defects or vacancies.

Irradiation of metallic and intermetallic phases have only been studied for Pu-based compounds. This compilation includes pure γ-Pu and group 13 intermetallics ($PuAl_2$, $PuGa_3$, $PuCoGa_5$, $PuCoIn_5$, $PuPt_2In_7$, and Pu_2PtGa_8).[211] As an α-emitter, Pu decay creates radiation-induced swelling in materials where the recoil energy and ballistic effects from the daughter products and the emitted α-particles cause damage to the lattice. These energetic events cause displacement of the atoms and ultimately lead to the formation of Frenkel pairs, vacancies, and self-interstitials (Fig. 12). These 0-D defects can then lead to 1-D defects, such as grain boundaries and lattice dislocations, resulting in macroscopic swelling and formation of voids.[212–214]

5.3. Oxides

Radiation effects in oxide materials are the most well studied solid state actinides due to the importance of these compounds for the nuclear fuel cycle. More specifically, the major focus is on the AnO_2 *fcc*-fluorite structure due to the use of UO_2 in light water power reactors and the impacts of γ-rays, α-particles, and heavy-ion bombardment.[215,216] However, the total number of studies for this group of compounds is quite limited, indicating that there are significant areas for continued discovery and advancement.

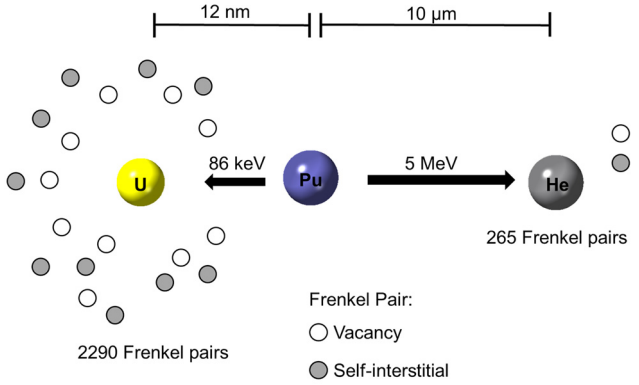

Fig. 12 Representation of Frenkel defect formation in δ-Pu. Adapted from Wolfer.[212]

Several studies have explored the optical spectroscopy associated with ThO_2 to better understand the nature of swelling that occurs upon irradiation. Upon γ-rays and ion beam irradiation, the starting material mainly remains intact; however, F-centers are created upon the formation of oxygen vacancies (V_O).[21,217–220] The presence of V_O sites can further perturb the lattice, creating dislocation loops and Frenkel defects from the Th(IV) cation shifting into an interstitial position and leaving behind a second lattice vacancy (Fig. 13).[221,222] These shifts from equilibrium positions in the lattice can then lead to volume expansions, thus explaining the swelling observed in ThO_2. Dennett *et al.*[223] further characterized this process for H^+-irradiation using spectroscopic techniques, observing the formation of ThO_{2-x}, ThO_{2+x}, and Th_4O_9 on the surface of ThO_2, further emphasizing the necessity to use both surface and bulk characterization techniques to understand the full effects of radiation exposure.

UO_2 has been investigated with a multitude of techniques, such as PXRD and Raman spectroscopy, which provide additional information into the formation of point defects that then grow into dislocation loops and lines upon dual ion beam irradiation.[225] Formation of dislocation loops and lines are further supported by Beauvy *et al.*[226] using UV-Vis-NIR spectroscopy they demonstrated that these defects are due to the oxidation of U(IV) to U(V) and the formation of V_O sites within the lattice. These point defects perturb the lattice and eventually lead to higher-dimensional defects. Guimbretière *et al.*[227] explored the effects of He^{2+} ion beam and internal α-particle irradiation using ^{239}Pu on UO_2 using Raman spectroscopy, where they observed a blue shift in the original T_{2g} peak and the ingrowth of additional peaks at higher wavenumbers associated with UO_{2+x} and U_4O_9. The presence of these phases supports the formation of V_O sites within the lattice and the oxidation of the U(VI) cation within these materials.

When Am(III) was incorporated as the internal α-particle source in UO_2, partial oxidation of both U and Am to U(V) and Am(IV) was observed regardless of the atmospheric conditions.[228,229] The use of an internal source provides criti-

 This journal is © the Partner Organisations 2025

Open Access Article. Published on 10 juli 2025. Downloaded on 20-05-2026 01:21:34.
This article is licensed under a Creative Commons Attribution 3.0 Unported Licence.

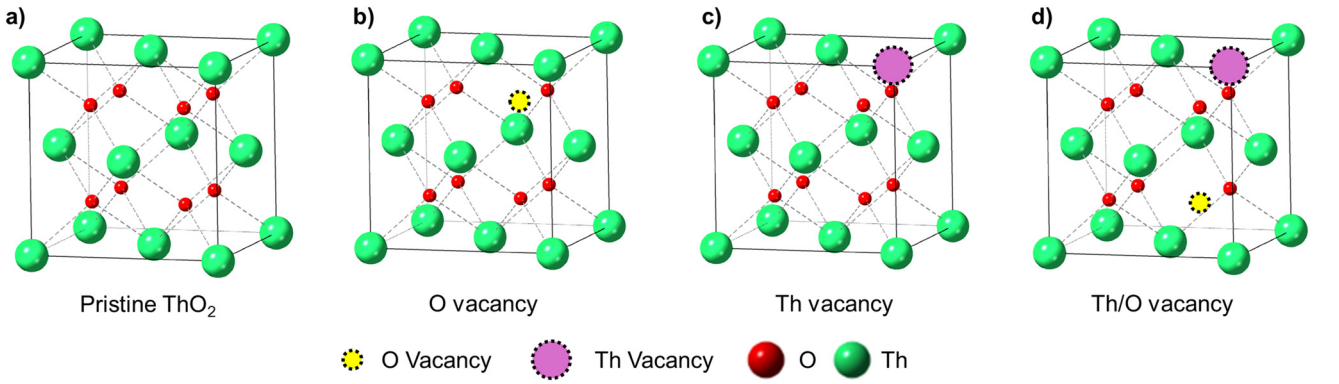

Fig. 13 Modified figure from Park *et al.*,[224] shows (a) the pristine ThO_2 unit cell. Radiation can result in the formation of a (b) F-center defect that can perturb the lattice to creat (c) Frenkel defects. These disruptions to the lattice can create (d) dislocation loops.

cal evaluation of materials that undergo constant irradiation by showing the long-term effects of prolonged exposure. As such, U(IV) typically oxidizes to U(VI); however, the incorporation of Am(III) into UO_2 results in the formation of U(V). It is also noted by Prieur *et al.*[229] that when U(V) is present in a mixed oxide with Am(III), the local environment around the U cation is perturbed, establishing new lattice equilibria to accommodate for the change in cation size, and suggests that U(V) becomes the preferred oxidation state in the material.

While oxidation of U(IV) is widely reported, only one study indicated that U(VI) oxides/oxyhydroxide phases are reduced to the tetravalent state. Tracy *et al.*[21] indicated that heavy-ion bombardment of γ-UO_3 and a mixed oxyhydroxide, metaschoepite (88% α-uranyl hydroxide, 12% $[(UO_2)_8(O_2)(OH)_{12}]\cdot 10H_2O$), under vacuum led to the formation of nanocrystalline UO_{2+x}. This reduction was suggested to occur through electronic excitation, followed by expulsion of oxygen along ion track cores. Tracy *et al.*[21] also indicates that uranium oxides, which can readily undergo metal redox reactions, exhibit radiation damage accumulation behavior different than that of oxides with stable metal centers like ThO_2. This study provides an intriguing mechanism for the reduction processes that may occur for U(VI) materials in the absence of O_2 but may not represent the final product in an aerobic environment. Benjamin *et al.*[230] noted that irradiation of metaschoepite by a He^{2+} ion beam did not result in the formation of U(IV), instead observing dehydration to γ-UO_3 followed by post-radiation transformation into studtite.

Redox changes of the actinide cation are not the only way that oxide materials are impacted by radiation. Mosley *et al.*[231] reported on the self-radiation of several Cm(III) oxides where the swelling of the lattice varied depending on the overall symmetry of the material. They observed that swelling of *fcc*-CmO_2 was twice that of *bcc*-Cm_2O_3, and furthermore, no swelling was noted for the monoclinic Cm_2O_3 phase. Mosley *et al.*[231] also reported the stabilization of *bcc*-Cm_2O_3, a high temperature metastable form, under ambient conditions. This observation indicates that radiolysis of solids may induce the formation of metastable phases not predicted to occur under standard conditions.

5.4. Peroxides

Peroxide materials have relevance in the nuclear fuel cycle and have been identified as secondary alteration phases on surfaces at waste sites, such as the corium lava at Chernobyl.[232] Multiple studies have been performed at the University of Notre Dame to investigate changes in peroxo-bearing U(VI) materials, including U(VI) triperoxide coordination complexes, large molecular U(VI) peroxide clusters, and studtite.[109,230,233–235] For both γ-particle and α-particle irradiation, the materials exhibited structural changes through the formation of hydroxide anions or formation of the amorphous U_2O_7 phase and weakening of the uranyl bond.[236] Interestingly, upon irradiation of the monomeric material $Li_4[UO_2(O_2)_3]\cdot 10H_2O$ (LiUT), formation of the $Li_{24}[UO_2O_2(OH)]_{24}$ (LiU_{24}) cluster was observed, which at high radiation doses (400 kGy) degrades into $Li_2[(UO_2)_3O_2(OH)_3]_2\cdot 7H_2O$.[109] Fairley *et al.*,[235] noted a red shift for the symmetric UO_2^{2+} stretch (ν_1) in the Raman spectra for the molecular clusters and studtite after irradiation by γ-rays; however, degradation of studtite and the U_{60} cluster to form amorphous U_2O_7 occurred upon He^{2+} ion irradiation. Uranyl peroxide clusters containing pyrophosphates also observed reduction of the metal cation into mixed oxidation states of U(IV), U(V), and U(VI).

Additional efforts by Emory *et al.*[233] noted that exposure of $Li_{28}[(UO_2)_{28}(O_2)_{42}]$ (LiU_{28}) to He^{2+} ion radiation leads to decomposition of the cluster at high doses and eventually direct air capture of CO_2. Fairley *et al.*[234] also reported the transformation of uranyl peroxide materials to uranyl tricarbonates upon radiation exposure under ambient conditions (Fig. 14), ultimately capturing CO_2 from the atmosphere. This work highlights potential formation mechanisms of secondary mineral phases containing uranyl triperoxides and their transformations into other mineral phases.

It is worth noting that the radical forms of the hydroxide and peroxide ligands ($^{\bullet}OH$ and $O_2^{\bullet-}$) could be present within the irradiated peroxide materials. This aspect was not evaluated in the previous studies and thus no conclusions can be made on their formation from direct irradiation. However,

Open Access Article. Published on 10 juli 2025. Downloaded on 20-05-2026 01:21:34.
This article is licensed under a Creative Commons Attribution 3.0 Unported Licence.

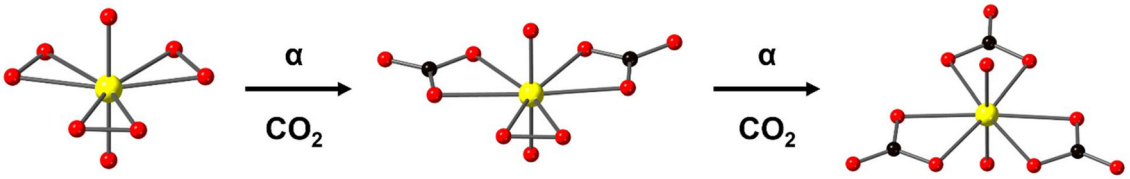

Fig. 14 Direct CO_2 capture by a uranyl triperoxide moiety upon exposure to α-radiation, resulting in the formation of a uranyl tricarbonates species. Adapted from Fairley *et al.*[234]

research by Kravchuk *et al.*[104] and Scherrer *et al.*[81,237] have previously identified the presence of $O_2^{\bullet-}$ within uranyl peroxide materials without exposure to external ionizing radiation, suggesting that superoxide species can exist within these materials. Two of these studies reported that uranyl triperoxides form uranyl peroxo-superoxide species over the course of a few weeks under inert conditions and that these uranyl peroxo-superoxide complexes will undergo direct air carbon capture under ambient conditions.[81,104] Thus, the formation of the uranyl superoxide has been linked to the first step in CO_2 capture, but more research into the radical formation is necessary to elucidate the associated mechanism taking place under irradiation.

5.5. Halogen containing materials

Actinide fluorides are important intermediate compounds in the formation of metallic actinide phases and are also used in the preparation of targets; thus, their behavior in high radiation fields is of interest. Steindler *et al.*[238] evaluated the behavior of PuF_6 upon γ-ray irradiation, observing reduction to PuF_4. Investigations by Stacy *et al.*[239] evaluated CaF_2 doped with An(III) (where An = U, Np, Pu, Am, or Cm). Upon γ-ray irradiation under ambient conditions, the majority of the An (III) readily oxidized to An(IV) within CaF_2, as evidenced with optical spectroscopy. The one exception is the Am(III) doped materials where Stacy *et al.*[239] and Edelstein *et al.*[240] both observed reduction of Am(III) to Am(II) concomitant with F-center formation, although it is not readily clear why the reduction occurs for just this one dopant. Due to valence state changes, multiple studies report a rearrangement of symmetry for the CaF_2 due to formation of defect sites, increase of interatomic distances, and structural disorder.

The only solid-state berkelium study was reported by Silver *et al.*[241] on the effects of self-irradiation on a mixture of Bk(III)/Bk(VI) iodates. They noted that $Bk(IO_3)_3$ converted to $Bk(IO_3)_4$ from the oxidation of Bk(III) to Bk(IV). This process occurs due to the high self-activity of ^{249}Bk where these materials preferentially oxidize to Bk(IV). More insight is necessary to understand the impact of the iodate ligands present on the material since Bk is a low-energy β-particle emitter that could potentially induce radical formation within the lattice itself, perturbing the metal–ligand coordination over time.

5.6. Nitrates

As discussed in section 4.3.6.1, actinide nitrates are ubiquitous in UNF separations processes, and their corresponding solid-state materials can help understand their atomistic-level decomposition and behavior due to direct radiation effects that will occur at high concentrations. Rao *et al.* investigated the γ-ray radiation induced formation of radicals in $[K(UO_2)(NO_3)_3]$, $[K_2(UO_2)(NO_3)_4]$, and $[(NH_4)(UO_2)(NO_3)_3]$ solids using EPR.[242] They observed the formation of two different signatures in their EPR spectra after irradiation but could not definitively assign these features to specific radical species. More recently, Kruse *et al.*[243] reported γ-ray radiation-induced changes in $[M(UO_2)(NO_3)_3]$ complexes, where M = Na^+, K^+, Rb^+, and observed similar signatures as those reported by Rao *et al.*[242] Additional DFT calculations and predicted EPR signatures performed on model complexes, including the second sphere coordination environment, demonstrated that the bidentate nitrate anion in uranyl trinitrate becomes monodentate following radiation exposure due to the formation of the $NO_3^{\bullet}$, as illustrated in Fig. 15. The use of solid-state materials provides insight into atomistic-level changes with control over the coordination environment and second-sphere interactions that can elucidate small changes upon irradiation. Although solid-state materials are traditionally regarded as immobile, the formation of molecular defects highlights the small but

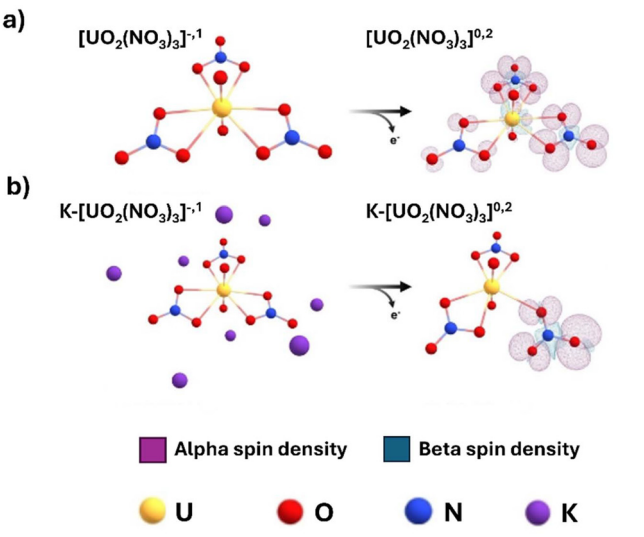

Fig. 15 (a) DFT calculation of uranyl trinitrate models without considering interactions of alkali metal counter cations. (b) DFT calculation of uranyl trinitrate where alkali metal counter cations are integrated into the calculation. Adapted from Kruse *et al.*[243]

This journal is © the Partner Organisations 2025

Open Access Article. Published on 10 juli 2025. Downloaded on 20-05-2026 01:21:34.
This article is licensed under a Creative Commons Attribution 3.0 Unported Licence.

significant changes to the solid that can cascade into further reactivity. These small changes may provide critical information that can assist solution-based irradiation studies.

5.7. Phosphorus-based materials

Phosphate materials, including monazite-based ceramics, are important materials that have been evaluated for the long-term storage of nuclear materials, but there are additional actinide phosphate phases that have also been evaluated at the atomistic level. EPR, thermoluminescence, and X-ray photoluminescence spectroscopy were used to evaluate the formation of radicals within γ- and heavy-ion irradiated $Th_4(PO_4)_4P_2O_7$.[244] Both phosphate- and diphosphate-based radicals were identified, which can behave as oxidizing agents and form additional species.[244] Additional degradation products were observed from heavy-ion irradiation of $Th_4(PO_4)_4P_2O_7$, including ThO_2, $(ThO)_3(PO_3)_2$, and P_4O_{10} on the surface of the starting material,[244] additional studies are necessary to determine the extent of degradation product formation throughout the bulk material.

Self-irradiation of phosphates has also been explored for $AnPO_4$ (An = Am(III), Pu(III)) and in both cases the crystalline starting material underwent rapid amorphization. Powder X-ray diffraction was used to evaluate crystallinity, and the lack of any discernable peaks occurred at 2.2×10^{18} Bq g^{-1} and 0.55×10^{18} Bq g^{-1} for $AmPO_4$ and $PuPO_4$, respectively. However, Dacheux *et al.*[245] noted that 2-billion-year-old (U,Th)PO_4 monazite samples were found to be well-crystallized even with observable radiation damage. These samples contain small nanodomains of lattice distortions and Seydoux-Guillaume *et al.*[246] suggested that the structure itself can undergo self-annealing to remove defects caused by irradiation. Nanodomains within the self-irradiated $AmPO_4$ sample were observed using transmission electron microscopy imaging and the ^{31}P nuclear magnetic resonance spectroscopy indicated no change in the local coordination environment.[247] This result suggests that over time there could be some annealing effect, but the exact mechanism is unclear.

5.8. Metal–organic frameworks (MOFs)

As a newer class of materials, MOFs are promising candidates for a range of applications (*i.e.*, asymmetric catalysis, gas storage/separation, nonlinear optics, chemical sensing) because of their unique properties, and are also being evaluated for their use in the nuclear fuel cycle.[248–250] While there are several studies that focus on transition metal and main-group MOFs for capture of fission products or other radionuclides important to the waste stream, this section will specifically focus on actinide-containing MOF materials.

Most studies in the literature on MOFs focus on the durability of the material upon irradiation and highlighted the importance of the organic linker[251–253] and the metal node.[254–256] Hastings *et al.*[255] reported the importance of the identity of the metal nodes within the MOF for obtaining increased structural stability, where thorium was found to enhance the stability of a UiO-66 MOF compared to plutonium. They also noted that the strength of the metal–ligand complexation is positively correlated with MOF structural stability upon irradiation and that self-irradiation within the Pu–UiO-66 MOF results in additional recoil effects that degrade the structural integrity of the material more readily. A Th-based MOF reported by Gilson *et al.*[254] reported the highest radiation stability of a MOF to date, which completely amorphized by 25 MGy of α-particle radiolysis. This study indicated that properties beyond absorption of energy by the metal node affect the radiation resistance of MOFs, such that the framework as a whole must be evaluated to holistically understand these properties. Zhang *et al.*[257] explored Pu(IV) and Am(III) MOFs (Pu–TPO and Am–TPO where TPO = tris(4-carboxyphenyl)-phosphineoxide) and demonstrated self-radiation resistance as no degradation of the material was initially noted for Pu–TPO and Am–TPO. However, α-particle radiation induced swelling was observed over the course of a few months for Pu–TPO. The authors suggested that the organic linker contributes to this stabilization due to the presence of extended π-systems where the delocalization of electrons can occur upon irradiation. However, α-particle and recoil energy within self-irradiated materials generally contribute to the amorphization of crystalline materials, so it is unclear how this material is more resistant to these types of forces. Further systematic work with both the metal and organic linkers are necessary to elucidate the rational design of MOFs with high structural stability towards radiation damage.

Gilson *et al.*[258] provided additional insights into how MOFs may degrade under γ-ray irradiation by utilizing vibrational spectroscopy. They reported the formation of a Np(V) MOF containing 4′,4″,4‴,4⁗-methanetetrayltetrabiphenyl-4-carboxylic acid that displayed structural stability until 3 MGy of γ-ray radiolysis at which point the amorphization of the material occurred. However, most of the spectroscopic signatures of the material remained unchanged up to 6 MGy of γ-ray irradiation. Only subtle changes in the vibrational spectroscopy are noted and are linked to carboxylate vibrational modes. This observation suggests it is the metal–ligand coordination that is most readily impacted following irradiation although the exact nature is still unknown. The stability of the material to γ-rays may be associated with the aromaticity of the tetracarboxylate ligand. However, it is interesting to note the redox activity of neptunium and the presence of actinyl–actinyl interactions that may also enhance disproportionation reactions. Reduction to Np(IV) would not be readily observed in the vibrational spectra and there are differences in the UV-Vis-NIR spectra reported by Gilson *et al.*[258] that may be indicative of redox changes.

One of the key properties of MOFs is their ability to have cavities or be porous in nature; thus, additional studies evaluated changes in porosity and uptake of guest molecules with exposure to ionizing radiation. Ionizing radiation exposure has been reported to enhance the sorption properties within main-group and transition metal MOFs,[259–262] but has not been evaluated for actinide-bearing materials. Li *et al.*[259] explored the structural radiation-resistance of two Th-MOFs built from aro-

Open Access Article. Published on 10 juli 2025. Downloaded on 20-05-2026 01:21:34.
This article is licensed under a Creative Commons Attribution 3.0 Unported Licence.

matic dicarboxylate linkers where structural stability was maintained up to 0.2 MGy. The authors explored the capability of the two MOFs to capture the fission product I_2, which is important in the proper disposal of nuclear waste, and both systems showed efficient I_2 adsorption (258–473 mg g^{-1}). However, these adsorption studies were only conducted pre-irradiation so the impact of irradiation on the I_2 uptake is unclear. It is important to expand these studies to understand not only the structural stability, but also the porous nature of the MOF upon ionizing radiation exposure, which can lead to changes in sorption capacity. This concern is demonstrated by Volkringer *et al.*[261] who completed a comprehensive study of various MOFs pre- and post-irradiation to understand changes in efficacy of N_2 sorption *via* BET analyses. Although this study does not include actinide-based MOFs, it represents an example of how the nature of the pores and impacts of irradiation on MOF materials can go beyond structural stability.

Lastly, it is important to note that MOFs are also being explored in radiomedicinal applications to assist in diagnostics, therapeutics, and a combination of both (theranostics). Mezenov *et al.*[263] reported a more in-depth analysis of MOFs, including non-actinide MOFs, and their changes to external stimuli such as radiation. Some MOFs, specifically a Th-MOF reported by Andreo *et al.*,[264] are also being explored as radiation detectors for imaging where autoluminescent properties from the decay of the actinide can aid as a sensor. Most studies in this area utilize MOFs without actinides; however, actinides can be promising candidates to advance this area of research due to their inherent radioactive decay which can be implemented in either detection and/or treatment.

6. Intersection of solution and solid-state: radiolysis effects of corrosion and environmental systems

While the last two sections of this review article focused on either aqueous solutions or solid-state materials, many chemical systems of interest are more complex. It is the intersection of these two-phase boundaries that can lead to important chemical reactivity. Chemistry occurring at surfaces and grain boundaries plays a significant role in the behavior of UNF in storage facilities, the evolution of nuclear materials over time, and the transport of actinides in environmental systems.[265,266] With this in mind, the current section focuses on exploring the impacts of water radiolysis on solid-state actinide materials.

Overwhelmingly, studies have shown that the γ-radiolysis of adsorbed water significantly affects the behavior of UO_2 fuel. This process enhances the oxidation of U(IV) to U(VI)[261,262] by reacting with H_2O_2 or $^{\bullet}OH$ from water radiolysis or through secondary species like $CO_3^{2-}/CO_3^{\bullet-}$ derived from dissolved CO_2.[262] These radiation-induced redox reactions produce secondary U(VI) alteration phases ($UO_{2.33}$) and significantly increase the dissolution rate of UO_2.[261,264–266] The rate of oxidation is dependent on the one-electron transfer by the oxidant. Ekeroth and Jonsson indicate that reactions with $^{\bullet}OH$ or $CO_3^{\bullet-}$ are diffusion controlled, but the reaction between UO_2 and H_2O_2 may be associated with a Fenton-like mechanism.[269,273] Christensen and Sunder also note that diffusion is not a major contributor to UO_2 oxidation; thus, only a thin layer of water (<100 μm)[274] is needed for this process to take place.[267,268,270,271]

Sunder *et al.*[267] also report that oxidation of UO_2 fuel is dependent on the flux of the α-particle radiation.[267] These studies were conducted using an internal α-particle radiation source (^{241}Am) and they observed that a dose equivalent to 5 μCi will convert UO_2 to $UO_{2.33}$, but a dose ≥250 μCi oxidizes the fuel to U_3O_7—a result dependent on accumulated dose. Additional studies using high energy He^{2+} ions (10^{10}–10^{11} He^{2+} cm^{-2} s^{-1}) supplied by a cyclotron found that UO_2 in the presence of water will alter to a hydrated uranyl peroxide upon irradiation.[275–279] Chemical experiments that introduced H_2O_2 to the solution also produced this hydrated U(VI) peroxide phase, but Corbel *et al.*[279] noted that the behavior of UO_2 dissolution is different between these two types of experiments. When H_2O_2 is produced by irradiation, the rate of uranium release from the interface is much higher than with simple H_2O_2 addition. This observation is consistent with H_2O_2 dissolution studies performed by Hickam *et al.*,[280] suggesting that it is not just H_2O_2 alone that enhances UO_2 dissolution in high radiation fields.

While the importance of H_2O_2 in the oxidation of UO_2 has been clearly demonstrated, there are some differences regarding the production of this molecular species between the specific type of incident radiation (γ-rays and α-particle irradiation). Jégou *et al.*[281] identified that the presence of gaseous O_2 enhances the production of H_2O_2 in γ-ray radiolysis and Sarrasin *et al.*[282] demonstrated using *in situ* Raman spectroscopy and ^{18}O labeled water that the peroxide bond contained a significant amount of ^{16}O. This observation indicates that the formation of H_2O_2 involved the dissolved $^{16}O_2$ and related radical species (*i.e.*, $HO_2^{\bullet}$, $O_2^{\bullet-}$). However, Perrot *et al.*[283] utilized the same approach for α-particles and found that the peroxide bond contains mostly ^{18}O, demonstrating that the formation of H_2O_2 in this case occurred through the recombination of $^{\bullet}OH$ produced from water radiolysis. These results align with expected LET effects and the typical yields for water radiolysis for the two types of radiation.

Formation of peroxide alteration phases has been further explored and found to be somewhat dependent on the chemical environment. The hydrated peroxide phase studtite and dehydrated phase metastudtite $[UO_2(O_2)(H_2O)_2]$ consume H_2O_2 in a reaction with UO_2^{2+}, leading to their formation as a solid layer for both γ-rays and α-particles (Fig. 16). Further α-particle radiolysis of studtite led to the formation of a reactive species and its conversion to metaschoepite, $[(UO_2)_8(O_2)(OH)_{12}]\cdot 10H_2O$, in the presence of water. Additional UO_2 alteration experiments also noted the formation of schoepite $[(UO_2)_8(O_2)(OH)_{12}]\cdot 12H_2O$.[278] These studies were performed

 This journal is © the Partner Organisations 2025

Open Access Article. Published on 10 juli 2025. Downloaded on 20-05-2026 01:21:34.
This article is licensed under a Creative Commons Attribution 3.0 Unported Licence.

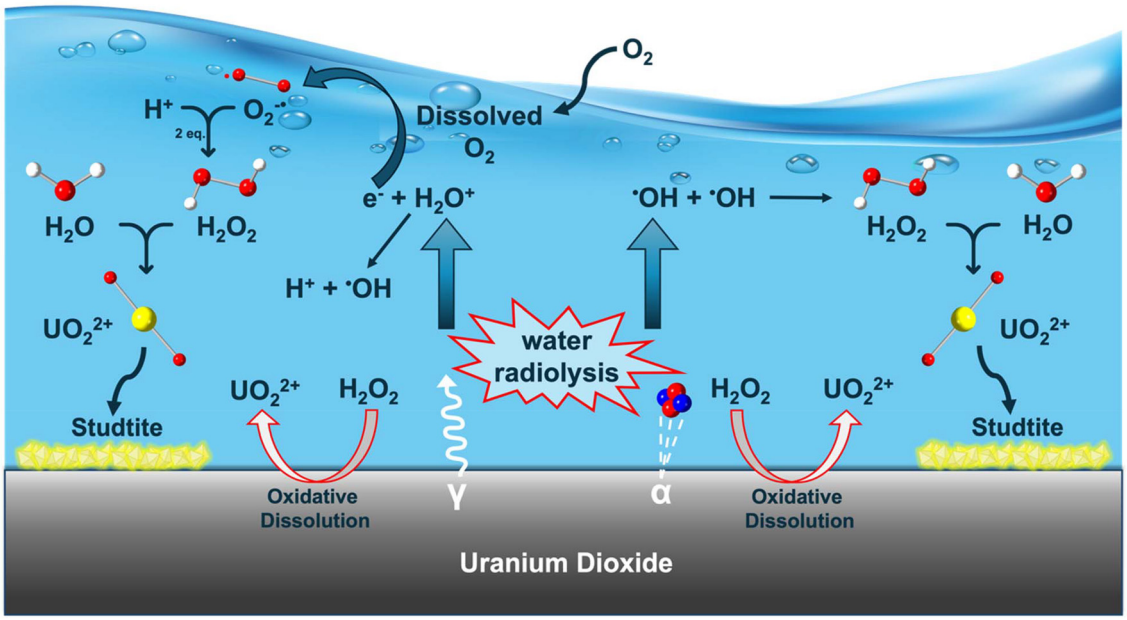

Fig. 16 Diagram of the formation of studtite from the oxidative dissolution of UO_2 from water radiolysis including both γ- and α-incident radiation pathways. Adapted from Perrot *et al.*[283]

with de-ionized water, but if UO_2 was exposed to environmentally relevant conditions, such as ground water, then the products and chemistry could be altered. Ground water contains various solutes that can act as radical scavengers that, when paired with neat water radiolysis, diminish the already low concentrations of H_2O_2 resulting in decreased schoepite formation. With a high initial H_2O_2 concentration that exceeds the scavenger concentration, studtite and/or metastudtite is most favorable.[284]

Although these studies have provided foundational information for the effects of water radiolysis on UO_2 species, other studies have also explored the behavior of real UNF for extended periods of time. Hanson *et al.*[194] exposed commercial UNF (c-UNF) to water without any external radiation source and observed the corrosion phases present on the surface of the fuel. Crystallites of metaschoepite were observed at short times on hydrated c-UNF particles; however, over two years of water contact, metaschoepite was no longer present and the c-UNF was instead coated with studtite and metastudtite. Thus, c-UNF under long-term storage conditions likely undergoes radiation-induced oxidative corrosion and the relationships between schoepite and studtite phases should be further explored to understand the nature of the reactive alteration phases.[272]

It is also important to highlight work by Jégou *et al.*[285] and Büppelmann *et al.*[286] that explored the impacts of radiation on transuranic oxide materials in aqueous solutions. Jégou *et al.*[285] investigated the impacts of γ-ray radiolysis on MOX-47, $(Pu,U)O_2$, material in water, resulting in the oxidation of Pu(IV) to Pu(V), and U(IV) to U(VI). Pu(IV) was found to be more stable over time than the U(IV) oxide materials, and soluble Pu(V) complexes were found to form $Pu(OH)_4$ colloids from hydrolysis upon aging.[285] Büppelmann *et al.*[286] explored the redox behavior of α-particle irradiated PuO_2 and $Am(IV)(OH)_4$ in high ionic strength (<5 M NaCl) solutions. With irradiation of the high-ionic strength solution in both air and Ar, Pu(IV) oxidized to Pu(VI).[286] Am(III) can also be oxidized to Am(V) under irradiation in air but remains stable in argon and 0.6 M NaCl. As the pH increased to 8 and the NaCl concentration increased to 3 M, oxidation of Am(III) to Am(V) was noted, indicating that pH and ionic strength play a role in the chemical species.

Increasing the complexity of the solution is important for understanding environmental transport; thus, Vladimirova *et al.*[287] explored the behavior of PuO_2 in ground water exposed to γ-rays. They observed reduction of PuO_2 to a more soluble Pu(III) form by the reaction with H_2O_2. The amount of Pu in solution can be linked to organic acids in ground water, particularly fulvic and mellitic acids, that form soluble complexes. Further dose accumulation studies noted that high doses such as 35 kGy result in the complete reduction of Pu(IV), whereas lower doses result in only 35% solubilized plutonium in ground water. This difference is due to disproportionation reactions where Pu(IV) interacts with water radiolysis products to produce Pu(III) and Pu(V), and H_2O_2 further reduces the remaining Pu(IV) to Pu(III). Thus, the direct interface of PuO_2 with ground water will generate radiolysis products to reduce Pu(IV) to Pu(III), increasing material solubility, leading to environmental contamination.

Although most studies in the literature focused on the oxidative dissolution of actinide oxides, some experiments observe the reduction and precipitation of oxide materials. Rath *et al.*[288] reported the electron beam of U(VI) nitrate hexa-

Open Access Article. Published on 10 juli 2025. Downloaded on 20-05-2026 01:21:34.
This article is licensed under a Creative Commons Attribution 3.0 Unported Licence.

hydrate dissolved in N_2-purged aqueous solutions containing 10 wt% propan-2-ol resulted in the formation of UO_2 nanoparticles. The particles were unstable in the presence of O_2, resulting in reoxidation to U(VI). However, if the solution was purged with N_2 and irradiated a second time, the UO_2 nanoparticles reformed. This study demonstrates that the irradiation of U(VI) bearing solutions, particularly in complex waste streams that contain organic solvents, can lead to the unanticipated formation of colloidal materials and particulates. Additional studies are needed to fully understand these processes.

7. Challenges, opportunities, and visions

This review has summarized most of the work completed thus far for the irradiation of both aqueous solution and solid-state actinide-containing systems. These ranged from cutting-edge experiments to explore the pico-second evolution of radical species in solution and changes to metal oxidation state, to focusing on the identification of radiolysis products and other long-lasting changes to actinide materials. Bridging the gap between pulse radiolysis and longer time scale dose accumulation studies can lead to a better mechanistic understanding of the behavior of actinides in these reactive environments that have important implications in the nuclear fuel cycle. In the following sections we highlight opportunities to enhance our understanding of actinides in high radiation fields through a variety of chemical approaches.

One of the main challenges with both actinide and radiation chemistry is that each require specialized facilities and licensing to complete the work. However, the infrastructure needed to irradiate materials and work with radioactive samples are quite different, so there are only a handful of facilities globally that can handle both. This limitation leads to challenges in developing this important chemistry more fully; thus, it is important to continue investments in these two areas. In addition, much of the infrastructure and workforce in actinide and radiation chemistry is aging, thus an influx of funds to support upgrades and educate the next generation is necessary to continue developing the field.

It is also important to continue expanding the chemical systems that are evaluated by irradiation experiments. While there have been significant and important efforts in some systems (*i.e.*, water, nitrate solutions, and oxide solids), it is somewhat surprising how few co-solutes and solid-state material classes have been explored to date. Additionally, studies on the radiolysis of organic solvents with actinides are needed because there is limited information regarding the actinide chemistry in these systems. Preliminary studies have been conducted on solely the organic solvent,[289,290] but the impact of radiolysis products in conjunction with actinides remains underexplored. With the development of next generation reactors and advanced reprocessing strategies for complex waste streams, it is important to increase our understanding of radiolytic effects on a broader spectrum of chemical environments.

Common analytical techniques utilized by inorganic chemists were listed in Fig. 2. These techniques fit within the toolbox of the inorganic chemist and can provide information on bonding and speciation that are crucial to developing a complete picture of actinide behavior within these systems. Some of these techniques are not routinely utilized in radiation chemistry, but the further development of these and other advanced methods to achieve shorter timescales can provide additional signatures to enhance our understanding of the chemical timescales for the metal species.

Continuing to explore and expand the time scales of actinide radiation chemistry experiments will lead to additional insights into the long-term behavior of these materials. Several studies have reported radiation-induced reaction kinetics and changes in actinide oxidation states, but few studies have reported steady-state dose accumulation products. Further, pulse radiolysis experiments provide important insight into the mechanistic details and yields of products upon radiolysis; however, few report the resulting complexes with the actinides present in solution. Bridging the physicochemical stages with the non-homogenous and homogenous stages would provide insights into the broader chemical system. Many actinide elements typically persist for tens to thousands of years due to the radioactive lifetime of species present;[291] therefore, long-term dose accumulation studies (*e.g.*, days, weeks, years) need to be conducted to fully understand the impacts of radiolysis on reprocessing and the storage of nuclear waste.[292,293] Since these timescales are difficult to achieve at irradiation facilities, continued work on internal radiation experiments are necessary to provide additional data for modeling chemical behavior.

One of the challenges with spectroscopic approaches is the deconvolution and interpretation of the resulting spectra. This effort can be particularly challenging in the case of actinides as the 5f-orbitals have complex electronic transitions, speciation, and redox behavior. Therefore, additional efforts must be put forward by inorganic chemists to provide a fundamental understanding of the chemical signatures for these actinide species. This advancement can occur by aqueous phase or solid-state model complexes and with the development of chemical surrogates (*i.e.*, chemical radical initiators, peroxide generators) to mimic specific radicals produced during radiolysis. Enhancements in the detection of low concentrations at fast time frames will enhance our understanding of actinide speciation in the presence of reactive species formed through radiolysis.

Additional efforts in developing existing and novel computational methods in the physical, physicochemical, and chemical stages could also enhance our understanding of actinides in high radiation fields. Much of the computational efforts in radiation chemistry track structure utilizes Monte Carlo simulations and deterministic methods, which enables important information on generation of radical species and their respective yields and kinetics.[294–297] These calculations are essential for pulse radiolysis experiments to account for the fast kinetics

 This journal is © the Partner Organisations 2025

Open Access Article. Published on 10 juli 2025. Downloaded on 20-05-2026 01:21:34.
This article is licensed under a Creative Commons Attribution 3.0 Unported Licence.

($\sim 10^{-12}$ s), and can extend to longer timescales as well to model the chemical speciation (*i.e.*, H_2O_2, H_2) of interest to inorganic chemists.[298–300] One of the challenges with these methodologies is that all equilibrium reactions must be accounted for and setting up these calculations can be time consuming, requiring ~90 reactions for neat water radiolysis alone.[298] The models described above only partially account for changes in actinide speciation and have focused solely on the solution, therefore the development of models for actinide speciation is necessary.

Some studies have explored aqueous solutions on the surface of UNF to understand the radiation-induced dissolution process.[301–304] These simulations are reported to be fairly accurate when homogeneous rate constants are used. Importantly, Eriksen *et al.*[305] notes spatial dose rate coefficients are needed for calculating the irradiation of materials at short times ($<10^{-6}$ s) but are less important at longer times (>1 s). In general, these calculations are time consuming, therefore, the use of spatial distribution will make calculations more expensive. The tradeoff is that without employing spatial distribution, the results are less accurate. For calculations over longer periods, a steady-state approach is fairly accurate; however, reaction mechanisms and kinetics cannot be reliably determined using this method. Thus, the user must recognize these models may assume poorly fitting rate coefficients and unrealistic mechanisms, even though the results may still match experimental yields. Therefore, reaction rate coefficients must be determined experimentally and used in the model. Additionally, mechanisms must be verified by the user to ensure they are chemically sound. A more in-depth review has been provided by Eriksen *et al.*[305] in regard to this predictive modelling approach for radiation-induced dissolution of actinide solids.

DFT methods are now commonly utilized by inorganic actinide chemists to understand speciation, determine energetics, predict spectral signatures, explain trends in bonding, and explore electronic structure within molecules and extended solids.[296] Recent solid-state irradiation studies[243] have implemented various DFT calculations, specifically for aid in radical characterization,[243] including the use of programs like ORCA[306] which can be used to calculate *g*-factors identified in EPR spectroscopy and are becoming quite accurate with the inclusion of relativistic effects (*i.e.*, ZORA),[307–309] necessary for actinides. Spin densities can be visualized using Chemcraft[310] programs as well, to provide important insights into the interaction between the metal cation and the radical species. To gain highly-accurate calculations, Complete Active Space Self-Consistent Field (CASSCF),[311,312] dynamic electron correlation N-Electron Valence state Perturbation Theory 2 (NEVPT2),[313] and spin orbit coupling using Quasi Degenerate Perturbation Theory (QDPT)[314,315] are being developed for these complex systems.[316] For *g*-factor calculations, a matrix can be calculated after employing CASSCF methods through Effective Hamiltonian,[317] which may enable more accurate predictions for irradiated materials.[318]

There are benefits and challenges associated with standard DFT that can arise within radiation chemistry; therefore, understanding its limitations is crucial. Benefits of DFT include geometry predictions, determination of bonding networks including bond orders, bond lengths, and bond angles, calculating dispersion forces—all of which have had great success in many computational studies.[296,319] However, the use of DFT requires the user to screen various basis sets and functionals to test which works best for each system.[320] Without proper screening of basis sets and functionals, large errors can easily arise. Benchmarking is essential for any set of calculations involving different actinide structures because a single basis set may not be universally accurate for all systems. Additional considerations include the treatment of the actinide and its 5f-orbitals. Different corrections can be made to treat the electrons in the f-orbitals as either localized or delocalized, which can also impact the results for actinide–ligand interactions, especially when determining radical signatures associated with the actinide complexes.[321–324] Overall, DFT typically does a poor job for calculating bulk solution chemistry.[325] However, when investigating the effects of a single outer-sphere shell of water or discrete network of water and an actinide moiety, DFT can still be used.[326,327] The dynamics in which electrons move throughout a system are important, and some solvation calculations have reported surface hopping dynamics of electrons;[328–330] however, gaining accuracy in these systems pushes towards gas- or condensed-phase calculations that may not accurately represent the behavior of the system.[331] Gas- and condensed-phase calculations typically represent ideal behavior of complex interactions. Ultimately, the environment chosen for the calculation is crucial and can easily complicate computational methods.

Additionally, DFT calculations use many approximations, such that typical calculations are usually ground-state calculations.[332] In terms of materials exposed to ionizing radiation, it is likely that both ground- and excited-states can arise. Thus, the use of a multireference methods such as CASSCF would be more favorable to account for excited-states. That said, there are also challenges with multireference methods, including the choice of chemical space—a common challenge in general when using DFT—and selecting specific orbitals and symmetries to calculate. Therefore, possessing chemical knowledge of the system can aid in determining the relevant chemical space and limiting the number of calculations to be run to a reasonable number to save computation time. Additionally, one can choose to make one part of their system multireference while the rest can be treated as periodic DFT, leaving many choices for the user to make. For a more comprehensive review of advantages and disadvantages with using DFT, we recommend a review written by Cohen *et al.*[332] and a perspective by Burke.[325]

In summary, continued development of instrumentation and data analysis procedures by inorganic and radiation chemists will lead to broader improvements in the identification and fundamental understanding of actinide species in both solution and solid-state chemistry. Inorganic chemists and their perspectives can provide critical insight into this realm of research, creating a unique perspective for the radiation chem-

Open Access Article. Published on 10 juli 2025. Downloaded on 20-05-2026 01:21:34.
This article is licensed under a Creative Commons Attribution 3.0 Unported Licence.

istry of actinide-containing materials. However, collaborations between inorganic and radiation chemists are imperative so that experiments are performed safely and interpreted correctly. These collaborations provide valuable insights into the behavior of actinides in high radiation fields, which will ultimately drive progress in the safe handling and storage of nuclear materials, improved strategies for UNF reprocessing, and aid in the remediation of environmental contamination.

Author contributions

All authors have participated in the writing of this manuscript and have given approval to the final version.

Data availability

The data supporting this article have been included as part of the ESI.†

Conflicts of interest

There are no conflicts to declare.

Acknowledgements

Kruse acknowledges support from the National Science Foundation Graduate Research Fellowship Program (NSF GRFP-1945994). Forbes was supported by U.S. DOE, Basic Energy Sciences, Heavy Elements Chemistry under award DE-SC0023995. Horne was supported by the U.S. DOE, Office of Science, Office of Basic Energy Sciences, Solar Photochemistry Program under award DE-SC0024191. LaVerne was supported by the Division of Chemical Sciences, Geosciences and Biosciences, Basic Energy Sciences, Office of Science, US-DOE through Award No. DE-FC02-04ER15533, document number NDRL-5458.

References

1 T. E. Albrecht-Schmitt, Actinide Chemistry at the Extreme, *Inorg. Chem.*, 2019, **58**(3), 1721–1723, DOI: **10.1021/acs.inorgchem.8b03603**.
2 T. Vitova, I. Pidchenko, D. Fellhauer, P. S. Bagus, Y. Joly, T. Pruessmann, S. Bahl, E. Gonzalez-Robles, J. Rothe, M. Altmaier, *et al.*, The role of the 5f valence orbitals of early actinides in chemical bonding, *Nat. Commun.*, 2017, **8**(1), 16053, DOI: **10.1038/ncomms16053**.
3 H. Matzke, Radiation effects in nuclear fuels, in *Radiation Effects in Solids*, Springer, 2007, pp. 401–420.
4 B. J. Mincher, G. Elias, L. R. Martin and S. P. Mezyk, Radiation chemistry and the nuclear fuel cycle, *J. Radioanal. Nucl. Chem.*, 2009, **282**, 645–649, DOI: **10.1007/s10967-009-0156-x**.
5 A. Pustovalov, Role and prospects of application of RTG on base of plutonium-238 for planetary exploration, in *5th European Conference on Thermoelectrics, Odessa, Ukraine*, 2007.
6 J. S. Dustin and R. A. Borrelli, Assessment of alternative radionuclides for use in a radioisotope thermoelectric generator, *Nucl. Eng. Des.*, 2021, **385**, 111475, DOI: **10.1016/j.nucengdes.2021.111475**.
7 J. Bell and L. Toth, Photo and Radiation Chemistry in Nuclear Fuel Reprocessin, *Radiochim. Acta*, 1978, **25**(3–4), 225–230, DOI: **10.1524/ract.1978.25.34.225**.
8 P. Paviet-Hartmann, B. Benedict and M. J. Lineberry, Nuclear Fuel Reprocessing, in *Nuclear Engineering Handbook*, CRC Press, 2009, pp. 333–384.
9 R. Ewing, Actinides and radiation effects: impact on the back-end of the nuclear fuel cycle, *Mineral. Mag.*, 2011, **75**(4), 2359–2377, DOI: **10.1180/minmag.2011.075.4.2359**.
10 R. C. Ewing, W. J. Weber and F. W. Clinard, Radiation effects in nuclear waste forms for high-level radioactive waste, *Prog. Nucl. Energy*, 1995, **29**(2), 63–127, DOI: **10.1016/0149-1970(94)00016-Y**.
11 R. C. Ewing and W. J. Weber, Actinide Waste Forms and Radiation Effects, in *The Chemistry of the Actinide and Transactinide Elements*, ed. L. R. Morss, N. M. Edelstein and J. Fuger, Springer, Netherlands, 2011, pp. 3813–3887. DOI: **10.1007/1-4020-3598-5_30**.
12 H. Matzke, J. W. Wald and W. J. Weber, Self-Radiation Damage in Actinide Host Phases of Nuclear Waste Forms, *MRS Proc.*, 1984, **44**, 679, DOI: **10.1557/PROC-44-679**, From Cambridge University Press Cambridge Core.
13 H. J. Matzke, Actinide behavior and radiation damage produced by α-decay in materials to solidify nuclear waste, *Inorg. Chim. Acta*, 1984, **94**(1), 142–143, DOI: **10.1016/S0020-1693(00)94605-X**.
14 C. Walther and M. A. Denecke, Actinide colloids and particles of environmental concern, *Chem. Rev.*, 2013, **113**(2), 995–1015, DOI: **10.1021/cr300343c**.
15 N. O. Eddy, O. Igwe, I. S. Eze, R. Garg, K. Akpomie, C. Timothy, G. Udeokpote, I. Ucheana and H. Paktin, Environmental and public health risk management, remediation and rehabilitation options for impacts of radionuclide mining, *Discover Sustainability*, 2025, **6**(1), 209, DOI: **10.1007/s43621-025-01047-6**.
16 D. Dhiman, R. Vatsa and A. Sood, Challenges and opportunities in developing Actinium-225 radiopharmaceuticals, *Nucl. Med. Commun.*, 2022, **43**(9), 970–977, DOI: **10.1097/MNM.0000000000001594**.
17 B. D. Wirth, How does radiation damage materials?, *Science*, 2007, **318**(5852), 923–924, DOI: **10.1126/science.1150394**.
18 G. R. Choppin, Solution chemistry of the actinides, *Radiochim. Acta*, 1983, **32**(1–3), 43–54, DOI: **10.1524/ract.1983.32.13.43**.
19 J. Bruno and R. C. Ewing, Spent Nuclear Fuel, *Elements*, 2006, **2**(6), 343–349, DOI: **10.2113/gselements.2.6.343**.

This journal is © the Partner Organisations 2025

Open Access Article. Published on 10 juli 2025. Downloaded on 20-05-2026 01:21:34.
This article is licensed under a Creative Commons Attribution 3.0 Unported Licence.

20 R. C. Ewing, W. J. Weber and J. Lian, Nuclear waste disposal—pyrochlore (A2B2O7): Nuclear waste form for the immobilization of plutonium and "minor" actinides, *J. Appl. Phys.*, 2004, **95**(11), 5949–5971, DOI: **10.1063/1.1707213**.

21 C. L. Tracy, M. Lang, J. M. Pray, F. Zhang, D. Popov, C. Park, C. Trautmann, M. Bender, D. Severin, V. A. Skuratov, *et al.*, Redox response of actinide materials to highly ionizing radiation, *Nat. Commun.*, 2015, **6**(1), 6133, DOI: **10.1038/ncomms7133**.

22 W. J. Weber, Radiation effects in nuclear waste glasses, *Nucl. Instrum. Methods Phys. Res., Sect. B*, 1988, **32**(1), 471–479, DOI: **10.1016/0168-583X(88)90257-1**.

23 W. J. Weber, A. Navrotsky, S. Stefanovsky, E. R. Vance and E. Vernaz, Materials Science of High-Level Nuclear Waste Immobilization, *MRS Bull.*, 2009, **34**(1), 46–53, DOI: **10.1557/mrs2009.12**.

24 J. W. T. Spinks and R. J. Woods, *An introduction to radiation chemistry*, John Wiley and Sons Inc., New York, NY (USA), 1990.

25 G. Choppin, J.-O. Liljenzin, J. Rydberg and C. Ekberg, Chapter 8 - Radiation Effects on Matter, in *Radiochemistry and Nuclear Chemistry*, ed. G. Choppin, J.-O. Liljenzin, J. Rydberg and C. Ekberg, Academic Press, 4th edn, 2013, pp. 209–237.

26 M. Seaton, The theory of excitation and ionization by electron impact, *At. Mol. Processes*, 1962, **13**, 375–420.

27 G. Kraft and M. Kramer, Linear energy transfer and track structure, in *Advances in radiation biology*, Elsevier, 1993, vol. 17, pp. 1–52.

28 M. Ragheb, Gamma rays interaction with matter, in *Nuclear, Plasma and Radiation Science. Inventing the Future*, 2011, pp. 17–22. **https://netfiles.uiuc.edu/mragheb/www**.

29 B. Collum, 2 - Radiation, in *Nuclear Facilities*, ed. B. Collum, Woodhead Publishing, 2017, pp. 45–60.

30 R. Ewing, The Design and Evaluation of Nuclear-Waste Forms: Clues from Mineralogy, *Can. Mineral.*, 2001, **39**, 697–715, DOI: **10.2113/gscanmin.39.3.697**.

31 S. Le Caër, Water Radiolysis: Influence of Oxide Surfaces on H2 Production under Ionizing Radiation, *Water*, 2011, **3**(1), 235–253, DOI: **10.3390/w3010235**.

32 A. K. Pikaev, V. P. Šilov and V. I. Spicyn, *Radioliz vodnych rastvorov lantanidov i aktinidov*, Nauka, 1983.

33 M. Smith, S. M. Pimblott and J. A. LaVerne, Hydroxyl radical yields in the heavy ion radiolysis of water, *Radiat. Phys. Chem.*, 2021, **188**, 109629, DOI: **10.1016/j.radphyschem.2021.109629**.

34 M. Huerta Parajon, P. Rajesh, T. Mu, S. M. Pimblott and J. A. LaVerne, H atom yields in the radiolysis of water, *Radiat. Phys. Chem.*, 2008, **77**(10), 1203–1207, DOI: **10.1016/j.radphyschem.2008.05.050**.

35 A. R. Cook, N. Dimitrijevic, B. W. Dreyfus, D. Meisel, L. A. Curtiss and D. M. Camaioni, Reducing Radicals in Nitrate Solutions. The NO32- System Revisited, *J. Phys. Chem. A*, 2001, **105**(14), 3658–3666, DOI: **10.1021/jp0038052**.

36 G. P. Horne, T. A. Donoclift, H. E. Sims, R. M. Orr and S. M. Pimblott, Multi-Scale Modeling of the Gamma Radiolysis of Nitrate Solutions, *J. Phys. Chem. B*, 2016, **120**(45), 11781–11789, DOI: **10.1021/acs.jpcb.6b06862**.

37 G. P. Horne, S. M. Pimblott and J. A. LaVerne, Inhibition of Radiolytic Molecular Hydrogen Formation by Quenching of Excited State Water, *J. Phys. Chem. B*, 2017, **121**(21), 5385–5390, DOI: **10.1021/acs.jpcb.7b02775**.

38 J. A. LaVerne and S. M. Pimblott, Scavenger and time dependences of radicals and molecular products in the electron radiolysis of water: examination of experiments and models, *J. Phys. Chem.*, 1991, **95**(8), 3196–3206, DOI: **10.1021/j100161a044**.

39 A. K. Pikaev, Environmental Application of Radiation Processing, *Isopenpraxis Isotopes Environ. Health Studies*, 1986, **22**(12), 439–443, DOI: **10.1515/9783112523445-006**.

40 J. Barilla, P. Simr and K. Sýkorová, Simulation of the Influence of N2O on the Chemical Stage of Water Radiolysis, *WSEAS Trans. Biol. Biomed.*, 2022, **19**, 47–62.

41 B. J. Mincher, M. Precek and A. Paulenova, The redox chemistry of neptunium in γ-irradiated aqueous nitric acid in the presence of an organic phase, *J. Radioanal. Nucl. Chem.*, 2016, **308**(3), 1005–1009, DOI: **10.1007/s10967-015-4530-6**.

42 N. M. Edelstein, J. Fuger, J. J. Katz and L. R. Morss, Summary and Comparison of Properties of the Actinide and Transactinide Elements, in *The Chemistry of the Actinide and Transactinide Elements*, ed. L. R. Morss, N. M. Edelstein and J. Fuger, Springer, Netherlands, 2011, pp. 1753–1835.

43 N. Takeno, *Atlas of Eh-pH diagrams*, Research Center for Deep Geological Environments, National Institute of Advanced Industrial Science and Technology, 2005.

44 G. P. Horne, T. S. Grimes, W. F. Bauer, C. J. Dares, S. M. Pimblott, S. P. Mezyk and B. J. Mincher, Effect of Ionizing Radiation on the Redox Chemistry of Penta- and Hexavalent Americium, *Inorg. Chem.*, 2019, **58**(13), 8551–8559, DOI: **10.1021/acs.inorgchem.9b00854**.

45 G. P. Horne, B. M. Rotermund, T. S. Grimes, J. M. Sperling, D. S. Meeker, P. R. Zalupski, N. Beck, Z. K. Huffman, D. G. Martinez, A. Beshay, *et al.*, Transient Radiation-Induced Berkelium(III) and Californium(III) Redox Chemistry in Aqueous Solution, *Inorg. Chem.*, 2022, **61**(28), 10822–10832, DOI: **10.1021/acs.inorgchem.2c01106**.

46 B. J. Mincher and S. P. Mezyk, Radiation chemical effects on radiochemistry: A review of examples important to nuclear power, *Radiochim. Acta*, 2009, **97**(9), 519–534, DOI: **10.1524/ract.2009.1646**.

47 K. E. Knope and L. Soderholm, Solution and Solid-State Structural Chemistry of Actinide Hydrates and Their Hydrolysis and Condensation Products, *Chem. Rev.*, 2013, **113**(2), 944–994, DOI: **10.1021/cr300212f**.

48 A. E. V. Gorden and M. L. McKee, Computational Study of Reduction Potentials of Th4+ Compounds and Hydrolysis

Open Access Article. Published on 10 juli 2025. Downloaded on 20-05-2026 01:21:34.
This article is licensed under a Creative Commons Attribution 3.0 Unported Licence.

of ThO2(H_2O)n, n = 1, 2, 4, *J. Phys. Chem. A*, 2016, **120**(41), 8169–8183, DOI: 10.1021/acs.jpca.6b08472.

49 G. P. Horne, T. S. Grimes, P. R. Zalupski, D. S. Meeker, T. E. Albrecht-Schönzart, A. R. Cook and S. P. Mezyk, Curium(III) radiation-induced reaction kinetics in aqueous media, *Dalton Trans.*, 2021, **50**(31), 10853–10859, DOI: 10.1039/D1DT01268A.

50 L. R. Morss, Comparative thermochemical and oxidation-reduction properties of lanthanides and actinides, *Handb. Phys. Chem. Rare Earths*, 1994, **18**, 239–291, DOI: 10.1016/S0168-1273(05)80045-5.

51 N. Mikheev, Lower oxidation states of lanthanides and actinides, *Inorg. Chim. Acta*, 1984, **94**(5), 241–248, DOI: 10.1016/S0020-1693(00)87451-4.

52 F. R. Dutra, M. Vasiliu, A. N. Gomez, D. Xia and D. A. Dixon, Prediction of Redox Potentials for U, Np, Pu, and Am in Aqueous Solution, *J. Phys. Chem. A*, 2024, **128**(28), 5612–5626, DOI: 10.1021/acs.jpca.4c02902.

53 A. V. Gogolev, V. P. Shilov, A. M. Fedoseev and A. K. Pikaev, *Radiokhimiya*, 1990, **32**, 121.

54 K. H. Schmidt, S. Gordon and R. C. Thompson, A pulse radiolysis study of the reduction of neptunium(V) by the hydrated electron, *J. Inorg. Nucl. Chem.*, 1980, **42**(4), 611–615, DOI: 10.1016/0022-1902(80)80093-5.

55 T. M. Nenoff, B. W. Jacobs, D. B. Robinson, P. P. Provencio, J. Huang, S. Ferreira and D. J. Hanson, Synthesis and Low Temperature In Situ Sintering of Uranium Oxide Nanoparticles, *Chem. Mater.*, 2011, **23**(23), 5185–5190, DOI: 10.1021/cm2020669.

56 J. Meesungnoen, J.-P. Jay-Gerin, A. Filali-Mouhim and S. Mankhetkorn, Monte-Carlo calculation of the primary H atom yield in liquid water radiolysis: effects of radiation type and temperature, *Chem. Phys. Lett.*, 2001, **335**(5), 458–464, DOI: 10.1016/S0009-2614(01)00073-2.

57 A. K. Pikaev, V. P. Shilov and A. V. Gogolev, Radiation chemistry of aqueous solutions of actinides, *Russ. Chem. Rev.*, 1997, **66**(9), 763, DOI: 10.1070/RC1997v066n09ABEH000284.

58 R. D. Saini and P. K. Bhattacharyya, Radiolytic oxidation of U(IV) sulphate in aqueous solution by alpha particles from cyclotron, *Int. J. Radiat. Appl. Instrum., Part C*, 1987, **29**(5), 375–379, DOI: 10.1016/1359-0197(87)90009-9.

59 A. V. Gogolev, V. P. Shilov, A. M. Fedoseev and A. K. Pikaev, The study of reactivity of actinide ions towards hydrated electrons and hydrogen atoms in acid aqueous solutions by a pulse radiolysis method, *Int. J. Radiat. Appl. Instrum., Part C*, 1991, **37**(3), 531–535, DOI: 10.1016/1359-0197(91)90031-V.

60 A. V. Gogolev, V. P. Shilov, A. M. Fedoseev and A. K. Pikaev, *Khim. Vys. Energy*, 1991, **25**, 472.

61 V. P. Shilov, A. V. Gogolev, A. M. Fedoseev and A. K. Pikaev, *Khim. Vys. Energy*, 1994, **28**, 114.

62 G. V. Buxton, C. L. Greenstock, W. Phillips Helman and A. B. Ross, Critical review of rate constants for reacitons of hydrated electrons hydrogen atoms and hydroxyl radical in aqueous solution, *J. Phys. Chem. Ref. Data*, 1988, **17**(2), 513–886, DOI: 10.1063/1.555805.

63 F. David, A. G. Maslennikov and V. P. Peretrukhin, Electrochemical reduction of actinide ions in aqueous solution, *J. Radioanal. Nucl. Chem.*, 1990, **143**(2), 415–426, DOI: 10.1007/BF02039610.

64 V. M. Berdnikov, Mechanism of OH Radical Reaction with Variable Valence Ions, *Zh. Fiz. Khim.*, 1973, **47**(11), 2753–2761.

65 E. Codorniu-Hernández and P. G. Kusalik, Mobility Mechanism of Hydroxyl Radicals in Aqueous Solution via Hydrogen Transfer, *J. Am. Chem. Soc.*, 2012, **134**(1), 532–538, DOI: 10.1021/ja208874t.

66 D. Golub, H. Cohen and D. Meyerstein, Kinetics and mechanism of single electron oxidations of the tervalent uranium ion, U3+(aq), by free radicals in aqueous solutions, *J. Chem. Soc., Dalton Trans.*, 1985, **4**, 641–644, DOI: 10.1039/DT9850000641.

67 C. H. Lierse, K. H. Schmidt and J. C. Sullivan, *Radiochim. Acta*, 1988, **44-45**(1), 71–72, DOI: 10.1524/ract.1988.4445.1.71.

68 C. Lierse, K. Schmidt and J. Sullivan, Reactions of radiolytically produced OH radicals with selected actinides in solution, *Radiochim. Acta*, 1988, **44**(1), 71–72.

69 G. R. Choppin and M. P. Jensen, Actinides in Solution: Complexation and Kinetics. in *The Chemistry of the Actinide and Transactinide Elements*, ed. L. R. Morss, N. M. Edelstein and J. Fuger, Springer, Netherlands, 2006, pp. 2524–2621. DOI: 10.1007/1-4020-3598-5_23.

70 J. Plasil, Oxidation–hydration weathering of uraninite: the current state-of-knowledge, *J. Geosci.*, 2014, **59**, 99–114, DOI: 10.3190/jgeosci.163.

71 F. Quilès and A. Burneau, Infrared and Raman spectra of uranyl(VI) oxo-hydroxo complexes in acid aqueous solutions: a chemometric study, *Vib. Spectrosc.*, 2000, **23**(2), 231–241, DOI: 10.1016/S0924-2031(00)00067-9.

72 B. Lottes and K. P. Carter, Capture and Stabilization of the Hydroxyl Radical in a Uranyl Peroxide Cluster, *Chem. – Eur. J.*, 2023, **29**(45), e202300749, DOI: 10.1002/chem.202300749.

73 A. K. Pikaev, V. P. Shilov, N. N. Krot and V. I. Spitsyn, Some aspects of radiation chemistry of aqueous solitions of neptunium and americium ions, *Radiat. Phys. Chem.*, 1980, **15**(2–3), 139–149, DOI: 10.1016/0146-5724(80)90124-7.

74 D. V. Kravchuk, L. J. Augustine, H. Rajapaksha, G. C. Benthin, E. R. Batista, P. Yang and T. Z. Forbes, Insights into the Mechanism of Neptunium Oxidation to the Heptavalent State, *Chem. – Eur. J.*, 2024, **30**(23), e202304049, DOI: 10.1002/chem.202304049.

75 E. Codorniu-Hernández and P. G. Kusalik, Probing the mechanisms of proton transfer in liquid water, *Proc. Natl. Acad. Sci. U. S. A.*, 2013, **110**(34), 13697–13698, DOI: 10.1073/pnas.1312350110.

76 J. A. LaVerne, R. H. Schuler and W. Burns, Track effects in radiation chemistry: production of hydroperoxyl radical

 This journal is © the Partner Organisations 2025

Open Access Article. Published on 10 juli 2025. Downloaded on 20-05-2026 01:21:34.
This article is licensed under a Creative Commons Attribution 3.0 Unported Licence.

within the track core in the heavy-particle radiolysis of water, *J. Phys. Chem.*, 1986, **90**(14), 3238–3242, DOI: 10.1021/j100405a037.

77 M. Hayyan, M. A. Hashim and I. M. AlNashef, Superoxide Ion: Generation and Chemical Implications, *Chem. Rev.*, 2016, **116**(5), 3029–3085, DOI: 10.1021/acs.chemrev.5b00407.

78 A. V. Gogolev, V. P. Shilov and A. K. Pikaev, *Khim. Vys. Energy*, 1996, **30**, 225.

79 D. Meisel, G. Czapski and A. Samuni, Hydroperoxy radical reactions. I. Electron paramagnetic resonance study of the complexation of hydroperoxyl radical with some metal ions, *J. Am. Chem. Soc.*, 1973, **95**(13), 4148–4153, DOI: 10.1021/ja00794a007.

80 J. K. Gibson, W. A. de Jong, P. D. Dau and Y. Gong, Heptavalent Actinide Tetroxides NpO4− and PuO4−: Oxidation of Pu(v) to Pu(vii) by Adding an Electron to PuO4, *J. Phys. Chem. A*, 2017, **121**(47), 9156–9162, DOI: 10.1021/acs.jpca.7b09721.

81 S. K. Scherrer, H. Rajapaksha, D. V. Kravchuk, S. E. Mason and T. Z. Forbes, Impacts of trace level chromium on formation of superoxide within uranyl triperoxide complexes, *Chem. Commun.*, 2024, **60**(76), 10584–10587, DOI: 10.1039/D4CC03194F.

82 A. J. Elliot and D. R. McCracken, Computer modelling of the radiolysis in an aqueous lithium salt blanket: Suppression of radiolysis by addition of hydrogen, *Fusion Eng. Des.*, 1990, **13**(1), 21–27, DOI: 10.1016/0920-3796(90)90028-5.

83 J. A. LaVerne, *Charged Particle and Photon Interactions with Matter: Radiation Chemical Effects of Heavy Ions*, CRC, 1st edn, 2003, pp. 27.

84 O. Roth and J. A. LaVerne, Effect of pH on H_2O_2 Production in the Radiolysis of Water, *J. Phys. Chem. A*, 2011, **115**(5), 700–708, DOI: 10.1021/jp1099927.

85 A. Hiroki, S. M. Pimblott and J. A. LaVerne, Hydrogen Peroxide Production in the Radiolysis of Water with High Radical Scavenger Concentrations, *J. Phys. Chem. A*, 2002, **106**(40), 9352–9358, DOI: 10.1021/jp0207578.

86 P. Bhattacharyya and R. Saini, Radiolytic oxidation of U(iv) to U(vi) in H_2SO4 and HCl media, *Radiat. Phys. Chem.*, 1979, **13**(1), 57–63.

87 V. P. Shilov, A. V. Gogolev and A. K. Pikaev, The formation of neptunium peroxo complexes upon reduction of neptunium(vi) by hydrogen peroxide in concentrated solutions of alkalis, *Mendeleev Commun.*, 1998, **8**(6), 220–221, DOI: 10.1070/MC1998v008n06ABEH000969.

88 I. G. Tananaev and V. I. Dzyubenko, *Radiokhimiya*, 1988, **30**, 842–845.

89 N. N. Krot, V. P. Shilov, V. B. Nikolaevskii, A. K. Pikaev, A. D. Gel'man and V. I. Spitsyn, Production of americium in septivalent state, *Dokl. Akad. Nauk SSSR*, 1974, **217**, 589–592.

90 V. Shilov, Mechanisms of Plutonium (III–VI) Redox Reactions in Solutions with pH above 1, *Radiochemistry*, 2023, **65**(3), 323–329.

91 A. E. Hixon and B. A. Powell, Plutonium environmental chemistry: mechanisms for the surface-mediated reduction of Pu (v/vi), *Environ. Sci.: Processes Impacts*, 2018, **20**(10), 1306–1322, DOI: 10.1039/C7EM00369B.

92 A. K. Pikaev, V. P. Shilov and V. I. Spitsyn, Application of pulsed radiolysis method for investigation of americium (4) properties in aqueous solutions, *Dokl. Akad. Nauk SSSR*, 1977, **232**(2), 387–390.

93 A. K. Pikaev, V. P. Shilov, V. I. Nikolaevskii, N. N. Krot and V. I. Spitsyn, *Radiokhimiya*, 1977, **19**, 720.

94 S. S. Galley, C. E. Van Alstine, L. Maron and T. E. Albrecht-Schmitt, Understanding the Scarcity of Thorium Peroxide Clusters, *Inorg. Chem.*, 2017, **56**(21), 12692–12694, DOI: 10.1021/acs.inorgchem.7b02216.

95 L. E. Sweet, J. F. Corbey, F. Gendron, J. Autschbach, B. K. McNamara, K. L. Ziegelgruber, L. M. Arrigo, S. M. Peper and J. M. Schwantes, Structure and Bonding Investigation of Plutonium Peroxocarbonate Complexes Using Cerium Surrogates and Electronic Structure Modeling, *Inorg. Chem.*, 2017, **56**(2), 791–801, DOI: 10.1021/acs.inorgchem.6b02235.

96 J. Margate, S. Bayle, T. Dumas, E. Dalodière, C. Tamain, D. Menut, P. Estevenon, P. Moisy, S. I. Nikitenko and M. Virot, Chronicles of plutonium peroxides: spectroscopic characterization of a new peroxo compound of Pu (iv), *Chem. Commun.*, 2024, **60**(49), 6260–6263, DOI: 10.1039/D4CC01186D.

97 W. Runde, L. F. Brodnax, G. S. Goff, S. M. Peper, F. L. Taw and B. L. Scott, Synthesis and structural characterization of a molecular plutonium(iv) compound constructed from dimeric building blocks, *Chem. Commun.*, 2007, **17**, 1728–1729, DOI: 10.1039/B617878B.

98 P. C. Burns and M. Nyman, Captivation with encapsulation: a dozen years of exploring uranyl peroxide capsules, *Dalton Trans.*, 2018, **47**(17), 5916–5927, DOI: 10.1039/C7DT04245K.

99 M. Nyman and P. C. Burns, A comprehensive comparison of transition-metal and actinyl polyoxometalates, *Chem. Soc. Rev.*, 2012, **41**(22), 7354–7367, DOI: 10.1039/C2CS35136F.

100 B. M. Lanee Snow and S. Sinkov, Obersvation of radiolytic field alternation of the uranyl cation in bicarbonate solution, in *Materials Research Society Symposium Proceedings*, 2007, 986, p. 177.

101 T. Forbes, P. Horan, T. Devine, D. McInnis and P. Burns, Alteration of dehydrated schoepite and soddyite to studtite, (UO2)(O-2)(H_2O)(2) (H_2O)(2), *Am. Mineral.*, 2011, **96**, 202–206, DOI: 10.2138/am.2011.3517.

102 A. S. Jayasinghe, L. C. Applegate, D. K. Unruh, J. Hutton and T. Z. Forbes, Utilizing Autoxidation of Solvents To Promote the Formation of Uranyl Peroxide Materials, *Cryst. Growth Des.*, 2019, **19**(3), 1756–1766, DOI: 10.1021/acs.cgd.8b01735.

103 D. V. Kravchuk and T. Z. Forbes, In Situ Generation of Organic Peroxide to Create a Nanotubular Uranyl Peroxide Phosphate, *Angew. Chem., Int. Ed.*, 2019, **58**(51), 18429–18433, DOI: 10.1002/anie.201910287.

Open Access Article. Published on 10 juli 2025. Downloaded on 20-05-2026 01:21:34.
This article is licensed under a Creative Commons Attribution 3.0 Unported Licence.

104 D. V. Kravchuk, N. N. Dahlen, S. J. Kruse, C. D. Malliakas, P. M. Shand and T. Z. Forbes, Isolation and Reactivity of Uranyl Superoxide, *Angew. Chem., Int. Ed.*, 2021, **60**(27), 15041–15048, DOI: 10.1002/anie.202103039.

105 K.-A. Kubatko and P. C. Burns, Expanding the Crystal Chemistry of Actinyl Peroxides: Open Sheets of Uranyl Polyhedra in Na5[(UO2)3(O2)4(OH)3](H2O)13, *Inorg. Chem.*, 2006, **45**(16), 6096–6098, DOI: 10.1021/ic0518677.

106 G. E. Sigmon, B. Weaver, K.-A. Kubatko and P. C. Burns, Crown and Bowl-Shaped Clusters of Uranyl Polyhedra, *Inorg. Chem.*, 2009, **48**(23), 10907–10909, DOI: 10.1021/ic9020355.

107 A. Arteaga, L. Zhang, S. Hickam, M. Dembowski, P. C. Burns and M. Nyman, Uranyl–Peroxide Capsule Self-Assembly in Slow Motion, *Chem. – Eur. J.*, 2019, **25**(24), 6087–6091, DOI: 10.1002/chem.201806227.

108 B. Vlaisavljevich, L. Gagliardi and P. C. Burns, Understanding the Structure and Formation of Uranyl Peroxide Nanoclusters by Quantum Chemical Calculations, *J. Am. Chem. Soc.*, 2010, **132**(41), 14503–14508, DOI: 10.1021/ja104964x.

109 D. E. Felton, M. Fairley, A. Arteaga, M. Nyman, J. A. LaVerne and P. C. Burns, Gamma-Ray-Induced Formation of Uranyl Peroxide Cage Clusters, *Inorg. Chem.*, 2022, **61**(30), 11916–11922, DOI: 10.1021/acs.inorgchem.2c01657.

110 S. Hickam, D. Ray, J. E. S. Szymanowski, R.-Y. Li, M. Dembowski, P. Smith, L. Gagliardi and P. C. Burns, Neptunyl Peroxide Chemistry: Synthesis and Spectroscopic Characterization of a Neptunyl Triperoxide Compound, Ca2[NpO2(O2)3]·9H2O, *Inorg. Chem.*, 2019, **58**(18), 12264–12271, DOI: 10.1021/acs.inorgchem.9b01712.

111 V. P. Shilov and A. M. Fedoseev, Oxidation of Np(IV) with hydrogen peroxide in carbonate solutions, *Radiochemistry*, 2013, **55**(3), 287–290, DOI: 10.1134/S1066362213030077.

112 V. P. Shilov and A. M. Fedoseev, Reaction of Np(VI) with H_2O_2 in carbonate solutions, *Radiochemistry*, 2010, **52**(3), 245–249, DOI: 10.1134/S1066362210030045.

113 P. C. Burns, K.-A. Kubatko, G. Sigmon, B. J. Fryer, J. E. Gagnon, M. R. Antonio and L. Soderholm, Actinyl Peroxide Nanospheres, *Angew. Chem., Int. Ed.*, 2005, **44**(14), 2135–2139, DOI: 10.1002/anie.200462445.

114 J. Qiu and P. C. Burns, Clusters of Actinides with Oxide, Peroxide, or Hydroxide Bridges, *Chem. Rev.*, 2013, **113**(2), 1097–1120, DOI: 10.1021/cr300159x.

115 C. Maillard and J.-M. Adnet, Plutonium(IV) peroxide formation in nitric medium and kinetics Pu(VI) reduction by hydrogen peroxide, *Radiochim. Acta*, 2001, **89**(8), 485–490, DOI: 10.1524/ract.2001.89.8.485.

116 K. Nash, M. E. Noon, S. Fried and J. C. Sullivan, The reaction between Pu(VI) and H_2O_2 in aqueous bicarbonate media. Formation of a Pu(VI) H_2O_2 complex (1), *Inorg. Nucl. Chem. Lett.*, 1980, **16**(1), 33–35, DOI: 10.1016/0020-1650(80)80089-4.

117 V. S. Koltunov, *Kinetics of Actinide Reactions*, Atomizdat, Moscow, 1974.

118 S. T. Arm, Direct Dissolution of Used Nuclear Fuel in PUREX Solvent: Review and Flowsheet Development, *Nucl. Technol.*, 2022, **208**(7), 1124–1136, DOI: 10.1080/00295450.2021.2018274.

119 Y. Katsumura, P. Jiang, R. Nagaishi, T. Oishi, K. Ishigure and Y. Yoshida, Pulse radiolysis study of aqueous nitric acid solutions: formation mechanism, yield, and reactivity of NO3 radical, *J. Phys. Chem.*, 1991, **95**(11), 4435–4439, DOI: 10.1021/j100164a050.

120 A. J. Elliot, A pulse radiolysis study of the temperature dependence of reactions involving H, OH and e-aq in aqueous solutions, *Int. J. Radiat. Appl. Instrum., Part C*, 1989, **34**(5), 753–758, DOI: 10.1016/1359-0197(89)90279-8.

121 A. J. Elliot and F. C. Sopchyshyn, The radiolysis at room temperature and 118 °C of aqueous solutions containing sodium nitrate and either sodium formate or 2-propanol, *Can. J. Chem.*, 1983, **61**(7), 1578–1582, DOI: 10.1139/v83-274.

122 M. Faraggi, D. Zehavi and M. Anbar, Radiolysis of aqueous nitrate solutions, *Trans. Faraday Soc.*, 1971, **67**, 701–710, DOI: 10.1039/TF9716700701.

123 F. Miner and J. Seed, Radiation chemistry of plutonium nitrate solutions, *Chem. Rev.*, 1967, **67**(3), 299–315, DOI: 10.1021/cr60247a003.

124 T. S. Grimes, G. P. Horne, C. J. Dares, S. M. Pimblott, S. P. Mezyk and B. J. Mincher, Kinetics of the Autoreduction of Hexavalent Americium in Aqueous Nitric Acid, *Inorg. Chem.*, 2017, **56**(14), 8295–8301, DOI: 10.1021/acs.inorgchem.7b00990.

125 G. P. Horne, C. R. Gregson, H. E. Sims, R. M. Orr, R. J. Taylor and S. M. Pimblott, Plutonium and americium alpha radiolysis of nitric acid solutions, *J. Phys. Chem. B*, 2017, **121**(4), 883–889, DOI: 10.1021/acs.jpcb.6b12061.

126 G. P. Horne, T. S. Grimes, B. J. Mincher and S. P. Mezyk, Reevaluation of Neptunium–Nitric Acid Radiation Chemistry by Multiscale Modeling, *J. Phys. Chem. B*, 2016, **120**(49), 12643–12649, DOI: 10.1021/acs.jpcb.6b09683.

127 P.-Y. Jiang, R. Nagaishi, T. Yotsuyanagi, Y. Katsumura and K. Ishigure, γ-Radiolysis study of concentrated nitric acid solutions, *J. Chem. Soc., Faraday Trans.*, 1994, **90**(1), 93–95, DOI: 10.1039/FT9949000093.

128 P. Y. Jiang, Y. Katsumura, K. Ishigure and Y. Yoshida, Reduction potential of the nitrate radical in aqueous solution, *Inorg. Chem.*, 1992, **31**(24), 5135–5136, DOI: 10.1021/ic00050a038.

129 R. Nagaishi, A model for radiolysis of nitric acid and its application to the radiation chemistry of uranium ion in nitric acid medium, *Radiat. Phys. Chem.*, 2001, **60**(4), 369–375, DOI: 10.1016/S0969-806X(00)00410-2.

130 J. W. Boyle and H. A. Mahlman, Radiation-Induced Decomposition of Thorium Nitrate Solutions, *Nucl. Sci. Eng.*, 1957, **2**(4), 492–500, DOI: 10.13182/NSE57-A25414.

131 V. P. Shilov, A. V. Gogolev, A. M. Fedoseev and A. K. Pikaev, Invstigation of reactivity of neptunoyl-ions to

This journal is © the Partner Organisations 2025

Open Access Article. Published on 10 juli 2025. Downloaded on 20-05-2026 01:21:34.
This article is licensed under a Creative Commons Attribution 3.0 Unported Licence.

inorganic free radicals by pulse radiolysis method, *Izv. Akad. Nauk SSSR, Ser. Khim.*, 1986, 456–458.

132 A. V. Gogolev, V. P. Shilov, A. M. Fedoseev, I. E. Makarov and A. K. Pikaev, Reactivity of neptunium and plutonium in relation to inorganic free radicals in aqueous solutions, *Radiokhimiya*, 1988, **30**(6), 761–766.

133 Z. R. Turel and P. R. Natarajan, *Lanthanide Actinide Res.*, 1990, **3**, 87–90.

134 M. Nagar and P. Natarajan, Studies on radiolytic oxidation of plutonium(III) in hydrochloric acid medium, *Int. J. Radiat. Appl. Instrum., Part C*, 1987, **30**(3), 169–172, DOI: **10.1016/1359-0197(87)90074-9**.

135 V. Ermakov, A. Rykov, G. Timofeev and G. Yakovlev, Investigations of the Kinetics of Redoc Reactions of the Actinide Elements. XX. Kinetics and Mechanism of the Interactions of Americium(III) and(V) with Peroxydisulfate ions in Nitric Acide Solution, *Sov. Radiochem. Engl. Transl.*, 1971, **13**(6), 851–857.

136 A. Ohyoshi, A. Jyo and T. Shinohara, Kinetics of the Reaction of Americium(III) with Peroxydisulfate, *Bull. Chem. Soc. Jpn.*, 1971, **44**(11), 3047–3051, DOI: **10.1246/bcsj.44.3047**.

137 L. B. Asprey, S. E. Stephanou and R. A. Penneman, A New Valence State of Americium, Am(VI), *J. Am. Chem. Soc.*, 1950, **72**(3), 1425–1426, DOI: **10.1021/ja01159a528**.

138 L. B. Asprey, S. E. Stephanou and R. A. Penneman, Hexavalent Americium1, *J. Am. Chem. Soc.*, 1951, **73**(12), 5715–5717, DOI: **10.1021/ja01156a065**.

139 L. M. Frolova, A. A. Frolov and V. Y. Vasil'ev, Radiation-chemical behaviour of neptunium ions in nitric acid solutions in the presence of curium-244, *Radiokhimiya*, 1984, **26**(1), 108–114.

140 G. Garaix, L. Venault, A. Costagliola, J. Maurin, M. Guigue, R. Omnee, G. Blain, J. Vandenborre, M. Fattahi, N. Vigier, *et al.*, Alpha radiolysis of nitric acid and sodium nitrate with 4He2+ beam of 13.5 MeV energy, *Radiat. Phys. Chem.*, 2015, **106**, 394–403, DOI: **10.1016/j.radphyschem.2014.08.008**.

141 M. Pages, Radiolysis of aqueous solutions of plutonium, *J. Chim. Phys. Phys.-Chim. Biol.*, 1962, **59**, 63.

142 A. V. Gogolev, I. E. Makarov and A. K. Pikaev, in *Proceedings of the VIth Tihany Symposium on Radiation Chemistry*, ed. E. P. Hedvig, Akademia Kiado, Budapest, 1987, pp. 161.

143 M. V. Vladimirova, I. A. Kulikov, O. A. Sosnovskii and A. A. Ryabova, Reduction of PuO22+ ions during gamma-radiolysis in aqueous solutions of HNO3, *At. Energy*, 1981, **51**(1), 55–57.

144 P. Di Bernardo, P. Zanonato, L. Rao, A. Bismondo and F. Endrizzi, Interaction of thorium(IV) with nitrate in aqueous solution: medium effect or weak complexation?, *Dalton Trans.*, 2011, **40**(36), 9101–9105, DOI: **10.1039/C1DT10325C**.

145 R. J. Lemire, J. Fuger, H. Nitsche, P. E. Potter, M. H. Rand, J. Rydberg, K. Spahiu, J. C. Sullivan, W. J. Ullman, P. Vitorge and H. Wanner, *Chemical Thermodynamics of Neptunium and Plutonium*, North Holland Elsevier Science Publishers, 2001.

146 M. Rand, J. Fuger, V. Neck, I. Grenthe and D. Rai, *Chemical Thermodynamics of Thorium*, 2008.

147 M. V. Vladimirova and O. A. Sosnovskii, Radiation-chemical reduction of PuO22+ and NpO22+ ions in the case of their simultaneous presence in HNO3 soutions, *Radiokhimiya*, 1980, **22**, 662–670.

148 M. V. Vladimirova, Radiation-chemical reduction of Pu(6) in 0.3–6.0 M HNO3, *Radiokhimiya*, 1980, **22**(5), 686–691.

149 S. D. Reilly and M. P. Neu, Pu(VI) Hydrolysis: Further Evidence for a Dimeric Plutonyl Hydroxide and Contrasts with U(VI) Chemistry, *Inorg. Chem.*, 2006, **45**(4), 1839–1846, DOI: **10.1021/ic051760j**.

150 R. Maurice, E. Renault, Y. Gong, P. X. Rutkowski and J. K. Gibson, Synthesis and Structures of Plutonyl Nitrate Complexes: Is Plutonium Heptavalent in PuO3(NO3)2− ?, *Inorg. Chem.*, 2015, **54**(5), 2367–2373, DOI: **10.1021/ic502969w**.

151 N. N. Andreichuk, K. V. Rotmanov, A. A. Frolov and V. Y. Vasil'ev, Reduction of Pu (6) in nitric acid solutions at alpha-irradiation, *Radiokhimiya*, 1984, **26**(1), 94–98.

152 N. N. Andreichuk, V. Y. Vasil'ev, N. B. Vysokoostrovskaya, V. M. Kalashnikov, V. I. Karasev, E. A. Karelin, V. B. Mishinev, V. M. Nikolaev and S. V. Osipov, Oxidation of plutonium (4) in nitric acid solutions with high specifi alpha-radioactivity, *Radiokhimiya*, 1976, **18**(1), 89–92.

153 M. V. Vladimirova, I. A. Kulikov, O. A. Sosnovskii and A. A. Ryabova, Reduction of PuO22+ in gamma radiolysis in aqueous HNO3, *Sov. At. Energy*, 1981, **51**, 475–478, DOI: **10.1007/BF01122566**.

154 M. Vladimirova, I. Kulikov, A. Ryabova and A. Milovanova, Radiation chemistry of Pu and Np aqueous solutions, *Radiokhimiya*, 1976, **18**(1), 172–177.

155 S. G. Patra, A. Mizrahi and D. Meyerstein, The Role of Carbonate in Catalytic Oxidations, *Acc. Chem. Res.*, 2020, **53**(10), 2189–2200, DOI: **10.1021/acs.accounts.0c00344**.

156 G. V. Buxton and A. J. Elliot, Rate constant for reaction of hydroxyl radicals with bicarbonate ions, *Int. J. Radiat. Appl. Instrum., Part C*, 1986, **27**(3), 241–243, DOI: **10.1016/1359-0197(86)90059-7**.

157 A. K. Pikaev, A. V. Gogolev and V. P. Shilov, Redox reactions of neptunium and plutonium in alkaline aqueous solutions upon gamma radiolysis, *Radiat. Phys. Chem.*, 1999, **56**(4), 483–491, DOI: **10.1016/S0969-806X(99)00334-5**.

158 A. Ikeda-Ohno, S. Tsushima, K. Takao, A. Rossberg, H. Funke, A. C. Scheinost, G. Bernhard, T. Yaita and C. Hennig, Neptunium Carbonato Complexes in Aqueous Solution: An Electrochemical, Spectroscopic, and Quantum Chemical Study, *Inorg. Chem.*, 2009, **48**(24), 11779–11787, DOI: **10.1021/ic901838r**.

159 L. Maya, Hydrolysis and carbonate complexation of dioxo-neptunium(V) in 1.0 M sodium perchlorate at 25.degree.C, *Inorg. Chem.*, 1983, **22**(14), 2093–2095, DOI: **10.1021/ic00156a031**.

Open Access Article. Published on 10 juli 2025. Downloaded on 20-05-2026 01:21:34.
This article is licensed under a Creative Commons Attribution 3.0 Unported Licence.

160 D. L. Clark, D. E. Hobart, P. D. Palmer, J. C. Sullivan and B. E. Stout, ^{13}C NMR characterization of actinyl(VI) carbonate complexes in aqueous solution, *J. Alloys Compd.*, 1993, **193**(1), 94–97, DOI: 10.1016/0925-8388(93)90319-I.

161 D. W. Wester and J. C. Sullivan, Electrochemical and spectroscopic studies of neptunium(VI), -(V) and -(IV) in carbonate-bicarbonate buffers, *J. Inorg. Nucl. Chem.*, 1981, **43**(11), 2919–2923, DOI: 10.1016/0022-1902(81)80643-4.

162 G. Ingmar, C. Riglet and P. Vitorge, Studies of metal-carbonate complexes. 13. Composition and equilibria of trinuclear neptunium(VI)- and plutonium(VI)-carbonate complexes, *Inorg. Chem.*, 1986, **25**(10), 1679–1684, DOI: 10.1021/ic00230a031.

163 L. Maya, Hydrolysis and carbonate complexation of dioxouranium(VI) in the neutral-pH range at 25.degree.C, *Inorg. Chem.*, 1982, **21**(7), 2895–2898, DOI: 10.1021/ic00137a077.

164 C. Madic, D. E. Hobart and G. M. Begun, Raman spectrometric studies of actinide(V) and -(VI) complexes in aqueous sodium carbonate solution and of solid sodium actinide(V) carbonate compounds, *Inorg. Chem.*, 1983, **22**(10), 1494–1503, DOI: 10.1021/ic00152a015.

165 M. I. Pratopo, T. Yamaguchi, H. Moriyama and K. Higashi, Adsorption of Np(IV) on Quartz in Carbonate Solutions, *Radiochim. Acta*, 1991, **55**, 209–213.

166 T. Yamaguchi, M. Pratopo, H. Moriyama and K. Higashi, Adsorption of cesium and neptunium(V) on bentonite, in *Proceedings of the third international conference on nuclear fuel reprocessing and waste management, RECOD'91*, 1991.

167 A. V. Gogolev, V. P. Shilov, A. M. Fedoseev and A. K. Pikaev, *Izv. Akad. Nauk SSSR, Ser. Khim.*, 1990, **2**, 8.

168 A. V. Gogolev, A. M. Fedoseev, V. P. Shilov and A. K. Pikaev, Kinetics of the radiation chemical reactions of tervalent and quadrivalent actinides and lanthanides in carbonate solutions, *Bull. Acad. Sci. USSR, Div. Chem. Sci.*, 1990, **39**, 21–25, DOI: 10.1007/BF00962995.

169 S. Gordon, J. Sullivan and A. B. Ross, Rate Constants for Reactions of Radiation–Produced Transients in Aqueous Solutions of Actinides, *J. Phys. Chem. Ref. Data*, 1986, **15**(4), 1357–1367, DOI: 10.1063/1.555768.

170 H. Nitsche and R. J. Silva, Investigation of the Carbonate Complexation of Pu(IV) in Aqueous Solution, *Radiochim. Acta*, 1996, **72**(2), 65–72, DOI: 10.1524/ract.1996.72.2.65.

171 W. A. Mulac, S. Gordon, K. H. Schmidt, D. Wester and J. C. Sullivan, Reactions of uranium(V), neptunium(V), and plutonium(V) with the carbonate radical, *Inorg. Chem.*, 1984, **23**(12), 1639–1641.

172 H. Capdevila, P. Vitorge, E. Giffaut and L. Delmau, Spectrophotometric Study of the Dissociation of the Pu(IV) Carbonate Limiting Complex, *Radiochim. Acta*, 1996, **74**(1), 93–98, DOI: 10.1524/ract.1996.74.special-issue.93.

173 R. E. Huie, C. L. Clifton and P. Neta, Electron transfer reaction rates and equilibria of the carbonate and sulfate radical anions, *Int. J. Radiat. Appl. Instrum., Part C*, 1991, **38**(5), 477–481, DOI: 10.1016/1359-0197(91)90065-A.

174 A. K. Pikaev and V. I. Zolotarevskii, Pulse radiolysis of aqueous solutions of sulfuric acid, *Bull. Acad. Sci. USSR, Div. Chem. Sci.*, 1967, **16**(1), 181–182, DOI: 10.1007/BF00907128.

175 P.-Y. Jiang, Y. Katsumura, R. Nagaishi, M. Domae, K. Ishikawa, K. Ishigure and Y. Yoshida, Pulse radiolysis study of concentrated sulfuric acid solutions. Formation mechanism, yield and reactivity of sulfate radicals, *J. Chem. Soc., Faraday Trans.*, 1992, **88**(12), 1653–1658, DOI: 10.1039/FT9928801653.

176 A. V. Gogolev, V. P. Shilov, A. M. Fedoseev and A. K. Pikaev, The Use of Conjugated Scavengers to Determine the Rate Constants of Fast Reactions in Aqueous Solutions by Pulse Radiolysis, *Mendeleev Commun.*, 1993, **3**(4), 155–156, DOI: 10.1070/MC1993v003n04ABEH000265.

177 A. K. Pikaev, A. V. Gogolev, V. P. Shilov and A. M. Fedoseev, Reactivity of ions of actinides towards inorganic free radicals in irradiated aqueous solutions, *Isotopenpraxis*, 1990, **26**(10), 465–469.

178 P. Hedvig, L. Nyikos, J. Dobó and R. Schiller, Proceedings of the Sixth Tihany Symposium on Radiation Chemistry: The 6th Tihany Symposium on Radiation Chemistry, Held at Balatonszéplak, Hungary, 21–26 September 1986, Organized by the Radiation Chemical Section of the Hungarian Chemical Society, in Co-operation with the International Atomic Energy Agency, Vienna, Akadémiai Kiadó, 1987.

179 A. K. Pikaev, V. P. Shilov and A. V. Gogolev, Radiation chemistry of aqueous solutions of actinides, *Usp. Khim.*, 1997, **66**, 845–873.

180 V. P. Shilov, A. V. Gogolev and A. K. Pikaev, Unusual radiolytic behavior of neptunium ions in aqueous bicarbonate solutions, *Dokl. Akad. Nauk*, 2000, **375**(3), 362–365.

181 A. V. Gogolev, V. P. Shilov, A. M. Fedoseev and A. K. Pikaev, Investigation of reactivity of neptunoyl-ions to inorganic free radicals by pulse radiolysis method. [Electrons], *Izv. Akad. Nauk SSSR, Ser. Khim.*, 1986, **2**, 456–458.

182 J. Boyle, J. Ghormley, C. Hochanadel, W. Kieffer and T. Sworski, The Radiation Chemistry of Aqueous Reactor Solutions, *Nucl. Sci. Eng. Technol.*, 1953, **3**, 25–42.

183 R. E. Wilson, Structural Periodicity in the Coordination Chemistry of Aqueous Pu(IV) Sulfates, *Inorg. Chem.*, 2012, **51**(16), 8942–8947, DOI: 10.1021/ic301025f.

184 G. E. Boris, Kinetics, mechanism and intermediates of some radiation-induced reactions in aqueous solutions, *Russ. Chem. Rev.*, 2004, **73**(1), 101, DOI: 10.1070/RC2004v073n01ABEH000865.

185 M. Domae, Y. Katsumura, P. Jiang, R. Nagaishi, K. Ishigure, T. Kozawa and Y. Yoshida, Pulse and γ-radiolysis of concentrated perchloric acid solutions, *J. Chem. Soc., Faraday Trans.*, 1996, **92**(12), 2245–2250.

186 C. Lierse, J. C. Sullivan and K. H. Schmidt, Rates of oxidation of selected actinides by Cl2, *Inorg. Chem.*, 1987, **26**(9), 1408–1410.

187 K. V. Rotmanov, N. N. Andreichuk and V. Y. Yasil'ev, Investigation of alpha-radiation effect on valent states of

 This journal is © the Partner Organisations 2025

Open Access Article. Published on 10 juli 2025. Downloaded on 20-05-2026 01:21:34.
This article is licensed under a Creative Commons Attribution 3.0 Unported Licence.

actinoids 14. Valent transformations of neptunium under alpha-irradiation of perchloric solutions, *Radiokhimiya*, 1995, **37**(1), 38–43.

188 T. W. Newton, D. E. Hobart and P. D. Palmer, The Formation of Pu(IV)-Colloid by the Alpha-reduction of Pu(V) or Pu(VI) in Aqueous Solutions, *Radiochim. Acta*, 1986, **39**(3), 139–148, DOI: 10.1524/ract.1986.39.3.139.

189 A. A. Frolov, L. M. Frolova and V. Y. Vasil'ev, Behavious of americium and berkelium ions in solutions under intensive alpha irradiation, *Radiokhimiya*, 1987, **29**(1), 79–87.

190 A. J. Zielen, J. C. Sullivan and D. Cohen, The photochemical reduction and the autoreduction of neptunium(VI), *J. Inorg. Nucl. Chem.*, 1958, **7**(4), 378–383, DOI: 10.1016/0022-1902(58)80246-8.

191 L. Manes and U. Benedict, Structural and thermodynamic properties of actinide solids and their relation to bonding, in *Actinides—Chemistry and Physical Properties*, ed. L. Manes, Springer Berlin Heidelberg, Berlin, Heidelberg, 1985, pp. 75–126.

192 J. Su, P. D. Dau, Y.-H. Qiu, H.-T. Liu, C.-F. Xu, D.-L. Huang, L.-S. Wang and J. Li, Probing the Electronic Structure and Chemical Bonding in Tricoordinate Uranyl Complexes UO2X3− (X = F, Cl, Br, I): Competition between Coulomb Repulsion and U–X Bonding, *Inorg. Chem.*, 2013, **52**(11), 6617–6626, DOI: 10.1021/ic4006482.

193 Q.-Y. Wu, C.-Z. Wang, J.-H. Lan, Z.-F. Chai and W.-Q. Shi, Electronic structures and bonding of the actinide halides An(TRENTIPS)X (An = Th–Pu; X = F–I): a theoretical perspective, *Dalton Trans.*, 2020, **49**(44), 15895–15902, DOI: 10.1039/D0DT02909B.

194 B. D. Hanson, B. McNamara, E. C. Buck, J. I. Friese, E. Jenson, K. Krupka and B. W. Arey, Corrosion of commercial spent nuclear fuel. 1. Formation of studtite and metastudtite, *Radiochim. Acta*, 2005, **93**(3), 159–168, DOI: 10.1524/ract.93.3.159.61613.

195 R. S. Forsyth and L. O. Werme, Spent fuel corrosion and dissolution, *J. Nucl. Mater.*, 1992, **190**, 3–19, DOI: 10.1016/0022-3115(92)90071-R.

196 S. J. Zinkle and G. S. Was, Materials challenges in nuclear energy, *Acta Mater.*, 2013, **61**(3), 735–758, DOI: 10.1016/j.actamat.2012.11.004.

197 M. I. Ojovan and O. G. Batyukhnova, Glasses for Nuclear Waste Immobilization WM'07 Conference, 2007 Waste Management Symposium – Global Accomplishments in Environmental and Radioactive Waste Management: Education and Opportunity for Next Generation of Waste Management Professionals, Tuscon, AZ, 2007.

198 S. Gin, P. Jollivet, M. Tribet, S. Peuget and S. Schuller, Radionuclides containment in nuclear glasses: an overview, *Radiochim. Acta*, 2017, **105**(11), 927–959, DOI: 10.1515/ract-2016-2658.

199 L. Thomé, S. Moll, A. Debelle, F. Garrido, G. Sattonnay and J. Jagielski, Radiation effects in nuclear ceramics, *Adv. Mater. Sci. Eng.*, 2012, **2012**(1), 905474, DOI: 10.1155/2012/905474.

200 W. J. Weber, Radiation and Thermal Ageing of Nuclear Waste Glass, *Procedia Mater. Sci.*, 2014, **7**, 237–246, DOI: 10.1016/j.mspro.2014.10.031.

201 M. Kurian and S. Thankachan, Introduction: Ceramics classification and applications, in *Ceramic catalysts*, Elsevier, 2023, pp. 1–17.

202 L. Y. Lin, D. Leitner, C. Benatti, G. Perdikakis, S. W. Krause, R. Rencsok, S. Nash and W. Wittmer, Investigation of ion induced damage in KBr, YAG:Ce, CaF2:Eu and CsI:Tl irradiated by various-energy protons, *J. Instrum.*, 2015, **10**(3), P03024, DOI: 10.1088/1748-0221/10/03/P03024.

203 K. Matsunaga, N. Narita, I. Tanaka and H. Adachi, Electronic states of F-centers in alkali halide crystals, *J. Phys. Soc. Jpn.*, 1996, **65**(8), 2564–2570, DOI: 10.1143/jpsj.65.2564.

204 F. Illas and G. Pacchioni, Optical properties of surface and bulk F centers in MgO from ab initio cluster model calculations, *J. Chem. Phys.*, 1998, **108**(18), 7835–7841, DOI: 10.1063/1.476220.

205 V. Vinetskiĭ, Y. K. Kalnin, E. Kotomin and A. Ovchinnikov, Radiation-stimulated aggregation of Frenkel defects in solids, *Sov. Phys. Usp.*, 1990, **33**(10), 793, DOI: 10.1070/PU1990v033n10ABEH002634.

206 T. R. Griffiths and J. Dixon, Electron irradiation of single crystal thorium dioxide and electron transfer reactions, *Inorg. Chim. Acta*, 2000, **300–302**, 305–313, DOI: 10.1016/S0020-1693(99)00597-6.

207 W. J. Weber and H. J. Matzke, Radiation effects in actinide host phases, *Radiat. Eff.*, 1986, **98**(1–4), 93–99, DOI: 10.1080/00337578608206101.

208 W. J. Weber, R. C. Ewing, C. Catlow, T. D. De La Rubia, L. W. Hobbs, C. Kinoshita, A. Motta, M. Nastasi, E. Salje and E. Vance, Radiation effects in crystalline ceramics for the immobilization of high-level nuclear waste and plutonium, *J. Mater. Res.*, 1998, **13**(6), 1434–1484, DOI: 10.1557/JMR.1998.0205.

209 C. L. Tracy, M. Lang, F. Zhang, S. Park, R. I. Palomares and R. C. Ewing, Review of recent experimental results on the behavior of actinide-bearing oxides and related materials in extreme environments, *Prog. Nucl. Energy*, 2018, **104**, 342–358, DOI: 10.1016/j.pnucene.2016.09.012.

210 Y. Ren, M. Shu, D. Xu, M. Liu, X. Dai, S. Wang and L. Li, Overview on Radiation Damage Effects and Protection Techniques in Microelectronic Devices, *Sci. Technol. Nucl. Install.*, 2024, **17**, 3616902, DOI: 10.1155/2024/3616902.

211 C. H. Booth, Y. Jiang, S. A. Medling, D. L. Wang, A. L. Costello, D. S. Schwartz, J. N. Mitchell, P. H. Tobash, E. D. Bauer, S. K. McCall, M. A. Wall and P. G. Allen, Self-irradiation damage to the local structure of plutonium and plutonium intermetallics, *J. Appl. Phys.*, 2013, **113**(9), 093502, DOI: 10.1063/1.4794016.

212 W. G. Wolfer, Radiation effects in plutonium, *Los Alamos Sci.*, 2000, **26**(2), 274–285.

213 I. Muller and W. J. Weber, Plutonium in crystalline ceramics and glasses, *MRS Bull.*, 2001, **26**(9), 698–706, DOI: 10.1557/mrs2001.180.

Open Access Article. Published on 10 juli 2025. Downloaded on 20-05-2026 01:21:34.
This article is licensed under a Creative Commons Attribution 3.0 Unported Licence.

214 D. M. Strachan, R. D. Scheele, J. P. Icenhower, E. C. Buck, A. E. Kozelisky, R. L. Sell, R. J. Elovich and W. C. Buchmiller, *Radiation Damage Effects in Candidate Ceramics for Plutonium Immobilization: Final Report*, PNNL-14588; NN6001020; TRN: US0401443, United States, 2004. DOI: 10.2172/15007189.

215 W. Goll, H.-P. Fuchs, R. Manzel and F. U. Schlemmer, Irradiation behavior of UO2/PuO2 fuel in light water reactors, *Nucl. Technol.*, 1993, **102**(1), 29–46, DOI: 10.13182/NT93-A34800.

216 J. Arborelius, K. Backman, L. Hallstadius, M. Limbäck, J. Nilsson, B. Rebensdorff, G. Zhou, K. Kitano, R. Löfström and G. Rönnberg, Advanced doped UO2 pellets in LWR applications, *J. Nucl. Sci. Technol.*, 2006, **43**(9), 967–976, DOI: 10.1080/18811248.2006.9711184.

217 T. R. Griffiths and J. Dixon, Optical absorption spectroscopy of thorium dioxide. Analysis of oxidising and reducing anneals and gamma and UV radiation on both flux-grown and arc-fused single crystals, *J. Chem. Soc., Faraday Trans.*, 1992, **88**(8), 1149–1160, DOI: 10.1039/FT9928801149, Scopus.

218 V. I. Neeley, J. B. Gruber and W. J. F. Gray, Centers in Thorium Oxide, *Phys. Rev.*, 1967, **158**(3), 809–813, DOI: 10.1103/PhysRev.158.809.

219 B. G. Childs, P. J. Harvey and J. B. Hallett, Color Centers and Point Defects in Irradiated Thoria, *J. Am. Ceram. Soc.*, 1970, **53**(8), 431–435, DOI: 10.1111/j.1151-2916.1970.tb12671.x.

220 P. Jegadeesan, S. Amirthapandian, G. Kaur, D. S. Kumar, A. Das, D. K. Avasthi, K. Ananthasivan and B. K. Panigrahi, Investigations on ion irradiation induced modifications in Th 5f occupancy in thoria, *J. Nucl. Mater.*, 2022, **570**, 153961, DOI: 10.1016/j.jnucmat.2022.153961.

221 C. A. Dennett, W. R. Deskins, M. Khafizov, Z. Hua, A. Khanolkar, K. Bawane, L. Fu, J. M. Mann, C. A. Marianetti, L. He, *et al.*, An integrated experimental and computational investigation of defect and microstructural effects on thermal transport in thorium dioxide, *Acta Mater.*, 2021, **213**, 116934, DOI: 10.1016/j.actamat.2021.116934.

222 K. Bawane, X. Liu, T. Yao, M. Khafizov, A. French, J. M. Mann, L. Shao, J. Gan, D. H. Hurley and L. He, TEM characterization of dislocation loops in proton irradiated single crystal ThO2, *J. Nucl. Mater.*, 2021, **552**, 152998, DOI: 10.1016/j.jnucmat.2021.152998.

223 C. A. Dennett, Z. Hua, A. Khanolkar, T. Yao, P. K. Morgan, T. A. Prusnick, N. Poudel, A. French, K. Gofryk, L. He, *et al.*, The influence of lattice defects, recombination, and clustering on thermal transport in single crystal thorium dioxide, *APL Mater.*, 2020, **8**(11), 111103, DOI: 10.1063/5.0025384.

224 J. Park, E. B. Farfán, K. Mitchell, A. Resnick, C. Enriquez and T. Yee, Sensitivity of thermal transport in thorium dioxide to defects, *J. Nucl. Mater.*, 2018, **504**, 198–205, DOI: 10.1016/j.jnucmat.2018.03.043.

225 M. Bricout, C. Onofri, A. Debelle, Y. Pipon, R. C. Belin, F. Garrido, F. Leprêtre and G. Gutierrez, Radiation damage in uranium dioxide: Coupled effect between electronic and nuclear energy losses, *J. Nucl. Mater.*, 2020, **531**, 151967, DOI: 10.1016/j.jnucmat.2019.151967.

226 M. Beauvy, C. Dalmasso and P. Iacconi, Irradiation effects of swift heavy ions in actinide oxides and actinide nitrides: Structure and optical properties, *Nucl. Instrum. Methods Phys. Res., Sect. B*, 2006, **250**(1), 137–141, DOI: 10.1016/j.nimb.2006.04.096.

227 G. Guimbretière, L. Desgranges, A. Canizarès, G. Carlot, R. Caraballo, C. Jégou, F. Duval, N. Raimboux, M. R. Ammar and P. Simon, Determination of in-depth damaged profile by Raman line scan in a pre-cut He2+ irradiated UO2, *Appl. Phys. Lett.*, 2012, **100**(25), 251914, DOI: 10.1063/1.4729588.

228 D. Horlait, F. Lebreton, P. Roussel and T. Delahaye, XRD Monitoring of α Self-Irradiation in Uranium–Americium Mixed Oxides, *Inorg. Chem.*, 2013, **52**(24), 14196–14204, DOI: 10.1021/ic402124s.

229 D. Prieur, F. Lebreton, P. M. Martin, M. Caisso, R. Butzbach, J. Somers and T. Delahaye, Comparative XRPD and XAS study of the impact of the synthesis process on the electronic and structural environments of uranium–americium mixed oxides, *J. Solid State Chem.*, 2015, **230**, 8–13, DOI: 10.1016/j.jssc.2015.03.037.

230 S. E. Benjamin, J. A. LaVerne, G. E. Sigmon and P. C. Burns, Investigation of Radiation Effects in the Uranyl Mineral Metaschoepite, *Inorg. Chem.*, 2023, **62**(29), 11602–11610, DOI: 10.1021/acs.inorgchem.3c01337.

231 W. Mosley, Self–radiation damage in curium–244 oxide and aluminate, *J. Am. Ceram. Soc.*, 1971, **54**(10), 475–479, DOI: 10.1111/j.1151-2916.1971.tb12182.x.

232 B. E. Burakov, E. E. Strykanova and E. B. Anderson, Secondary Uranium Minerals on the Surface of Chernobyl "Lava", *MRS Proc.*, 1996, **465**, 1309, DOI: 10.1557/PROC-465-1309.

233 Z. C. Emory, J. A. LaVerne and P. C. Burns, Activation of uranyl peroxides by ionizing radiation prior to uranyl carbonate formation, *Dalton Trans.*, 2024, **53**, 17169–17178, DOI: 10.1039/D4DT01841A.

234 M. Fairley, G. E. Sigmon and J. A. LaVerne, Solid-State Transformation of Uranyl Peroxide Materials through High-Level Irradiation, *Inorg. Chem.*, 2023, **62**(48), 19780–19785, DOI: 10.1021/acs.inorgchem.3c03373.

235 M. Fairley, N. M. Myers, J. E. S. Szymanowski, G. E. Sigmon, P. C. Burns and J. A. LaVerne, Stability of Solid Uranyl Peroxides under Irradiation, *Inorg. Chem.*, 2019, **58**(20), 14112–14119, DOI: 10.1021/acs.inorgchem.9b02132.

236 M. Fairley, D. E. Felton, G. E. Sigmon, J. E. S. Szymanowski, N. A. Poole, M. Nyman, P. C. Burns and J. A. LaVerne, Radiation-Induced Solid-State Transformations of Uranyl Peroxides, *Inorg. Chem.*, 2022, **61**(2), 882–889, DOI: 10.1021/acs.inorgchem.1c02603.

 This journal is © the Partner Organisations 2025

Open Access Article. Published on 10 juli 2025. Downloaded on 20-05-2026 01:21:34.
This article is licensed under a Creative Commons Attribution 3.0 Unported Licence.

237 S. K. Scherrer, C. Gates, H. Rajapaksha, S. M. Greer, B. W. Stein and T. Z. Forbes, Superoxide Radicals in Uranyl Peroxide Solids: Lasting Signatures Identified by Electron Paramagnetic Resonance Spectroscopy, *Angew. Chem.*, 2024, **136**(21), e202400379, DOI: 10.1002/anie.202400379.

238 M. Steindler, D. Steidl and J. Fischer, The decomposition of plutonium hexafluoride by gamma radiation, *J. Inorg. Nucl. Chem.*, 1964, **26**(11), 1869–1878.

239 J. J. Stacy, N. Edelstein and R. D. McLaughlin, Effects of Gamma Irradiation on Actinide Ions in Calcium Fluoride, *J. Chem. Phys.*, 1972, **57**(11), 4980–4988, DOI: 10.1063/1.1678168.

240 N. Edelstein, W. Easley and R. McLaughlin, Formation and Characterization of Divalent Americium in CaF2 Crystals, *J. Chem. Phys.*, 1966, **44**(8), 3130–3131, DOI: 10.1063/1.1727193.

241 M. A. Silver, S. K. Cary, A. J. Garza, R. E. Baumbach, A. A. Arico, G. A. Galmin, K.-W. Chen, J. A. Johnson, J. C. Wang, R. J. Clark, A. Chemey, T. M. Eaton, M. L. Marsh, K. Seidler, S. S. Galley, L. van de Burgt, A. L. Gray, D. E. Hobart, K. Hanson, S. M. Van Cleve, F. Gendron, J. Autschbach, G. E. Scuseria, L. Maron, M. Speldrich, P. Kogerler, C. Celis-Barros, D. Perez-Hernandez, R. Arratia-Perez, M. Ruf and T. E. Albrecht-Schmidtt, Electronic Structure and Properties of Berkelium Iodates, *J. Am. Chem. Soc.*, 2017, **139**(38), 13361–13375, DOI: 10.1021/jacs.7b05569.

242 T. K. Gundu Rao, K. V. Lingam and B. N. Bhattacharya, ESR of γ-irradiated single crystals of rubidium uranyl nitrate: NO3 radical, *J. Magn. Reson.*, 1974, **16**(3), 369–376, DOI: 10.1016/0022-2364(74)90218-2.

243 S. J. Kruse, H. Rajapaksha, J. A. LaVerne, S. E. Mason and T. Z. Forbes, Radiation-Induced Defects in Uranyl Trinitrate Solids, *Chem. – Eur. J.*, 2024, **30**(35), e202400956, DOI: 10.1002/chem.202400956.

244 E. Pichot, N. Dacheux, J. Emery, J. Chaumont, V. Brandel and M. Genet, Preliminary study of irradiation effects on thorium phosphate-diphosphate, *J. Nucl. Mater.*, 2001, **289**(3), 219–226, DOI: 10.1016/S0022-3115(01)00437-8.

245 N. Dacheux, N. Clavier and R. Podor, Versatile Monazite: Resolving geological records and solving challenges in materials science. Monazite as a promising long-term radioactive waste matrix: Benefits of high-structural flexibility and chemical durability, *Am. Mineral.*, 2013, **98**(5–6), 833–847, DOI: 10.2138/am.2013.4307.

246 A.-M. Seydoux-Guillaume, X. Deschanels, C. Baumier, S. Neumeier, W. J. Weber and S. Peuget, Why natural monazite never becomes amorphous: Experimental evidence for alpha self-healing, *Am. Mineral.*, 2018, **103**(5), 824–827, DOI: 10.2138/am-2018-6447.

247 L. Martel, M. A. Islam, K. Popa, J.-F. Vigier, E. Colineau, H. Bolvin and J.-C. Griveau, Local Structure and Magnetism of La1−xMxPO4 (M = Sm, 239Pu, 241Am) Explained by Experimental and Computational Analyses, *J. Phys. Chem. C*, 2021, **125**(40), 22163–22174, DOI: 10.1021/acs.jpcc.1c03957.

248 C. Wang, D. Liu and W. Lin, Metal–Organic Frameworks as A Tunable Platform for Designing Functional Molecular Materials, *J. Am. Chem. Soc.*, 2013, **135**(36), 13222–13234, DOI: 10.1021/ja308229p.

249 D. Banerjee, A. J. Cairns, J. Liu, R. K. Motkuri, S. K. Nune, C. A. Fernandez, R. Krishna, D. M. Strachan and P. K. Thallapally, Potential of metal–organic frameworks for separation of xenon and krypton, *Acc. Chem. Res.*, 2015, **48**(2), 211–219, DOI: 10.1021/ar5003126.

250 T. Vazhappilly, A. K. Pathak, M. Sundararajan, B. Modak, S. Kancharlapalli and N. Choudhury, Multiscale Modelling and Simulations for Nuclear Fuels, Waste Management, and Radiation Damages, *BARC Newsl.*, 2024, 24–29.

251 M. Fairley, S. E. Gilson, S. L. Hanna, A. Mishra, J. G. Knapp, K. B. Idrees, S. Chheda, H. Traustason, T. Islamoglu, P. C. Burns, *et al.*, Linker Contribution toward Stability of Metal–Organic Frameworks under Ionizing Radiation, *Chem. Mater.*, 2021, **33**(23), 9285–9294, DOI: 10.1021/acs.chemmater.1c02999.

252 L. Wang, M. Ma, H. Wang, H. Xiong, X. Chen, F. Wei and B. Shen, Real-Space Imaging of the Molecular Changes in Metal–Organic Frameworks under Electron Irradiation, *ACS Nano*, 2023, **17**(5), 4740–4747, DOI: 10.1021/acsnano.2c11110.

253 K. Lv, M. Patzschke, J. März, E. Bazarkina, K. O. Kvashnina and M. Schmidt, Selective Crystallization of a Highly Radiation-Resistant Isonicotinic Acid-Based Metal–Organic Framework as a Primary Actinide Waste Form, *ACS Mater. Lett.*, 2023, **5**(2), 536–542, DOI: 10.1021/acsmaterialslett.2c01087.

254 S. E. Gilson, M. Fairley, P. Julien, A. G. Oliver, S. L. Hanna, G. Arntz, O. K. Farha, J. A. LaVerne and P. C. Burns, Unprecedented Radiation Resistant Thorium–Binaphthol Metal–Organic Framework, *J. Am. Chem. Soc.*, 2020, **142**(31), 13299–13304, DOI: 10.1021/jacs.0c05272.

255 A. M. Hastings, M. Fairley, M. C. Wasson, D. Campisi, A. Sarkar, Z. C. Emory, K. Brunson, D. B. Fast, T. Islamoglu, M. Nyman, *et al.*, Role of Metal Selection in the Radiation Stability of Isostructural M-UiO-66 Metal–Organic Frameworks, *Chem. Mater.*, 2022, **34**(18), 8403–8417, DOI: 10.1021/acs.chemmater.2c02170.

256 Y. Zhang, Y. Du, L. Li, Y. Tao, K. Li, H. Zhang, Y. Wang, L. Chen, Y. Wang, Z. Chai, *et al.*, A Tetravalent Plutonium Organic Framework Containing [Pu2O16] Dimers as Secondary Building Units: Synthesis, Structure, and Radiation Stability, *Chin. J. Chem.*, 2023, **41**(13), 1552–1556, DOI: 10.1002/cjoc.202200833.

257 Y. Zhang, K. Li, S. Zhang, X. Wang, H. Zhang, Y. Wang, Y. Wang, Z. Chai and S. Wang, A Trivalent Americium Organic Framework with Decent Structural Stability against Self-Irradiation, *Chin. J. Chem.*, 2022, **40**(7), 801–805, DOI: 10.1002/cjoc.202100724.

258 S. E. Gilson, M. Fairley, S. L. Hanna, J. E. S. Szymanowski, P. Julien, Z. Chen, O. K. Farha, J. A. LaVerne and

Open Access Article. Published on 10 juli 2025. Downloaded on 20-05-2026 01:21:34.
This article is licensed under a Creative Commons Attribution 3.0 Unported Licence.

P. C. Burns, Unusual Metal–Organic Framework Topology and Radiation Resistance through Neptunyl Coordination Chemistry, *J. Am. Chem. Soc.*, 2021, **143**(42), 17354–17359, DOI: 10.1021/jacs.1c08854.

259 Z.-J. Li, Z. Yue, Y. Ju, X. Wu, Y. Ren, S. Wang, Y. Li, Z.-H. Zhang, X. Guo, J. Lin, *et al.*, Ultrastable Thorium Metal–Organic Frameworks for Efficient Iodine Adsorption, *Inorg. Chem.*, 2020, **59**(7), 4435–4442, DOI: 10.1021/acs.inorgchem.9b03602.

260 A. G. Al Lafi, B. Assfour and T. Assaad, Spectroscopic investigations of gamma-ray irradiation effects on metal organic framework, *J. Mater. Sci.*, 2021, **56**(21), 12154–12170, DOI: 10.1007/s10853-021-06051-5.

261 C. Volkringer, C. Falaise, P. Devaux, R. Giovine, V. Stevenson, F. Pourpoint, O. Lafon, M. Osmond, C. Jeanjacques, B. Marcillaud, *et al.*, Stability of metal–organic frameworks under gamma irradiation, *Chem. Commun.*, 2016, **52**(84), 12502–12505, DOI: 10.1039/C6CC06878B.

262 J. M. Dorhout, M. P. Wilkerson and K. R. Czerwinski, Irradiation and isolation of fission products from uranium metal–organic frameworks, *J. Radioanal. Nucl. Chem.*, 2019, **320**(2), 415–424, DOI: 10.1007/s10967-019-06478-w.

263 Y. A. Mezenov, A. A. Krasilin, V. P. Dzyuba, A. Nominé and V. A. Milichko, Metal–Organic Frameworks in Modern Physics: Highlights and Perspectives, *Adv. Sci.*, 2019, **6**(17), 1900506, DOI: 10.1002/advs.201900506.

264 J. Andreo, E. Priola, G. Alberto, P. Benzi, D. Marabello, D. M. Proserpio, C. Lamberti and E. Diana, Autoluminescent Metal–Organic Frameworks (MOFs): Self-Photoemission of a Highly Stable Thorium MOF, *J. Am. Chem. Soc.*, 2018, **140**(43), 14144–14149, DOI: 10.1021/jacs.8b07113.

265 R. Forsyth, *Spent nuclear fuel. A review of properties of possible relevance to corrosion processes*, 1995.

266 B. Grambow, *Spent fuel. Dissolution and oxidation*, Swedish Nuclear Fuel and Waste Management Co., 1989.

267 S. Sunder and D. W. Shoesmith, *Chemistry of UO2 fuel dissolution in relation to the disposal of used nuclear fuel*, 1991.

268 D. W. Shoesmith, J. Tait, S. Sunder, W. Gray, S. Steward, R. Russo and J. Rudnicki, *Factors affecting the differences in reactivity and dissolution rates between UO2 and spent nuclear fuel*, Atomic Energy of Canada Ltd., 1996.

269 E. Ekeroth, O. Roth and M. Jonsson, The relative impact of radiolysis products in radiation induced oxidative dissolution of UO2, *J. Nucl. Mater.*, 2006, **355**(1), 38–46, DOI: 10.1016/j.jnucmat.2006.04.001.

270 D. W. Shoesmith and S. Sunder, *An electrochemistry-based model for the dissolution of uranium dioxide*, Atomic Energy of Canada Limited, 1991.

271 L. H. Johnson and D. W. Shoesmith, *Radioactive Waste Forms of the Future*, North-Holland, Amsterdam, 1988.

272 R. C. Ewing, Long-term storage of spent nuclear fuel, *Nat. Mater.*, 2015, **14**, 252–257, DOI: 10.1038/nmat4226.

273 E. Ekeroth and M. Jonsson, Oxidation of UO2 by radiolytic oxidants, *J. Nucl. Mater.*, 2003, **322**(2–3), 242–248.

274 H. Christensen and S. Sunder, An evaluation of water layer thickness effective in the oxidation of UO2 fuel due to radiolysis of water, *J. Nucl. Mater.*, 1996, **238**(1), 70–77, DOI: 10.1016/S0022-3115(96)00342-X.

275 C. Corbel, J. F. Lucchini, G. Sattonnay, M. F. Barthe, F. Huet, P. Dehaudt, C. Ardois, B. Hickel and C. Jegou, Increase of the uranium release t an UO2/H_2O interface under He2+ ion beam irradition, *Nucl. Instrum. Methods Phys. Res., Sect. B*, 2001, **179**(2), 225–229, DOI: 10.1016/S0168-583X(01)00519-5.

276 G. Sattonnay, C. Ardois, C. Corbel, J. F. Lucchini, M. F. Barthe, F. Garrido and D. Gosset, Alpha-radiolysis effects on UO2 alteration in water, *J. Nucl. Mater.*, 2001, **288**(1), 11–19, DOI: 10.1016/S0022-3115(00)00714-5.

277 C. Corbel, J. F. Lucchini, G. Sattonnay, M. F. Barthe, F. Huet, P. Dehaudt, C. Ardois, B. Hickel and J. L. Paul, Uranium Oxide Mass Loss Rate in Water for an Interface Under Alpha-Irradiation, *MRS Online Proc. Libr.*, 1999, **608**(41), DOI: 10.1557/PROC-608-41.

278 A. Canizarès, G. Guimbretière, Y. A. Tobon, N. Raimboux, R. Omnée, M. Perdicakis, B. Muzeau, E. Leoni, M. S. Alam, E. Mendes, *et al.*, In situ Raman monitoring of materials under irradiation: study of uranium dioxide alteration by water radiolysis, *J. Raman Spectrosc.*, 2012, **43**(10), 1492–1497, DOI: 10.1002/jrs.4088.

279 C. Corbel, G. Sattonnay, S. Guilbert, F. Garrido, M. F. Barthe and C. Jegou, Addition versus radiolytic production effects of hydrogen peroxide on aqueous corrosion of UO2, *J. Nucl. Mater.*, 2006, **348**(1), 1–17, DOI: 10.1016/j.jnucmat.2005.05.009.

280 S. Hickam, J. Breier, Y. Cripe, E. Cole and P. C. Burns, Effects of H_2O_2 Concentration on Formation of Uranyl Peroxide Species Probed by Dissolution of Uranium Nitride and Uranium Dioxide, *Inorg. Chem.*, 2019, **58**(9), 5858–5864, DOI: 10.1021/acs.inorgchem.9b00231.

281 C. Jégou, B. Muzeau, V. Broudic, S. Peuget, A. Poulesquen, D. Roudil and C. Corbel, Effect of external gamma irradiation on dissolution of the spent UO2 fuel matrix, *J. Nucl. Mater.*, 2005, **341**(1), 62–82, DOI: 10.1016/j.jnucmat.2005.01.008.

282 L. Sarrasin, S. Miro, C. Jégou, M. Tribet, V. Broudic, C. Marques and S. Peuget, Studtite Formation Assessed by Raman Spectroscopy and 18O Isotopic Labeling during the Oxidative Dissolution of a MOX Fuel, *J. Phys. Chem. C*, 2021, **125**(35), 19209–19218, DOI: 10.1021/acs.jpcc.1c04392.

283 A. Perrot, A. Canizares, S. Miro, L. Claparede, R. Podor, T. Sauvage, S. Peuget, C. Jegou and N. Dacheux, In situ Raman monitoring of studtite formation under alpha radiolysis in 18O-labeled water, *J. Nucl. Mater.*, 2024, **600**, 155267, DOI: 10.1016/j.jnucmat.2024.155267.

284 M. Amme, Contrary effects of the water radiolysis product H_2O_2 upon the dissolution of nuclear fuel in natural ground water and deionized water, *Radiochim. Acta*, 2001, **90**(7), 399–406, DOI: 10.1524/ract.2002.90.7_2002.399.

Open Access Article. Published on 10 juli 2025. Downloaded on 20-05-2026 01:21:34. This article is licensed under a Creative Commons Attribution 3.0 Unported Licence.

285 C. Jégou, R. Caraballo, J. De Bonfils, V. Broudic, S. Peuget, T. Vercouter and D. Roudil, Oxidizing dissolution of spent MOX47 fuel subjected to water radiolysis: Solution chemistry and surface characterization by Raman spectroscopy, *J. Nucl. Mater.*, 2010, **399**(1), 68–80, DOI: **10.1016/j.jnucmat.2010.01.004**.

286 K. Büppelmann, S. Magirius, C. Lierse and J. I. Kim, Radiolytic oxidation of americium(III) to americium(V) and plutonium(IV) to plutonium(VI) in saline solution, *J. Less-Common Met.*, 1986, **122**, 329–336, DOI: **10.1016/0022-5088(86)90427-3**.

287 M. V. Vladimirova, D. A. Fedoseev and M. A. Dunaeva, Radiation-Chemical Behavior of Plutonium in the Heterogeneous System PuO2-Ground Water, *Radiochemistry*, 2002, **44**(5), 498–500, DOI: **10.1023/A:1021191710917**.

288 M. C. Rath, D. B. Naik and S. K. Sarkar, Reversible growth of UO2 nanoparticles in aqueous solutions through 7 MeV electron beam irradiation, *J. Nucl. Mater.*, 2013, **438**(1), 26–31, DOI: **10.1016/j.jnucmat.2013.02.005**.

289 R. E. Umpleby, J. K. Conrad, J. R. Wilbanks, K. D. Schaller and G. P. Horne, Radiolytic evaluation of acetohydroxamic acid (AHA) under biphasic (HNO3:n-dodecane and TBP/DEHBA/DEHiBA) used nuclear fuel reprocessing conditions, *Radiat. Phys. Chem.*, 2023, **207**, 110799, DOI: **10.1016/j.radphyschem.2023.110799**.

290 R. G. Deokar and A. R. Cook, Early-stage oxidation and subsequent damage of the used nuclear fuel extractant TODGA; electron pulse radiolysis and theoretical insights, *Phys. Chem. Chem. Phys.*, 2024, **26**(46), 29060–29069, DOI: **10.1039/D4CP03678F**.

291 J. Veliscek-Carolan, Separation of actinides from spent nuclear fuel: A review, *J. Hazard. Mater.*, 2016, **318**, 266–281, DOI: **10.1016/j.jhazmat.2016.07.027**.

292 M. E. Kraft, Nuclear power and the challenge of high-level waste disposal in the United States, *Polity*, 2013, **45**(2), 265–280.

293 R. Wymer, Reprocessing of Nuclear Fuel: Overview/critique of Worldwide Experience and Engineering/technology Challenges for Separations, in *Chemical Separation Technologies and Related Methods of Nuclear Waste Management: Applications, Problems, and Research Needs*, 1999, pp. 29–52.

294 L. L. Daemen, G. S. Kanner, R. S. Lillard, D. P. Butt, T. O. Brun and W. F. Sommer, Modeling of water radiolysis at spallation neutron sources. In Conference: 126. annual meeting of the Minerals, Metals and Materials Society, Orlando, FL (United States), 9–13 Feb 1997; Other Information: PBD: [1998], United States, 1998.

295 Z. Cai, X. Li, Y. Katsumura and O. Urabe, Radiolysis of bicarbonate and carbonate aqueous solutions: product analysis and simulation of radiolytic processes, *Nucl. Technol.*, 2001, **136**(2), 231–240, DOI: **10.13182/NT01-A3241**.

296 V. Vallet, P. Macak, U. Wahlgren and I. Grenthe, Actinide Chemistry in Solution, Quantum Chemical Methods and Models, *Theor. Chem. Acc.*, 2006, **115**(2), 145–160, DOI: **10.1007/s00214-005-0051-7**.

297 D. D. Macdonald, G. R. Engelhardt and A. Petrov, A Critical Review of Radiolysis Issues in Water-Cooled Fission and Fusion Reactors: Part I, Assessment of Radiolysis Models, *Corros. Mater. Degrad.*, 2022, **3**(3), 470–535, DOI: **10.3390/cmd3030028**.

298 S. M. Pimblott and J. A. LaVerne, Molecular product formation in the electron radiolysis of water, *Radiat. Res.*, 1992, **129**(3), 265–271, DOI: **10.2307/3578025**.

299 J. A. LaVerne and S. M. Pimblott, Diffusion-kinetic modeling of the electron radiolysis of water at elevated temperatures, *J. Phys. Chem.*, 1993, **97**(13), 3291–3297.

300 K. Iwamatsu, S. Sundin and J. A. LaVerne, Hydrogen peroxide kinetics in water radiolysis, *Radiat. Phys. Chem.*, 2018, **145**, 207–212, DOI: **10.1016/j.radphyschem.2017.11.002**.

301 M. M. Hossain, E. Ekeroth and M. Jonsson, Effects of HCO3- on the kinetics of UO2 oxidation by H_2O_2, *J. Nucl. Mater.*, 2006, **358**(2–3), 202–208, DOI: **10.1016/j.jnucmat.2006.07.008**, Scopus.

302 I. Casas, J. De Pablo, F. Clarens, J. Giménez, J. Merino, J. Bruno and A. Martínez-Esparza, Combined effect of H_2O_2 and HCO3 - on UO2(s) dissolution rates under anoxic conditions, *Radiochim. Acta*, 2009, **97**(9), 485–490, DOI: **10.1524/ract.2009.1641**.

303 P. G. Lucuta, R. A. Verrall, H. Matzke and B. J. Palmer, Microstructural features of SIMFUEL - Simulated high-burnup UO2-based nuclear fuel, *J. Nucl. Mater.*, 1991, **178**(1), 48–60, DOI: **10.1016/0022-3115(91)90455-G**.

304 F. Garisto, The energy spectrum of α-particles emitted from used CANDU™ fuel, *Ann. Nucl. Energy*, 1989, **16**(1), 33–38, DOI: **10.1016/0306-4549(89)90118-7**.

305 T. E. Eriksen, D. W. Shoesmith and M. Jonsson, Radiation induced dissolution of UO2 based nuclear fuel – A critical review of predictive modelling approaches, *J. Nucl. Mater.*, 2012, **420**(1), 409–423, DOI: **10.1016/j.jnucmat.2011.10.027**.

306 F. Neese, F. Wennmohs, U. Becker and C. Riplinger, The ORCA quantum chemistry program package, *J. Chem. Phys.*, 2020, **152**(22), 224108, DOI: **10.1063/5.0004608**.

307 E. V. Lenthe, E.-J. Baerends and J. G. Snijders, Relativistic regular two–component Hamiltonians, *J. Chem. Phys.*, 1993, **99**(6), 4597–4610, DOI: **10.1063/1.466059**.

308 C. van Wüllen, Molecular density functional calculations in the regular relativistic approximation: Method, application to coinage metal diatomics, hydrides, fluorides and chlorides, and comparison with first-order relativistic calculations, *J. Chem. Phys.*, 1998, **109**(2), 392–399, DOI: **10.1063/1.476576**.

309 D. A. Pantazis, X.-Y. Chen, C. R. Landis and F. Neese, All-Electron Scalar Relativistic Basis Sets for Third-Row Transition Metal Atoms, *J. Chem. Theory Comput.*, 2008, **4**(6), 908–919, DOI: **10.1021/ct800047t**.

310 *Chemcraft*, 2009. **https://www.chemcraftprog.com**.

311 J. Iliopoulos, C. Itzykson and A. Martin, Functional methods and perturbation theory, *Rev. Mod. Phys.*, 1975, **47**(1), 165, DOI: **10.1103/RevModPhys.47.165**.

Open Access Article. Published on 10 juli 2025. Downloaded on 20-05-2026 01:21:34.
This article is licensed under a Creative Commons Attribution 3.0 Unported Licence.

312 S. Chattopadhyay, R. K. Chaudhuri, U. S. Mahapatra, A. Ghosh and S. S. Ray, State–specific multireference perturbation theory: development and present status, *Wiley Interdiscip. Rev.: Comput. Mol. Sci.*, 2016, **6**(3), 266–291.
313 V. von Burg, *Modern Approaches Towards the Electron Correlation Problem*, ETH Zurich, 2022.
314 H. Zhai, Degenerate quantum gases with spin–orbit coupling: a review, *Rep. Prog. Phys.*, 2015, **78**(2), 026001, DOI: 10.1088/0034-4885/78/2/026001.
315 C. M. Marian, Spin-orbit coupling in molecules, *Rev. Comput. Chem.*, 2001, **17**, 99–204, DOI: 10.1002/0471224413.
316 Y. Guo, K. Sivalingam, E. F. Valeev and F. Neese, Explicitly correlated N-electron valence state perturbation theory (NEVPT2-F12), *J. Chem. Phys.*, 2017, **147**(6), 064110, DOI: 10.1063/1.4996560.
317 H. Bolvin, From ab initio calculations to model Hamiltonians: the effective Hamiltonian technique as an efficient tool to describe mixed-valence molecules, *J. Phys. Chem. A*, 2003, **107**(25), 5071–5078, DOI: 10.1021/jp034176+.
318 F. Neese, Efficient and accurate approximations to the molecular spin-orbit coupling operator and their use in molecular g-tensor calculations, *The Journal of Chemical Physics*, 2005, **122**(3), 034107, DOI: 10.1063/1.1829047.
319 J.-P. Dognon, Theoretical insights into the chemical bonding in actinide complexes, *Coord. Chem. Rev.*, 2014, **266–267**, 110–122, DOI: 10.1016/j.ccr.2013.11.018.
320 K. A. Peterson, Correlation consistent basis sets for actinides. I. The Th and U atoms, *J. Chem. Phys.*, 2015, **142**(7), 074105, DOI: 10.1063/1.4907596.
321 J. T. Pegg, X. Aparicio-Anglès, M. Storr and N. H. de Leeuw, DFT+U study of the structures and properties of the actinide dioxides, *J. Nucl. Mater.*, 2017, **492**, 269–278, DOI: 10.1016/j.jnucmat.2017.05.025.
322 D. Gryaznov, E. Heifets and D. Sedmidubsky, Density functional theory calculations on magnetic properties of actinide compounds, *Phys. Chem. Chem. Phys.*, 2010, **12**(38), 12273–12278, DOI: 10.1039/C0CP00372G.
323 B. Sadigh, A. Kutepov, A. Landa and P. Söderlind, Assessing Relativistic Effects and Electron Correlation in the Actinide Metals Th to Pu, *Appl. Sci.*, 2019, **9**(23), 5020, DOI: 10.3390/app9235020.
324 C. Clavaguéra-Sarrio, V. Vallet, D. Maynau and C. J. Marsden, Can density functional methods be used for open-shell actinide molecules? Comparison with multiconfigurational spin-orbit studies, *J. Chem. Phys.*, 2004, **121**(11), 5312–5321, DOI: 10.1063/1.1784412.
325 K. Burke, Perspective on density functional theory, *J. Chem. Phys.*, 2012, **136**(15), 150901, DOI: 10.1063/1.4704546.
326 D. S. Sholl and J. A. Steckel, *Density functional theory: a practical introduction*, John Wiley & Sons, 2022.
327 J. Neugebauer and T. Hickel, Density functional theory in materials science, *Wiley Interdiscip. Rev.: Comput. Mol. Sci.*, 2013, **3**(5), 438–448, DOI: 10.1002/wcms.1125.
328 J. W. Park and T. Shiozaki, On-the-Fly CASPT2 Surface-Hopping Dynamics, *J. Chem. Theory Comput.*, 2017, **13**(8), 3676–3683, DOI: 10.1021/acs.jctc.7b00559.
329 J. M. Toldo, M. T. do Casal, E. Ventura, S. A. do Monte and M. Barbatti, Surface hopping modeling of charge and energy transfer in active environments, *Phys. Chem. Chem. Phys.*, 2023, **25**(12), 8293–8316, DOI: 10.1039/D3CP00247K.
330 K. F. Wong and P. J. Rossky, Mean-Field Molecular Dynamics with Surface Hopping: Application to the Aqueous Solvated Electron, *J. Phys. Chem. A*, 2001, **105**(12), 2546–2556, DOI: 10.1021/jp0037652.
331 R. P. Sutton, Fundamental PVT Calculations for Associated and Gas/Condensate Natural-Gas Systems, *SPE Reservoir Eval. Eng.*, 2007, **10**(3), 270–284, DOI: 10.2118/97099-pa.
332 A. J. Cohen, P. Mori-Sánchez and W. Yang, Challenges for Density Functional Theory, *Chem. Rev.*, 2012, **112**(1), 289–320, DOI: 10.1021/cr200107z.

This journal is © the Partner Organisations 2025